UC Davis
UC Davis Electronic Theses and Dissertations

Title
Model Building from the Hierarchy Problem to Flavor Physics

Permalink
https://escholarship.org/uc/item/0pj027fr

Author
Chung, Yi

Publication Date
2022

Peer reviewed|Thesis/dissertation

eScholarship.org Powered by the California Digital Library
University of California

Model Building from the Hierarchy Problem to Flavor Physics

By

YI CHUNG

DISSERTATION

Submitted in partial satisfaction of the requirements for the degree of

DOCTOR OF PHILOSOPHY

in

Physics

in the

OFFICE OF GRADUATE STUDIES

of the

UNIVERSITY OF CALIFORNIA

DAVIS

Approved:

Hsin-Chia Cheng, Chair

Markus Luty

John Terning

Committee in Charge

2022

Copyright © 2022 by
Yi Chung
All rights reserved.

To mom and dad

who support me unconditionally.

Contents

List of Figures

List of Tables

Abstract

Model Building from the Hierarchy Problem to Flavor Physics

This dissertation includes several models motivated by the theoretical and experimental problems in the Standard Model of particle physics. The models are based on the composite Higgs models with different cosets. We show that, with enlarged symmetries and cosets, we are able to address the hierarchy problem together with the fine-tuning issue in the Higgs potential, the mass hierarchy between different fermions, and the current B-meson anomalies. A detailed study of phenomenology, including direct and indirect searches, is also presented. The models will be tested in the future, which might unveil the deep connection between Higgs physics and flavor physics.

Chapter 1

Introduction

The Standard Model (SM) of particle physics is the most successful model, which describes the properties of all the known elementary particles. Since the Large Hadron Collider (LHC) started up in 2008, about 140 fb^{-1} of data have been collected and analyzed. So far, the observations from the two main collaborations, ATLAS and CMS, are consistent with the SM predictions, including the famous discovery of the Higgs boson in July 2012, which strengthens the validity of the SM. However, there are still theoretical considerations and experimental results that indicate the SM is incomplete. To understand these issues, we can first briefly overview the SM Lagrangian through the following terms

$$\mathcal{L}_{\text{SM}} = -\frac{1}{4}\left(F^a_{\mu\nu}\right)^2 + |D_\mu H|^2 + i\bar{\psi}\not{D}\psi - m_H^2|H|^2 - \lambda_H|H|^4 - Y_{ij}\bar{\psi}_{L,i}H\psi_{R,j} \ , \qquad (1.0.1)$$

which can be categorized into three different sectors.

First, the **Gauge sector**, which describes the properties of vector bosons and their interaction with charged particles, is the most well-understood one among all. The gauge theory helps us write down the relevant interactions related to spin-one particles, which are included in the first three terms of Eq. (1.0.1). They are based on the SM gauge group

$$SU(3)_C \times SU(2)_W \times U(1)_Y \ , \qquad (1.0.2)$$

which is composed of two parts - strong interaction and electroweak interaction.

The theory of the strong interaction is constructed through the non-abelian $SU(3)_C$ gauge group with quarks, also known as quantum chromodynamics (QCD). QCD has several salient properties. First, it is asymptotically free, which means its coupling becomes

weaker as the energy scale increases. The property allows us to address QCD perturbatively in high-energy collisions, such as in the LHC. On the other hand, the theory becomes non-perturbative when the energy is below the scale $\Lambda_{QCD} \sim 200$ MeV. The strong interaction will lead to a fermionic condensate and break the chiral symmetry. At this energy scale, QCD with quarks and gluons no longer provides a good description. Instead, the degrees of freedom become composite particles like mesons and hadrons. One way to describe the low-energy dynamics of QCD is by an effective field theory (EFT) constructed through the underlying symmetry, such as the chiral perturbation theory. Building the low-energy EFT based on symmetry is an important method in studying composite theory, such as composite Higgs models.

The rest, $SU(2)_W \times U(1)_Y$, is known as electroweak gauge symmetry. The key feature is that the symmetry is broken down to the $U(1)_{EM}$, the electromagnetism with the photon. The other three gauge bosons become massive and are known as $W^{\pm}$ and Z bosons, which mediate the weak force. The way the symmetry is spontaneously broken brings us to the next and the most important sector.

The **Higgs sector**, responsible for the electroweak symmetry breaking (EWSB), is the core of the SM. The Higgs potential, i.e. the fourth and fifth terms in Eq. (1.0.1), is the most mysterious part of the SM Lagrangian. Especially, the coefficient of the Higgs quadratic term, m_H^2, is the only dimensionful parameter in Eq. (1.0.1). The mass of the Higgs field is not protected by any symmetry and thus is UV-sensitive. Therefore, the generic scale should be around Planck scale $M_{\rm Pl} \sim 10^{19}$ GeV, which is much larger than the observed value $m_H \sim 100$ GeV. The problem is known as the **Hierarchy problem**, which is eager for a solution to explain the hierarchy between the electroweak scale and the Planck scale. It is also the main motivation for both the model building (theory side) and the searches of new physics (experimental side) beyond the Standard Model (BSM) in the past few decades.

An attractive solution to introduce the electroweak scale is through an asymptotically-free gauge theory, just like QCD, which introduces the scale Λ_{QCD} and breaks the chiral symmetry. Based on this idea, theorists constructed the first BSM model for the hierarchy

problem, Technicolor (TC) models. However, the models are ruled out due to the discovery of the light Higgs boson. The successor, Composite Higgs Models (CHM), on the other hand, introduce the Higgs boson as a pseudo-Nambu Goldstone boson (pNGB), like the pions in QCD. In this way, the Higgs boson is predicted to be much lighter than other composite resonances. The models not only explain the origin of the electroweak scale but also predict the spectrum we observed in the LHC.

The construction of CHMs is analogous to the chiral perturbation theory, where the chiral symmetry is broken below the compositeness scale Λ_{QCD}. In the low-energy regime of QCD, considering only the up quark and the down quark, the $SU(2)_L \times SU(2)_R$ global symmetry is broken down to $SU(2)_V$ once a quark-antiquark pair forms a condensate and acquires a non-zero VEV. The chiral symmetry breaking will introduce three pNGBs, i.e. pions. In CHMs, we also introduce some global symmetry G, which is broken down to the subgroup H with a symmetry breaking scale $f \sim 1$ TeV. The coset G/H should introduce at least four pNGBs to play the roles of the Higgs doublet. Among all kinds of coset, the most popular one is the $SO(5)/SO(4)$ coset, which introduces exactly four pNGBs and is known as the minimal composite Higgs model (MCHM). However, the coset can be well beyond the minimal choice and results in a richer mechanism and phenomenology. *The additional mechanism might allow us to solve not only the problem in the Higgs sector but also other issues in the SM.* This is the main motivation of this dissertation. In the following chapters, we are going to explore a series of models, all based on composite Higgs models but with larger cosets, aiming at solving different problems together with the hierarchy problem. Before that, let us go back to the issue in the SM.

The last sector, the little-understood one, is the **Yukawa sector**, which describes the interaction between the fermion fields and the Higgs field. Although it is written as merely one term in Eq. (1.0.1), it actually includes more parameters than the other two sectors. Unlike the gauge sector, which only includes three different couplings (one for each gauge interaction), the Yukawa couplings do not follow any underlying rule and thus can all be different. That is, even we don't count the mysterious neutrino sector, the other SM fermions already require three 3×3 complex Yukawa matrices, i.e. 27 complex couplings

in total. They will lead to more than ten physical observables, including fermion masses and mixings. The problem is not just about the number of parameters but also their values. The masses of these SM fermions span over six orders of magnitude. The mixing matrix also shows a weird pattern. It is close to the identity in the quark sector but far from identity in the lepton sector. The issue is known as the **flavor puzzle**, which represents the mysterious structure of SM Yukawa couplings.

Besides the theoretical issues, many experimental results indicate that the SM is not complete. For example, multiple observations have shown the existence of Dark Matter and Dark Energy, which are not predicted in the SM. Also, the abundance of matter over anti-matter derived from the SM mechanism is not enough to explain the observed Universe. However, these examples are originated from astrophysics and cosmology, where the solutions might be beyond the scope of particle physics. Even if they are within particle physics, it is unclear whether the scale of the solution is reachable. In this dissertation, we focus on the TeV-scale new physics, and there is no guarantee that they should be related to any of the issues mentioned in this paragraph.

The direct searches of TeV-scale new physics have already been conducted by ATLAS and CMS collaborations. No significant discrepancies have been found so far, which have ruled out most of the minimal models aiming at explaining the hierarchy problem. However, in the other direction, the indirect searches conducted by the LHCb collaboration show a series of consistent deviations in the semileptonic B-meson decays. The discrepancy first showed up in the measurement of the angular observables P_5' of a $b \to s\mu\mu$ decay. Since then, the LHCb have measured branching ratios in many different $b \to s\ell^+\ell^-$ decays. Among them, the most important measurement is the test of lepton flavor universality (LFU), which measure the ratio of branching ratios

$$R_{K^{(*)}} \equiv \frac{Br(B \to K^{(*)}\mu^+\mu^-)}{Br(B \to K^{(*)}e^+e^-)} \simeq 1 \ . \tag{1.0.3}$$

The theoretical prediction of the LFU is clean (not sensitive to hadronic uncertainties) and thus can provide clear evidence for the possible deviation. So far, none of these measurements is statistically significant enough to reach the discovery level, but the combined analysis shows a consistent deviation from the SM prediction. Most important of all, they

point to the new physics around the TeV-scale, which is precisely the scale we expect for a solution to the hierarchy problem! Therefore, it will be the only experimental issue that we are going to address in this dissertation.

Outline of Dissertation

This dissertation explores the possibility of solving the hierarchy problem together with other SM issues as mentioned within the framework of composite Higgs models. Three CHMs, each with a different setup and intent, are studied in the content.

In chapter 2, we first try to solve the problem within CHMs. In most CHMs, the tuning is required to reproduce a Higgs VEV v much less than the symmetry breaking scale f of CHMs, which requires some level of tuning. We show that, within a $SU(6)/Sp(6)$ composite Higgs model, there is an enhanced symmetry on the fermion resonances, which can help minimize the Higgs quadratic term. An additional Higgs quartic term can also be generated through the collective symmetry breaking. Combining the two mechanisms, we are able to reach a minimal tuning and get a more natural Higgs potential.

Chapter 3 is an attempt to address the hierarchy problem with the flavor puzzle together at the electroweak scale. The model is also based on $SU(6)/Sp(6)$ coset but with an $U(1)$ subgroup identified as the flavor symmetry. We realize the Froggatt-Nielsen (FN) mechanism within the framework of CHMs. The flavon field arises as a pNGB of the broken symmetry, and composite fermionic resonances of the strong dynamics can play the roles of the FN fields (vector-like fermions). The model can be viewed as a composite UV completion of the Froggatt-Nielsen mechanism.

The last model in chapter 4 targets the B-meson anomalies. One popular solution is a massive neutral vector boson Z' of some flavor-dependent $U(1)'$ gauge symmetry. We find that, in a $SU(4)/Sp(4)$ fundamental composite Higgs model, a TeV-scale Z' boson can naturally arise and explain the neutral current B anomalies. We explore the allowed parameter space and study the corresponding Z' phenomenology.

Finally, chapter 5 contains the conclusion and outlook.

Chapter 2

A More Natural Composite Higgs Model

Hsin-Chia Cheng and Yi Chung

Center for Quantum Mathematics and Physics (QMAP), Department of Physics, University of California, Davis, CA 95616, U.S.A.

Composite Higgs models provide an attractive solution to the hierarchy problem. However, many realistic models suffer from tuning problems in the Higgs potential. There are often large contributions from the UV dynamics of the composite resonances to the Higgs potential, and tuning between the quadratic term and the quartic term is required to separate the electroweak breaking scale and the compositeness scale. We consider a composite Higgs model based on the $SU(6)/Sp(6)$ coset, where an enhanced symmetry on the fermion resonances can minimize the Higgs quadratic term. Moreover, a Higgs quartic term from the collective symmetry breaking of the little Higgs mechanism can be realized by the partial compositeness couplings between elementary Standard Model fermions and the composite operators, without introducing new elementary fields beyond the Standard Model and the composite sector. The model contains two Higgs doublets, as well as several additional pseudo-Nambu-Goldstone bosons. To avoid tuning, the extra Higgs bosons are expected to be relatively light and may be probed in the future LHC runs. The deviations of the Higgs couplings and the weak gauge boson couplings also provide important tests as they are expected to be close to the current limits in this model.

2.1 Introduction

The Standard Model (SM) of particle physics successfully describes all known elementary particles and their interactions. At the center of SM is the mechanism of electroweak symmetry breaking (EWSB), which is responsible for the masses of gauge bosons and fermions. The discovery of Higgs bosons in 2012 [1, 2] filled in the last missing piece of the SM. However, the Higgs boson itself brings new questions and puzzles that need to be answered. As a minimal model to realize EWSB, the Higgs field is characterized by the potential

$$V(H) = -\mu^2|H|^2 + \lambda|H|^4 \tag{2.1.1}$$

with just two parameters. The two parameters are now fixed by the observed Higgs vacuum expectation value (VEV) $v \simeq 246$ GeV and Higgs boson mass $M_h \simeq 125$ GeV as

$$\mu^2 \simeq (88 \text{ GeV})^2 , \qquad \lambda \simeq 0.13 . \tag{2.1.2}$$

However, SM does not address the UV-sensitive nature of scalar bosons. The Higgs mass-squared receives quadratically divergent radiative corrections from the interactions with SM fields, which leads to the well-known hierarchy problem. To avoid the large quadratic corrections, the most natural way is to invoke some new symmetry such that the quadratic contributions cancel in the symmetric limit. This requires the presence of new particles related to SM particles by the new symmetry, such as top partners, in order to cut off the divergent loop contributions.

One such appealing solution to the hierarchy problem is the composite Higgs model (CHM), where the Higgs doublet is the pseudo-Nambu-Goldstone boson (pNGB) of a spontaneously broken global symmetry of the underlying strong dynamics [3, 4]. Through the analogy of the chiral symmetry breaking in quantum chromodynamics (QCD), which naturally introduces light scalar fields, i.e., pions, we can construct models with light Higgs bosons in a similar way. In a CHM, an approximate global symmetry G is spontaneously broken by some strong dynamics down to a subgroup H with a symmetry breaking scale f. The heavy resonances of the strong dynamics are expected to be around the compositeness scale $\sim 4\pi f$ generically. The pNGBs of the symmetry breaking, on the other hand, can

naturally be light with masses $< f$ as they are protected by the shift symmetry. The potential of the Higgs field arises from the explicit symmetry breaking effects, such as the interactions with other SM fields. The largest coupling of the Higgs field in SM is to the top quark. As a result, for naturalness, the top partners which regulate the top loop contribution to the Higgs potential should not be too heavy. The top loop contribution to the Higgs mass term can be estimated as

$$\Delta\mu^2 \sim \frac{N_c}{8\pi^2} y_t^2 M_T^2 \sim (220 \text{ GeV})^2 \left(\frac{M_T}{1.2 \text{ TeV}}\right)^2, \tag{2.1.3}$$

where M_T is the top partner mass. On the other hand, the bounds on the SM colored top partners have reached beyond 1 TeV from the collider searches [27, 28]. Compared with Eq. (2.1.2), we see that the models with colored top partners (including both the minimal supersymmetric standard model (MSSM) and the CHM) already require some unavoidable $\mathcal{O}(10\%)$ tuning, albeit not unimaginable.

In most CHMs, however, the tuning is much worse than that is shown in Eq. (2.1.3). Depending on the coset G/H and the representations of composite operators that couple to the top quarks, the strongly interacting resonances of the top sector in the UV often give a bigger contribution to the Higgs potential than Eq. (2.1.3), which requires more tuning to cancel. Another problem is that, unlike the pions, the Higgs field needs to develop a nonzero VEV v. The current experimental constraints require $v < f/3$. On the other hand, for a generic pNGB potential, the natural VEV for the pNGB is either 0 or f. To obtain a VEV much less than f, a significant quartic Higgs potential compared to the quadratic term is needed. In little Higgs models [7, 8, 9], a Higgs quartic term can be generated without inducing a large quadratic term from the collective symmetry breaking. Such a mechanism is not present in most CHMs, which is another cause of the fine-tuning issue.

In this study, our goal is to find a more natural CHM by removing the additional tuning beyond Eq. (2.1.3). We first identify the cosets and the composite operator representations that couple to the top quarks, which can preserve a larger symmetry for the resonances to suppress the UV contribution to the Higgs potential. Next, we implement the collective symmetry breaking to generate a Higgs quartic potential while keeping the quadratic term

at the level of Eq. (2.1.3). In this way we can naturally separate the scales of v and f, resulting in a more natural CHM.

This paper is organized as follows. In section 2.2, we review the tuning problems in CHMs and identify the sources of the extra tuning, using the $SO(5)/SO(4)$ CHMs as an example. In section 4.2, we introduce the $SU(6)/Sp(6)$ CHM, including the interactions that produce the SM Yukawa couplings, and show how the large UV contribution to the Higgs potential is avoided. We then move on to the next step to generate an independent Higgs quartic term from collective symmetry breaking in section 2.4. The resulting Higgs potential of the 2HDM is discussed in section 2.5. The complete potential and spectrum of all the pNGBs in our model are summarized in section 2.6 with numerical estimation. Section 4.5 and Section 2.8 are devoted to the phenomenology of this model. Section 4.5 focuses on the collider searches and constraints. The analyses of the indirect constraints from the precision experimental measurements are presented in Section 2.8. Section 4.7 contains our summaries and conclusions. In Appendix A we briefly discuss the possibility of constructing a similar model based on the $SU(5)/SO(5)$ coset. We point out the differences and some drawbacks of such a model. Appendix B contains the details of the interactions between elementary fermions and composite operators for a realistic implementation of the $SU(6)/Sp(6)$ CHM model.

2.2 Tuning in General Composite Higgs Models

We first give a brief review of the tuning problem of the Higgs potential in general CHMs, which was comprehensively discussed in Ref. [10, 11]. This will help to motivate possible solutions. As an illustration, we consider the Minimal Composite Higgs Models (MCHMs) [12] with the symmetry breaking $SO(5) \to SO(4)$. The four pNGBs are identified as the SM Higgs doublet. The SM gauge group $SU(2)_W \times U(1)_Y$ is embedded in $SO(5) \times U(1)_X$, with the extra $U(1)_X$ accounting for the hypercharges of SM fermions. The explicit breaking of the global symmetry introduces a pNGB potential such that at the minimum the $SO(5)$ breaking VEV f is slightly rotated away from the direction that preserves the $SU(2)_W \times U(1)_Y$ gauge group. The misalignment leads to the EWSB at a

scale $v \ll f$.

The explicit global symmetry breaking comes from SM gauge interactions and Yukawa interactions. The SM Yukawa couplings arise from the partial compositeness mechanism [20]: elementary fermions mix with composite operators of the same SM quantum numbers from the strong dynamics,

$$\mathcal{L} = \lambda_L \bar{q}_L O_R + \lambda_R \bar{q}_R O_L, \tag{2.2.1}$$

where q_L, q_R are elementary fermions and O_L, O_R are composite operators of some representations of G ($= SO(5)$ in MCHMs). The values of couplings λ_L, λ_R depend on the UV theory of these interactions and are treated as free parameters to produce viable models. With these interactions, the observed SM fermions will be mixtures of elementary fermions and composite resonances. The SM fermions can then couple to the Higgs field through the portion of the strong sector with couplings given by

$$y \simeq \frac{\lambda_L \lambda_R}{g_\psi} \simeq \epsilon_L \cdot g_\psi \cdot \epsilon_R \ , \tag{2.2.2}$$

where g_ψ is a coupling of the strong resonances and is expected to be $\gg 1$, $\epsilon_{L,R}$ are ratios $\lambda_{L,R}/g_\psi$, which are expected to be small. The resonances created by $O_{L,R}$ have masses $\sim g_\psi f$, and play the roles of SM fermion partners. They cut off the divergent contributions to the Higgs potential and make it finite. Notice that the operators belong to representations of the global symmetry G, but the resonances are divided into representations of H after the symmetry breaking. Because the elementary fermions in general do not fill the whole representations of G, the partial compositeness couplings λ_L, λ_R explicitly break the global symmetry G and generate a nontrivial Higgs potential.

The pNGB Higgs field parametrizes the coset G/H so the potential is periodic in the Higgs field. The Higgs potential can be expanded in $\sin(H/f)$ and up to the quartic term it takes the form

$$V(H) = -\hat{\alpha} f^2 \sin^2 \frac{H}{f} + \hat{\beta} f^2 \sin^4 \frac{H}{f} \ , \tag{2.2.3}$$

where $\hat{\alpha}$ and $\hat{\beta}$ have mass dimension two and $\hat{\alpha}$ corresponds to the mass-squared parameter of the Higgs field while $\hat{\beta}/f^2$ will contribute to the quartic term. By expanding $\sin(H/f)$,

higher powers of H can be generated from each term, but for convenience, we will simply call the first term quadratic term and the second term quartic term. The parameters $\hat{\alpha}$ and $\hat{\beta}$ are model dependent and are generated by explicit breaking parameters, like λ_L and λ_R. Given the potential, we can get the VEV and Higgs mass parameterized as

$$v = \sqrt{\frac{\hat{\alpha}}{2\hat{\beta}}}\, f, \qquad M_h^2 = 8\hat{\beta}\frac{v^2}{f^2}(1 - \frac{v^2}{f^2}) \ . \tag{2.2.4}$$

The misalignment of the minimum from the SM gauge symmetry preserving direction is parametrized by

$$\xi \equiv \frac{v^2}{f^2} = \sin^2\langle\theta\rangle = \frac{\hat{\alpha}}{2\hat{\beta}} \ll 1 \ , \tag{2.2.5}$$

where angle $\langle\theta\rangle \equiv \langle h\rangle/f$. Therefore, for a realistic model, we need $\hat{\alpha} \ll \hat{\beta}$ and at the same time, the correct size of $\hat{\beta}$ to get the observed Higgs boson mass $M_h \simeq 125$ GeV.

From the most explicit symmetry breaking effects of the composite Higgs models, one typically gets $\hat{\alpha} > \hat{\beta}$, which is the source of the tuning problem. For example, in MCHM$_5$ [11, 12], the SM fermions mix with composite operators O_L, $O_R \in \mathbf{5}$ of $SO(5)$. After the symmetry breaking, the composite resonances split into $\mathbf{4}$ and $\mathbf{1}$ representations of $SO(4)$. The mass difference between $\mathbf{4}$ and $\mathbf{1}$ resonances generates a Higgs potential at the compositeness (UV) scale with

$$\hat{\alpha} \sim \frac{N_c}{16\pi^2}\lambda_{L,R}^2 M_\psi^2 \sim \epsilon_{L,R}^2 \frac{N_c g_\psi^4}{16\pi^2} f^2, \tag{2.2.6a}$$

$$\hat{\beta} \sim \frac{N_c}{16\pi^2}\lambda_{L,R}^4 f^2 \sim \epsilon_{L,R}^4 \frac{N_c g_\psi^4}{16\pi^2} f^2. \tag{2.2.6b}$$

The quartic term coefficient $\hat{\beta}$ arises at a higher order in ϵ than $\hat{\alpha}$, so generically $\hat{\beta} \ll \hat{\alpha}$ is expected instead. It is then required more fine-tuning to achieve the correct EWSB. In some models, it is possible to have $\hat{\alpha} \sim \hat{\beta}$. For example, MCHM$_{14}$ [10] with O_L, $O_R \in \mathbf{14}$ of $SO(5)$ can lead to the potential with

$$\hat{\alpha} \sim \hat{\beta} \sim \frac{N_c}{16\pi^2}\lambda_{L,R}^2 M_\psi^2 \sim \epsilon_{L,R}^2 \frac{N_c g_\psi^4}{16\pi^2} f^2, \tag{2.2.7}$$

where $\hat{\beta}$ arises at the same order as $\hat{\alpha}$. It requires less tuning to achieve $\xi \ll 1$. This has been called "minimal tuning." But even so, the UV contribution of Eq. (2.2.7) to $\hat{\alpha}$ is

larger than the IR contribution from the top quark loop

$$\Delta m_{\rm IR}^2 \sim \frac{N_c}{16\pi^2} y_t^2 M_T^2 \sim \epsilon_{L,R}^4 \frac{N_c g_\psi^4}{16\pi^2} f^2, \tag{2.2.8}$$

which already requires some levels of fine-tuning as shown in Eq. (2.1.3). This additional UV contribution actually worsens the condition and requires more tuning. A less-tuned scenario is to have a composite right-handed top quark (which is a singlet of G). In this case, $\epsilon_R \sim 1$ but does not contribute to the Higgs potential. The Higgs potential is controlled by $\lambda_L \sim y_t$, which can be smaller.

From the above discussion, one can see that to obtain a more natural Higgs potential in CHM, it would be desirable to suppress the contribution from the composite top-partner resonances to the quadratic term. For example, a maximal symmetry was proposed in Ref. [14] to keep the degeneracy of the whole G representation of the top-partner resonances. However, the maximal symmetry is somewhat ad hoc within a simple model and its natural realization requires more complicated model constructions by doubling the global symmetry groups or invoking a holographic extra dimension [15, 16]. We will look for cosets G/H such that the representation of the top-partner resonances do not split even after the symmetry breaking of $G \to H$ so that it preserves a global symmetry G in any single partial compositeness coupling to prevent unwanted large contributions to the Higgs potential. Besides, we need some additional contribution to the quartic term without inducing the corresponding quadratic term simultaneously to make $\hat{\beta} > \hat{\alpha}$ naturally. This may be achieved by the collective symmetry breaking of the little Higgs mechanism [7, 8, 9]. Previous attempts include adding exotic elementary fermions to an $SU(5)/SO(5)$ CHM model [17] and a holographic model with double copies of the global symmetry [18]. Another way of generating the quartic term without the quadratic term using the Higgs dependent kinetic mixing requires both new elementary fermions and an enlarged global symmetry or an extra dimension [19]. We will take a more economical approach by implementing the little Higgs mechanism without adding exotic elementary fermions or invoking multiple copies of the global symmetry, but simply using the couplings that mix SM fermions with composite resonances.

2.3 The $SU(6)/Sp(6)$ Composite Higgs Model

Among the possible cosets, the cosets $SU(5)/SO(5)$ and $SU(6)/Sp(6)$ are potential candidates to realize the ideas discussed at the end of the previous section. If the composite operator $O_{L,R} \in \mathbf{5}(\mathbf{6})$ of $SU(5)(SU(6))$, the corresponding resonances do not split under the unbroken subgroup $SO(5)(Sp(6))$.[1] Since they are still complete multiplets of G, there is an enhanced symmetry for each mixing coupling $\lambda_{L,R}$, which protects the pNGB potential. The cosets were also some earliest ones employed in little Higgs models [9, 16] where the collective symmetry breaking for the quartic coupling was realized. In CHMs, it requires different explicit implementations if no extension of the SM gauge group or extra elementary fermions are introduced. The $SU(5)/SO(5)$ model has a general problem that an $SU(2)$ triplet scalar VEV violates the custodial $SU(2)$ symmetry, leading to strong experimental constraints. We will focus on the $SU(6)/Sp(6)$ model[2] here and leave a brief discussion of the $SU(5)/SO(5)$ model in Appendix A.

2.3.1 Basics of $SU(6)/Sp(6)$

To parametrize the $SU(6)/Sp(6)$ non-linear sigma model, we can use a sigma field Σ^{ij}, which transforms as an anti-symmetric tensor representation **15** of $SU(6)$, where $i, j = 1, \ldots 6$ are $SU(6)$ indices. The transformation can be expressed as $\Sigma \to g\Sigma g^T$ with $g \in SU(6)$ or as $\Sigma^{ij} \to g^i{}_k g^j{}_\ell \Sigma^{k\ell}$ with indices explicitly written out. The scalar field Σ has an anti-symmetric VEV $\langle\Sigma\rangle = \Sigma_0^{\alpha\beta}$ (with α, β representing $Sp(6)$ index), where

$$\Sigma_0 = \begin{pmatrix} 0 & -\mathbb{I} \\ \mathbb{I} & 0 \end{pmatrix}, \tag{2.3.1}$$

and $\mathbb{I}$ is the 3×3 identity matrix. The Σ VEV breaks $SU(6)$ down to $Sp(6)$, producing 14 Nambu-Goldstone bosons.

The 35 $SU(6)$ generators can be divided into the unbroken ones and broken ones with

[1] Naïvely they can split into two real representations, but if they carry charges under the extra $U(1)_X$ gauge group which is required to obtain the correct hypercharge, they need to remain complex.

[2] A CHM with the $SU(6)/Sp(6)$ coset were considered in Ref. [17], but for a different prospect.

each type satisfying

$$\begin{cases} \text{unbroken generators} & T_a : T_a\Sigma_0 + \Sigma_0 T_a^T = 0 \ , \\ \text{broken generators} & X_a : X_a\Sigma_0 - \Sigma_0 X_a^T = 0 \ . \end{cases} \tag{2.3.2}$$

The Nambu-Goldstone fields can be written as a matrix with the broken generator:

$$\xi(x) = \xi^i{}_\alpha(x) \equiv e^{\frac{i\pi_a(x)X_a}{2f}}. \tag{2.3.3}$$

Under $SU(6)$, the ξ field transforms as $\xi \to g\xi h^\dagger$ where $g \in SU(6)$ and $h \in Sp(6)$, so ξ carries one $SU(6)$ index and one $Sp(6)$ index. The relation between ξ and Σ field is given by

$$\Sigma(x) = \Sigma^{ij}(x) \equiv \xi\Sigma_0\xi^T = e^{\frac{i\pi_a(x)X_a}{2f}}\Sigma_0 e^{\frac{i\pi_a(x)X_a^T}{2f}} = e^{\frac{i\pi_a(x)X_a}{f}}\Sigma_0 \ . \tag{2.3.4}$$

The complex conjugation raises or lowers the indices. The fundamental representation of $Sp(6)$ is (pseudo-)real and the $Sp(6)$ index can be raised or lowered by $\Sigma_0^{\alpha\beta}$ or $\Sigma_{0,\alpha\beta}$.

The broken generators and the corresponding fields in the matrix can be organized as follows ($\epsilon = i\sigma^2$):

$$\pi_a X_a = \begin{pmatrix} \frac{1}{\sqrt{2}}\phi_a\sigma^a - \frac{\eta}{\sqrt{6}}\mathbf{1} & H_2 & \epsilon s & H_1 \\ H_2^\dagger & \frac{2\eta}{\sqrt{6}} & -H_1^T & 0 \\ \epsilon^T s^* & -H_1^* & \frac{1}{\sqrt{2}}\phi_a\sigma^{a*} - \frac{\eta}{\sqrt{6}}\mathbf{1} & H_2^* \\ H_1^\dagger & 0 & H_2^T & \frac{2\eta}{\sqrt{6}} \end{pmatrix} . \tag{2.3.5}$$

In this matrix, there are 14 independent fields. They are (under $SU(2)_W$): a real triplet ϕ_a, a real singlet η, a complex singlet s, and two Higgs (complex) doublets H_1 and H_2. We effectively end up with a two-Higgs-doublet model (2HDM). The observed Higgs boson will correspond to a mixture of h_1 and h_2 inside two Higgs doublets $H_1 = H_{1/2} \supset \frac{1}{\sqrt{2}}\binom{0}{h_1}$ and $H_2 = H_{-1/2} \supset \frac{1}{\sqrt{2}}\binom{h_2}{0}$. Using the Nambu-Goldstone matrix, we can construct the low energy effective Lagrangian for the Higgs fields and all the other pNGBs.

2.3.2 The Gauge Sector

The SM electroweak gauge group $SU(2)_W \times U(1)_Y$ is embedded in $SU(6) \times U(1)_X$ with generators given by

$$SU(2)_W : \frac{1}{2}\begin{pmatrix} \sigma^a & 0 & 0 & 0 \\ 0 & 0 & 0 & 0 \\ 0 & 0 & -\sigma^{a*} & 0 \\ 0 & 0 & 0 & 0 \end{pmatrix}, \quad U(1)_Y : \frac{1}{2}\begin{pmatrix} 0 & 0 & 0 & 0 & 0 & 0 \\ 0 & 0 & 0 & 0 & 0 & 0 \\ 0 & 0 & 1 & 0 & 0 & 0 \\ 0 & 0 & 0 & 0 & 0 & 0 \\ 0 & 0 & 0 & 0 & 0 & 0 \\ 0 & 0 & 0 & 0 & 0 & -1 \end{pmatrix} + X\mathbf{I} \, . \tag{2.3.6}$$

The extra $U(1)_X$ factor accounts for the different hypercharges of the fermion representations but is not relevant for the bosonic fields. These generators belong to $Sp(6) \times U(1)_X$ and not broken by Σ_0. Using the Σ field, the Lagrangian for kinetic terms of Higgs boson comes from

$$\mathcal{L}_h = \frac{f^2}{4}\mathrm{tr}\left[(D_\mu \Sigma)(D^\mu \Sigma)^\dagger\right] + \cdots \, , \tag{2.3.7}$$

where D_μ is the electroweak covariant derivative. Expanding this, we get

$$\mathcal{L}_h = \frac{1}{2}(\partial_\mu h_1)(\partial^\mu h_1) + \frac{1}{2}(\partial_\mu h_2)(\partial^\mu h_2) + \frac{f^2}{2} g_W^2 \left(\sin^2 \frac{\sqrt{h_1^2 + h_2^2}}{\sqrt{2} f}\right)\left[W_\mu^+ W^{-\mu} + \frac{Z_\mu Z^\mu}{2\cos\theta_W}\right] \, . \tag{2.3.8}$$

The non-linear behavior of Higgs boson in CHM is apparent from the dependence of trigonometric functions.

The W boson acquires a mass when h_1 and h_2 obtain nonzero VEVs V_1 and V_2 of

$$m_W^2 = \frac{f^2}{2} g_W^2 \left(\sin^2 \frac{\sqrt{V_1^2 + V_2^2}}{\sqrt{2} f}\right) = \frac{1}{4} g_W^2 (v_1^2 + v_2^2) = \frac{1}{4} g_W^2 v^2, \tag{2.3.9}$$

where

$$v_i \equiv \sqrt{2} f \frac{V_i}{\sqrt{V_1^2 + V_2^2}} \sin \frac{\sqrt{V_1^2 + V_2^2}}{\sqrt{2} f} \approx V_i = \langle h_i \rangle \, . \tag{2.3.10}$$

The parameter that parametrizes the nonlinearity of the CHM is given by

$$\xi \equiv \frac{v^2}{f^2} = 2 \, \sin^2 \frac{\sqrt{V_1^2 + V_2^2}}{\sqrt{2} f} \, . \tag{2.3.11}$$

2.3.3 The Gauge Contribution to the pNGB Potential

SM gauge interactions explicitly break the $SU(6)$ global symmetry, so they contribute to the potential of the Higgs fields as well as other pNGBs. SM gauge bosons couple to pNGBs through the mixing with composite resonances:

$$\mathcal{L} = gW_{\mu,a}J_W^{\mu,a} + g'B_\mu J_Y^\mu \ . \tag{2.3.12}$$

The J_W and J_Y belong to the composite operators in an adjoint representation **35** of $SU(6)$. After the symmetry breaking, the composite operators are decomposed into **21** and **14** of $Sp(6)$. The masses of composite resonances of different representations of $Sp(6)$ are in general different and this will generate a potential for pNGBs at $\mathcal{O}(g^2)$. For $SU(2)_W$, it only breaks the global symmetry partially and generates mass terms for the two Higgs doublets and the scalar triplet ϕ:

$$SU(2)_W : \ (\text{for } H_1, H_2)\ c_w \frac{1}{16\pi^2}\frac{3g^2}{2}g_\rho^2 f^2 \approx c_w \frac{3}{32\pi^2}g^2 M_\rho^2, \tag{2.3.13}$$

$$(\text{for } \phi)\ c_w \frac{1}{16\pi^2}4g^2 g_\rho^2 f^2 \approx c_w \frac{1}{4\pi^2}g^2 M_\rho^2, \tag{2.3.14}$$

where $g_\rho f \sim M_\rho$ is the mass of the vector resonances ρ which act as the gauge boson partners to cut off the $SU(2)_W$ gauge loop contribution to the pNGB masses, and c_w is a $\mathcal{O}(1)$ constant. Similarly, for $U(1)_Y$, the interaction also breaks the global symmetry partially. It only generates mass terms for H_1, H_2:

$$U(1)_Y : \ c' \frac{1}{32\pi^2}g'^2 g_\rho^2 f^2 \approx c' \frac{1}{32\pi^2}g'^2 M_\rho^2, \tag{2.3.15}$$

where c' is also an $\mathcal{O}(1)$ constant.

Combining these two contributions, we get the mass terms of the pNGBs from the gauge contributions at the leading order as

$$\begin{aligned} &M_\eta^2 = M_s^2 = 0, \qquad\qquad M_\phi^2 = c_w \frac{1}{4\pi^2}g^2 M_\rho^2 \ , \\ &M_{H_1}^2 = M_{H_2}^2 = c_w \frac{3}{32\pi^2}g^2 M_\rho^2 + c' \frac{1}{32\pi^2}g'^2 M_\rho^2 \approx \left(\frac{3g^2 + g'^2(c'/c_w)}{8g^2}\right) M_\phi^2 \ . \end{aligned} \tag{2.3.16}$$

From the gauge contributions only, we expect that $M_\phi > M_{H_1} = M_{H_2}$ and they are below the symmetry breaking scale f. The $SU(2)_W \times U(1)_Y$ singlets s and η do not receive masses from the gauge interactions at this order, but they will obtain masses elsewhere which will be discussed later.

2.3.4 The Yukawa Sector

For partial compositeness, the elementary quarks and leptons couple to composite operators of $G = SU(6)$. To be able to mix with the elementary fermions, the representations of the composite operators must contain states with the same SM quantum numbers as the SM fermions. For our purpose, we can consider $\mathbf{6}$ and $\bar{\mathbf{6}}$ of $SU(6)$ as they don't split under the $Sp(6)$ subgroup. To account for the correct hypercharge, e.g., $q_L = 2_{1/6}$, $q_R = 1_{2/3}$ for up-type quarks and $q_R = 1_{-1/3}$ for down-type quarks, the composite operators need to carry additional charges under the $U(1)_X$ outside $SU(6)$ and the SM hypercharge is a linear combination of the $SU(6)$ generator $\mathrm{diag}(0, 0, 1/2, 0, 0, -1/2)$ and X. The composite operator as a $\mathbf{6}_{1/6}$ of $SU(6)$ (where the subscript $1/6$ denotes its $U(1)_X$ charge) can be decomposed under SM $SU(2)_W \times U(1)_Y$ gauge group as

$$O^i_{L,R} \sim \xi^i{}_\alpha Q^\alpha_{L,R} \sim \mathbf{6}_{1/6} = \mathbf{2}_{1/6} \oplus \mathbf{1}_{2/3} \oplus \bar{\mathbf{2}}_{1/6} \oplus \mathbf{1}_{-1/3}, \tag{2.3.17}$$

where $Q_{L,R}$ are the corresponding composite resonances. The composite states $Q_{L,R}$ created by these operators belong to the $\mathbf{6}$ representations of $Sp(6)$ and play the roles of SM fermion composite partners. For $SU(2)$, $\mathbf{2}$ and $\bar{\mathbf{2}}$ are equivalent and related by the ϵ tensor. We make the distinction to keep track of the order of the fermions in a doublet. We see that the composite states have the appropriate quantum numbers to mix with the SM quarks.

The left-handed elementary top quark can mix with either the first two components or the 4th and 5th components of the sextet. If we assume that it couples to the first two components, the mixing term can be expressed as

$$\lambda_L \bar{q}_{La} \Lambda^a{}_i O^i_R = \lambda_L \bar{q}_{La} \Lambda^a{}_i \left(\xi^i{}_\alpha Q^\alpha_R\right) \tag{2.3.18}$$

where a represents an $SU(2)_W$ index, and

$$(\Lambda)^a{}_i = \Lambda = \begin{pmatrix} 1 & 0 & 0 & 0 & 0 & 0 \\ 0 & 1 & 0 & 0 & 0 & 0 \end{pmatrix} \tag{2.3.19}$$

is the spurion which keeps track of the symmetry breaking.

To get the top Yukawa coupling, we couple the elementary right-handed quark to the $\bar{\mathbf{6}}_{1/6}$, which decomposes under $SU(2)_W \times U(1)_Y$ as

$$O'_{L,Rj} \sim \xi_j^{*\beta} \Sigma_{0\beta\alpha} Q^\alpha_{L,R} \sim \bar{\mathbf{6}}_{1/6} = \bar{\mathbf{2}}_{1/6} \oplus \mathbf{1}_{-1/3} \oplus \mathbf{2}_{1/6} \oplus \mathbf{1}_{2/3} \ . \tag{2.3.20}$$

The right-handed top quark mixes with the last component of the $\bar{\mathbf{6}}_{1/6}$, which can be written as

$$\lambda_{t_R} \bar{t}_R \Gamma_{t_R}{}^j O'_{Lj} = \lambda_{t_R} \bar{t}_R \Gamma_{t_R}{}^j \left(\xi_j^{*\beta} \Sigma_{0\beta\alpha} Q^\alpha_L \right), \tag{2.3.21}$$

where $\Gamma_{t_R} = (0\ 0\ 0\ 0\ 0\ 1)$ is the corresponding spurion.

Combining λ_L and λ_{t_R} couplings, we can generate the SM Yukawa coupling for the top quark (and similarly for other up-type quarks),[3]

$$\sim \lambda_L \lambda_{t_R} \bar{q}_{La} \Lambda^a{}_i \xi^i{}_\alpha \Sigma_0^{\alpha\beta} \xi_\beta^{Tj} \Gamma^\dagger_{t_R j} t_R = \lambda_L \lambda_{t_R} \bar{q}_{La} \Lambda^a{}_i \Sigma^{ij} \Gamma^\dagger_{t_R j} t_R \supset \lambda_L \lambda_{t_R} \left(\bar{q}_L H_2 t_R \right) \ . \tag{2.3.22}$$

Similarly, for the bottom quark (or in general down-type quarks), we can couple b_R to the third component of $\bar{\mathbf{6}}_{1/6}$ with the coupling λ_{b_R} and spurion $\Gamma_{b_R} = (0\ 0\ 1\ 0\ 0\ 0)$. This generates a bottom Yukawa coupling of

$$\sim \lambda_L \lambda_{b_R} \bar{q}_{La} \Lambda^a{}_i \xi^i{}_\alpha \Sigma_0^{\alpha\beta} \xi_\beta^{Tj} \Gamma^\dagger_{b_R j} b_R = \lambda_L \lambda_{b_R} \bar{q}_{La} \Lambda^a{}_i \Sigma^{ij} \Gamma^\dagger_{b_R j} b_R \supset \lambda_L \lambda_{b_R} \left(\bar{q}_L H_1 b_R \right) \ . \tag{2.3.23}$$

Alternatively, we could also couple the left-handed elementary quarks to $\bar{\mathbf{6}}_{1/6}$ and right-handed elementary quarks to $\mathbf{6}_{1/6}$,

$$\lambda'_L \bar{q}_{La} \epsilon^{ab} \Omega_b{}^i O'_{Ri} = \lambda'_L \bar{q}_{La} \epsilon^{ab} \Omega_b{}^i \left(\xi_i^{*\beta} \Sigma_{0\beta\alpha} Q^\alpha_R \right), \tag{2.3.24}$$

where

$$(\Omega)_a{}^i = \Omega = \begin{pmatrix} 1 & 0 & 0 & 0 & 0 & 0 \\ 0 & 1 & 0 & 0 & 0 & 0 \end{pmatrix} \tag{2.3.25}$$

[3]If we had coupled the left-handed quarks to the 4th and 5th components of O_R,

$$\tilde{\lambda}_L \bar{q}_{La} \epsilon^{ab} \Lambda'_{bi} O^i_R = \tilde{\lambda}_L \bar{q}_{La} \epsilon^{ab} \Lambda'_{bi} \left(\xi^i{}_\alpha Q^\alpha_R \right) + \text{h.c.},$$

with the spurion

$$(\Lambda')_{bi} = \Lambda' = \begin{pmatrix} 0 & 0 & 0 & 1 & 0 & 0 \\ 0 & 0 & 0 & 0 & 1 & 0 \end{pmatrix}.$$

The combination of $\tilde{\lambda}_L$ and λ_{t_R} would generate an up-type Yukawa coupling with H_1, $\sim \tilde{\lambda}_L \lambda_{t_R} \left(\bar{q}_L \tilde{H}_1 t_R \right)$.

and

$$\lambda'_{b_R}\bar{b}_R\Gamma'_{b_R j}O_L^j = \lambda'_{b_R}\bar{b}_R\Gamma'_{b_R j}\left(\xi^j{}_\alpha Q_L^\alpha\right), \tag{2.3.26}$$

where $\Gamma'_{b_R} = (0\ 0\ 0\ 0\ 0\ 1)$. Combining λ'_L and λ'_{b_R} coupling, we can generate the SM Yukawa coupling for bottom quark as

$$\sim \lambda'_L\lambda'_{b_R}\bar{q}_{La}\epsilon^{ab}\Omega_b{}^i\xi_i^{*\beta}\Sigma_{0\beta\alpha}\xi^{\dagger\alpha}{}_j\Gamma'^{*j}_{b_R}b_R = \lambda'_L\lambda'_{b_R}\bar{q}_{La}\epsilon^{ab}\Omega_b{}^i\Sigma^\dagger_{ij}\Gamma'^{*j}_{b_R}b_R \supset \lambda'_L\lambda'_{b_R}\left(\bar{q}_L\tilde{H}_2 b_R\right), \tag{2.3.27}$$

where $\tilde{H} \equiv \epsilon H^*$. In this case, the bottom mass also comes from VEV of H_2. Note that the combination of λ_L and λ'_{b_R} (or λ'_L and λ_{b_R}) does not generate the SM Yukawa coupling because it does not depend on Σ.

The lepton Yukawa couplings can be similarly constructed by coupling elementary leptons to $\mathbf{6}$ and $\bar{\mathbf{6}}$ with $X = -1/2$. In 2HDMs, if the SM quarks have general couplings to both Higgs doublets, large tree-level flavor-changing effects can be induced. To avoid them, it is favorable to impose the natural flavor conservation [21, 22] such that all up-type quarks couple to one Higgs doublet and all down-type quarks couple to either the same Higgs doublet (Type-I) or the other Higgs doublet (Type-II or flipped depending on the lepton assignment). We can obtain all different possibilities by choosing the partial compositeness couplings. For Type-II and flipped models, the $b \to s\gamma$ put strong constraints on the charged Higgs boson mass ($\gtrsim 600$ GeV) [38] which would require more tuning in the Higgs potential. Therefore, we will assume the Type-I 2HDM for the remaining of the paper, with the top Yukawa coupling coming from $\lambda_L\lambda_{t_R}$ and the bottom Yukawa coupling coming from $\lambda'_L\lambda'_{b_R}$.

2.3.5 The Top Contribution to the pNGB Potential

The partial compositeness coupling λ_L or λ_R individually cannot generate a potential for the pNGBs by itself, because the coupling Eq. (2.3.18) [or (3.3.6)] preserves an $SU(6)$ symmetry represented by the α index. Although α is an $Sp(6)$ index, without Σ_0, it cannot distinguish $Sp(6)$ from $SU(6)$. To generate a nontrivial Higgs potential, we need at least an insertion of Σ_0, which distinguishes $Sp(6)$ from $SU(6)$. It first arises through the combination of λ_L and λ_R in Eq. (3.3.7), which is just the top Yukawa coupling.

Therefore, the first nontrivial Higgs potential shows up at the next order, i.e., $\mathcal{O}(\lambda_L^2\lambda_R^2)$, as

$$\sim -\frac{N_c}{8\pi^2}\lambda_L^2\lambda_R^2 f^4 \left|(\Lambda)^a{}_i(\Gamma^*)_j\Sigma^{ij}\right|^2 \tag{2.3.28}$$

It gives a contribution to the H_2 squared-mass term of the order

$$\Delta M_{H_2}^2 \sim -\frac{N_c}{8\pi^2}\lambda_L^2\lambda_R^2 f^2 \sim -\frac{N_c}{8\pi^2}y_t^2 M_T^2 \ , \tag{2.3.29}$$

which is the same as the IR contribution from the top loop estimated in Eq. (2.1.3). Therefore, in this model, we avoid the potentially large $\mathcal{O}(\lambda^2)$ UV contribution and achieve the minimal tuning for the quadratic part of the Higgs potential.

2.4 Collective Higgs Quartics from Fermion Partial Compositeness Couplings

In the previous section, we show that in the $SU(6)/Sp(6)$ CHM the UV contribution from the strong dynamics to the Higgs potential is suppressed, minimizing the tuning of the quadratic term. However, we need some additional quartic Higgs potential to further reduce the tuning and to obtain a 125 GeV Higgs boson, as the IR contribution from the top quark loop to the Higgs quartic term is not enough. Generating a Higgs quartic coupling without inducing the corresponding quadratic term is the hallmark of the little Higgs mechanism. For example, in the original $SU(6)/Sp(6)$ little Higgs model [16], a Higgs quartic term from the collective symmetry breaking can be generated by gauging two copies of $SU(2)$, with generators given by

$$Q_1^a = \frac{1}{2}\begin{pmatrix} \sigma^a & 0 & 0 & 0 \\ 0 & 0 & 0 & 0 \\ 0 & 0 & 0_{2\times 2} & 0 \\ 0 & 0 & 0 & 0 \end{pmatrix} \quad \text{and} \quad Q_2^a = -\frac{1}{2}\begin{pmatrix} 0_{2\times 2} & 0 & 0 & 0 \\ 0 & 0 & 0 & 0 \\ 0 & 0 & \sigma^{a*} & 0 \\ 0 & 0 & 0 & 0 \end{pmatrix} \tag{2.4.1}$$

and gauge couplings g_1 and g_2. The two $SU(2)$'s are broken down to the diagonal $SU(2)_W$ by the Σ VEV. The potential for the pNGBs generated by the two gauge couplings takes the form

$$g_1^2 f^2 \left|s + \frac{i}{2f}\tilde{H_2}^\dagger H_1\right|^2 + g_2^2 f^2 \left|s - \frac{i}{2f}\tilde{H_2}^\dagger H_1\right|^2 . \tag{2.4.2}$$

The g_1^2 term preserves the $SU(4)$ symmetry of the $3,4,5,6$ entries which contains the shift symmetry of H_1 and H_2. If only the first term of the potential exists, the $\tilde{H_2}^\dagger H_1$ dependence can be absorbed into s by a field redefinition and the term just corresponds to a mass term for s. Similarly, the g_2^2 term preserves the $SU(4)$ symmetry of the $1,2,3,6$ entries under which H_1 and H_2 remain as Nambu-Goldstone bosons, but with a different shift symmetry. The combination of both terms breaks either of the shift symmetries, and a quartic Higgs potential is generated after integrating out the s field,

$$\lambda \left| \tilde{H_2}^\dagger H_1 \right|^2 \quad \text{with} \quad \lambda = \frac{g_1^2 g_2^2}{g_1^2 + g_2^2} \ . \tag{2.4.3}$$

The possibility of gauging two copies of $SU(2)$ gauge group is subject to the strong experimental constraints on W' and Z'. We would like to generate the quartic Higgs potential without introducing additional elementary fields to the $SU(6)/Sp(6)$ CHM, so we will consider the collective symmetry breaking from the interactions between the elementary fermions and the resonances of the strong dynamics.

From the discussion of the previous section, we see that the elementary quark doublets may couple to composite operators of $SU(6)$ representations $\mathbf{6}$ and/or $\bar{\mathbf{6}}$, and each contains two doublets of the same SM quantum numbers:

$$\mathbf{6}_{1/6} = \mathbf{2}_{1/6} \oplus \mathbf{1}_{2/3} \oplus \bar{\mathbf{2}}_{1/6} \oplus \mathbf{1}_{-1/3}, \tag{2.4.4a}$$

$$\bar{\mathbf{6}}_{1/6} = \bar{\mathbf{2}}_{1/6} \oplus \mathbf{1}_{-1/3} \oplus \mathbf{2}_{1/6} \oplus \mathbf{1}_{2/3} \ . \tag{2.4.4b}$$

Both operators can create the same resonances which belong to $\mathbf{6}$ of the $Sp(6)$ group.

Now consider two elementary quark doublets couple to the first two components of the composite operators of $\mathbf{6}$ and $\bar{\mathbf{6}}$ respectively, while both representations contain the same resonances:

$$\lambda_L \bar{q}_{La} \Lambda^a{}_i O_R^i = \lambda_L \bar{q}_{La} \Lambda^a{}_i \left(\xi^i{}_\alpha Q_R^\alpha \right), \tag{2.4.5}$$

where

$$(\Lambda)^a{}_i = \Lambda = \begin{pmatrix} 1 & 0 & 0 & 0 & 0 & 0 \\ 0 & 1 & 0 & 0 & 0 & 0 \end{pmatrix} \ , \tag{2.4.6}$$

and

$$\lambda'_L \bar{q}'_{La} \epsilon^{ab} \Omega_b{}^i O'_{Ri} = \lambda'_L \bar{q}'_{La} \epsilon^{ab} \Omega_b{}^i \left(\xi_i^{*\beta} \Sigma_{0\beta\alpha} Q_R^\alpha \right), \tag{2.4.7}$$

where

$$(\Omega)_a{}^i = \Omega = \begin{pmatrix} 1 & 0 & 0 & 0 & 0 & 0 \\ 0 & 1 & 0 & 0 & 0 & 0 \end{pmatrix} . \tag{2.4.8}$$

The combination of the two interactions breaks the $SU(6)$ global symmetry explicitly but preserves an $SU(4)$ symmetry of the $3, 4, 5, 6$ entries. It leads to a potential for the pNGBs at $\mathcal{O}(\lambda_L^2 \lambda_L'^2)$ of the form

$$[(\Lambda)^a{}_i (\Omega^*)^b{}_j \Sigma^{ij}][(\Omega)_b{}^m (\Lambda^*)_a{}^n \Sigma^*_{mn}] , \tag{2.4.9}$$

which can easily be checked by drawing a one-loop diagram, with q_L, q'_L, Q_R running in the loop.

After expanding it we obtain

$$\sim \frac{N_c}{8\pi^2} \lambda_L^2 \lambda_L'^2 f^4 \left| (\Lambda)^a{}_i (\Omega^*)^b{}_j \Sigma^{ij} \right|^2 \quad \to \quad \frac{N_c}{4\pi^2} \lambda_L^2 \lambda_L'^2 f^2 \left| s + \frac{i}{2f} \tilde{H}_2{}^\dagger H_1 \right|^2 . \tag{2.4.10}$$

(The factor of 2 comes from the trace which reflects the degrees of freedom running in the loop, as both elementary fermions are doublets.) This is one of the terms needed for the collective symmetry breaking. The coefficient is estimated from the dimensional analysis. Notice that we have chosen different (generations of) elementary quark doublets, q_L and q'_L in the two couplings. If q_L and q'_L were the same, the loop can be closed at $\mathcal{O}(\lambda_L \lambda'_L)$ and a large s tadpole term and Higgs quadratic term will be generated,

$$\sim \frac{N_c}{8\pi^2} \lambda_L \lambda'_L f^4 \left(\epsilon_{ab} (\Lambda)^a{}_i (\Omega^*)^b{}_j \Sigma^{ij} \right) \quad \to \quad \frac{N_c}{4\pi^2} \lambda_L \lambda'_L g_\psi^2 f^3 \left(s + \frac{i}{2f} \tilde{H}_2{}^\dagger H_1 \right) . \tag{2.4.11}$$

Such a term is actually needed for a realistic EWSB, but it would be too large if it were generated together with Eq. (2.4.10) that will produce the Higgs quartic term. It can be generated of an appropriate size in a similar way involving some other different fermions and composite operators with smaller couplings.

The way that the mass term for s can be generated without the tadpole term can be understood from the symmetry point of view. In addition to the $SU(2)_W \times U(1)_Y$, the Σ_0 preserves a global $U(1)$ Peccei-Quinn (PQ) [19] subgroup of $Sp(6)$. This global $U(1)$

symmetry corresponds to the unbroken generator

$$U(1)_{PQ} : \frac{1}{2}\begin{pmatrix} 1 & 0 & 0 & 0 & 0 & 0 \\ 0 & 1 & 0 & 0 & 0 & 0 \\ 0 & 0 & 0 & 0 & 0 & 0 \\ 0 & 0 & 0 & -1 & 0 & 0 \\ 0 & 0 & 0 & 0 & -1 & 0 \\ 0 & 0 & 0 & 0 & 0 & 0 \end{pmatrix}, \tag{2.4.12}$$

under which s has charge 1, both H_1, H_2 have charge 1/2, and the rest of pNGBs have charge 0. The s mass term is invariant under $U(1)_{PQ}$ while the tadpole term has charge 1 so it will not be induced if the interactions can preserve the $U(1)_{PQ}$ symmetry. On the other hand, the composite operators in Eqs. (3.7.13), (3.7.15) have the following PQ charges for their components (assuming that they don't carry an additional overall charge),

$$\mathbf{6}_0 = \mathbf{2}_{1/2} \oplus \mathbf{1}_0 \oplus \bar{\mathbf{2}}_{-1/2} \oplus \mathbf{1}_0, \tag{2.4.13a}$$

$$\bar{\mathbf{6}}_0 = \bar{\mathbf{2}}_{-1/2} \oplus \mathbf{1}_0 \oplus \mathbf{2}_{1/2} \oplus \mathbf{1}_0, \tag{2.4.13b}$$

where the subscript here denotes the PQ charge instead of the X charge. We see that q_L and q'_L couple to components of different PQ charges. If q_L and q'_L are different, it is possible to assign PQ charges, i.e., 1/2 for q_L and $-1/2$ for q'_L, so that the interactions Eqs. (3.7.13), (3.7.15) preserve the PQ symmetry and the s tadpole term will not be generated. If q_L and q'_L are the same, then there is no consistent charge assignment that can preserve the PQ symmetry, and hence the s tadpole term can be induced. Furthermore, if different generations of quarks carry different PQ charges, The $U(1)_{PQ}$ preserving interactions will not induce flavor-changing neutral currents (FCNC) as they violate the PQ symmetry.

The second term required in realizing the collective symmetry breaking can be generated similarly by a different set of quarks (or leptons). They should couple to the 4th

and 5th components of the $\mathbf{6}$ and $\bar{\mathbf{6}}$ operators through the spurions

$$(\Lambda')_{ai} = \begin{pmatrix} 0 & 0 & 0 & 1 & 0 & 0 \\ 0 & 0 & 0 & 0 & 1 & 0 \end{pmatrix} \quad \text{and} \quad (\Omega')^{ai} = \begin{pmatrix} 0 & 0 & 0 & 1 & 0 & 0 \\ 0 & 0 & 0 & 0 & 1 & 0 \end{pmatrix}, \tag{2.4.14}$$

which preserve the $SU(4)$ symmetry of the 1,2,3,6 entries.

The combination of Λ' and Ω' can then introduce the potential

$$\sim \frac{N_c}{8\pi^2}\lambda_L^2\lambda_L'^2 f^4 \left|(\Lambda')_{ai}(\Omega'^*)_{bj}\Sigma^{ij}\right|^2 \quad \to \quad \frac{N_c}{4\pi^2}\lambda_L^2\lambda_L'^2 f^2 \left|s - \frac{i}{2f}\tilde{H_2}^\dagger H_1\right|^2, \tag{2.4.15}$$

which provides the other term needed for the collective symmetry breaking.

To generate all the terms required for the Higgs quartic potential from collective symmetry breaking, we need to use several different quarks and/or leptons, with different PQ charge assignments. As we mentioned earlier, we also need some smaller PQ-violating couplings between the elementary fermions and the composite operators, in order to generate a proper-sized $\tilde{H_2}^\dagger H_1$ term,

$$m_{12}^2 \sim \frac{N_c}{8\pi^2}\lambda_L\lambda_L''g_\psi^2 f^2, \tag{2.4.16}$$

where λ_L'' represents the smaller $U(1)_{PQ}$ violating coupling. A more detailed coupling assignment for a realistic model is presented in Appendix B. With all the collective symmetry breaking interactions discussed above, we obtain a pNGB potential,

$$c_{k\ell}\frac{N_c}{4\pi^2}\lambda_{k_L}^2\lambda_{\ell_L}'^2 f^2 \left|s + \frac{i}{2f}\tilde{H_2}^\dagger H_1\right|^2 + c_{mn}\frac{N_c'}{4\pi^2}\lambda_{m_L}^2\lambda_{n_L}'^2 f^2 \left|s - \frac{i}{2f}\tilde{H_2}^\dagger H_1\right|^2, \tag{2.4.17}$$

where $c_{k\ell}$, c_{mn} are $\mathcal{O}(1)$ constants depending on the UV completion,[4] and the indices k, ℓ, m, n here label different fermions. After integrating out the massive s field, we obtain a quartic term for the Higgs doublets (take $N_c, N_c' = 3$) as

$$\lambda_{12}\left|\tilde{H_2}^\dagger H_1\right|^2 \quad \text{with} \quad \lambda_{12} = \frac{3}{4\pi^2}\frac{c_{k\ell}c_{mn}\lambda_{k_L}^2\lambda_{\ell_L}'^2\lambda_{m_L}^2\lambda_{n_L}'^2}{c_{k\ell}\lambda_{k_L}^2\lambda_{\ell_L}'^2 + c_{mn}\lambda_{m_L}^2\lambda_{n_L}'^2}. \tag{2.4.18}$$

[4] In the Discrete CHMs [26] or UV completions with Weinberg's sum rules [27, 28] for the MCHM, the analogous finite quartic potentials have the coefficient $c \sim 2$.

Assuming $\lambda_{k_L}\lambda'_{\ell_L} \sim \lambda_{m_L}\lambda'_{n_L}$ and $c_{k\ell} \sim c_{mn} \sim 2$, then in our estimate

$$\lambda_{12} \sim \frac{3}{4\pi^2}\lambda_{k_L}^2\lambda_{\ell_L}'^2 \ . \tag{2.4.19}$$

Including this quartic term, the coefficients of the Higgs potential in this model are estimated to be

$$\hat{\alpha} \sim \frac{3}{16\pi^2}\lambda_{t_L}^2\lambda_{t_R}^2 f^2, \quad \hat{\beta} \sim \frac{3}{16\pi^2}\lambda_{k_L}^2\lambda_{\ell_L}'^2 f^2 \ . \tag{2.4.20}$$

Therefore we can further improve upon the minimal tuning ($\hat{\alpha} \sim \hat{\beta}$) case by requiring

$$\lambda'_L > \lambda_{t_R} \implies \hat{\beta} > \hat{\alpha} \ . \tag{2.4.21}$$

Of course, however, $\hat{\beta}$ can not be arbitrarily large because it is determined by the Higgs boson mass from Eq. (2.2.4). The required numerical parameters will be discussed in the next section.

2.5 The Higgs Potential in the 2HDM

The $SU(6)/Sp(6)$ model contains two Higgs doublets. To analyze the EWSB and the Higgs boson masses, we need to consider the Higgs potential in a 2HDM. A review of 2HDM can be found in Ref. [29]. The other pNGBs do not affect the Higgs potential much (they either are heavy or couple mostly quadratically to the Higgs doublets), so we will postpone their discussion to the next section. The Higgs potential in our model can be parameterized as

$$\begin{aligned} V(H_1, H_2) = {} & m_1^2 H_1^\dagger H_1 + m_2^2 H_2^\dagger H_2 - m_{12}^2 \left(\tilde{H_2}^\dagger H_1 + \text{h.c.} \right) \\ & + \frac{\lambda_1}{2}\left(H_1^\dagger H_1\right)^2 + \frac{\lambda_2}{2}\left(H_2^\dagger H_2\right)^2 + \lambda_{12}\left|\tilde{H_2}^\dagger H_1\right|^2 \ . \end{aligned} \tag{2.5.1}$$

Notice that, in CHMs, due to the non-linearity of pNGBs, the Higgs potential should include trigonometric functions instead of polynomials. Also, to match the potential here to the SM Higgs potential, an additional factor of $\cos\langle\theta\rangle$ will appear. However, since the deviation is strongly constrained by Higgs coupling measurements, we will take $\langle\theta\rangle \ll 1$ and expand $\sin x \sim x$ in the following discussion for simplicity.

In the 2HDM potential (2.5.1), both Higgs doublets develop nonzero VEVs. Denote the VEVs of H_1 and H_2 to be v_1 and v_2 respectively, and their ratio is defined as $\tan\beta \equiv v_2/v_1$. The total VEV v satisfies

$$v^2 = v_1^2 + v_2^2 = v^2\cos^2\beta + v^2\sin^2\beta = (246\text{ GeV})^2 \ . \tag{2.5.2}$$

H_2 couples to the top quark and gets a large negative loop-induced contribution to its quadratic term, so it is natural to expect $v_2 > v_1$. On the other hand, the main quartic term coming from the collective symmetry breaking is λ_{12}. To have a large enough effective quartic term for the 125 GeV Higgs boson, we do not want either $\sin\beta\,(\equiv s_\beta)$ or $\cos\beta\,(\equiv c_\beta)$ to be too small. The current constraints [24, 31, 32] have ruled out the region $\tan\beta$ near 1, so we will consider a benchmark with a medium value,

$$\tan\beta \sim 3 \ . \tag{2.5.3}$$

Also, the light neutral eigenstate should be close to the SM Higgs boson, which imposes some conditions on the parameters in the Higgs potential (2.5.1). In Subsec. 2.5.1, we first discuss the quadratic potential, which will determine the spectrum of additional Higgs bosons in this model. Then, we will discuss the alignment issue in Subsec. 2.5.2 and the corresponding values of the quartic terms in the Higgs potential.

2.5.1 Estimating the Mass Terms

The experimental constraints require that the 2HDM should be close to the alignment limit ($\beta - \alpha = \pi/2$) [33, 34, 35, 36], where α is the mixing angle between the mass eigenstates of the two CP-even Higgs boson and the corresponding components in H_1, H_2 (after removing the VEVs),

$$h = -h_1\,\sin\alpha + h_2\,\cos\alpha \ . \tag{2.5.4}$$

To simplify the discussion of the quadratic terms, we assume that the alignment holds approximately,

$$h \approx h_1\,\cos\beta + h_2\,\sin\beta = h_{\rm SM}, \tag{2.5.5}$$

then we can calculate the SM Higgs potential by the transformation

$$\begin{pmatrix} H_1 \\ H_2 \end{pmatrix} = \begin{pmatrix} \cos\beta & -\sin\beta \\ \sin\beta & \cos\beta \end{pmatrix} \begin{pmatrix} H_{\rm SM} \\ H_{\rm heavy} \end{pmatrix} \ . \tag{2.5.6}$$

The potential of the light SM Higgs doublet becomes (keeping the terms with $H_{\rm SM}$ only and rewriting $H_{\rm SM} \to H$)

$$\begin{aligned} V(H) = & \left(m_1^2 \cos^2\beta + m_2^2 \sin^2\beta - 2m_{12}^2 \sin\beta\cos\beta\right) |H|^2 \\ & + \left(\frac{\lambda_1}{2}\cos^4\beta + \frac{\lambda_2}{2}\sin^4\beta + \lambda_{12}\sin^2\beta\cos^2\beta\right) |H|^4 \ . \end{aligned} \tag{2.5.7}$$

Matching the quadratic term with the SM Higgs potential implies that

$$-\mu^2 = m_1^2 \cos^2\beta + m_2^2 \sin^2\beta - 2m_{12}^2 \sin\beta\cos\beta \approx -\left(88 \text{ GeV}\right)^2 \ . \tag{2.5.8}$$

As shown in the previous section, these mass terms get contributions from different sources: m_1 comes from gauge contributions, m_2 gets an additional large negative contribution from the top quark besides the gauge contributions, and m_{12} comes from the PQ-violating interactions. No natural cancellation among the three terms in Eq. (2.5.8) is warranted. Therefore, the absolute values of all three terms should be of the same order as μ^2 to avoid tuning. For example, for $\tan\beta = 3$ Eq. (2.5.8) can be satisfied by $m_1^2 \sim \left(360 \text{ GeV}\right)^2$, $m_2^2 \sim \left(120 \text{ GeV}\right)^2$, and $m_{12}^2 \sim \left(210 \text{ GeV}\right)^2$ without strong cancellations among the three terms. These numbers are based on the alignment approximation. More accurate values need to include the whole 2HDM potential and will be given after the discussion of the quartic terms.

2.5.2 Estimating the Quartic Terms

There are three quartic couplings in the Higgs potential (2.5.1): λ_1, λ_2, and λ_{12}. The effective quartic coupling for the light Higgs, which can be seen from Eq. (2.5.7), is a combination of the three quartic couplings and $\tan\beta$. To obtain a 125 GeV Higgs boson we need

$$\frac{\lambda_1}{2}\cos^4\beta + \frac{\lambda_2}{2}\sin^4\beta + \lambda_{12}\sin^2\beta\cos^2\beta \approx 0.13 \ . \tag{2.5.9}$$

λ_1 is mainly induced by the SM gauge loops and is expected to be small. λ_2 receives the top quark loop contribution,

$$\lambda_2 \sim \frac{3y_t^4}{4\pi^2} \ln \frac{M_T}{v} \sim 0.1. \tag{2.5.10}$$

This implies that we need λ_{12} which comes from the collective symmetry breaking to satisfy

$$\lambda_{12} \mathrm{s}_\beta^2 \mathrm{c}_\beta^2 \sim 0.1 \quad \Rightarrow \quad \lambda_{12} \sim 1 \quad \text{for } \tan\beta = 3 \, . \tag{2.5.11}$$

If it arises from the collective quartic term obtained in Eq. (2.4.19), it corresponds to

$$\lambda_L \lambda'_L \sim 3.6 \quad \Rightarrow \quad \sqrt{\lambda_L \lambda'_L} \sim 1.9 \, . \tag{2.5.12}$$

These couplings between the elementary states and composite operators are quite large. However, the smallness of SM Yukawa couplings can be obtained by small λ_R couplings. There are other experimental constraints with these large λ_L couplings, which will be discussed in the following sections.

We have been assuming that the 2HDM potential is approximately in the alignment regime. Let us go back to check how well the alignment can be achieved. A simple way to achieve the alignment is the decoupling limit where the extra Higgs bosons are heavy. However, this would require more tuning in the Higgs mass parameters. In our model $\lambda_{12} > \lambda_2, \lambda_1$. Under this condition, we need $\tan\beta \sim 1$ to achieve the exact alignment if the extra Higgs bosons are not too heavy. This is not compatible with the experiment constraints. Therefore we expect some misalignment and need to check whether the misalignment can be kept within the experimental constraints.

Solving the eigenvalue equations, we can get the following equations for the factor $c_{\beta-\alpha}$,

$$c_{\beta-\alpha} = \frac{1}{M_A^2 \tan\beta} \left(\lambda_1 v_1^2 \left(\frac{-s_\alpha}{c_\beta} \right) + \lambda_{12} v_2^2 \left(\frac{c_\alpha}{s_\beta} \right) - M_h^2 \left(\frac{-s_\alpha}{c_\beta} \right) \right), \tag{2.5.13}$$

$$= \frac{1}{M_A^2 \cot\beta} \left(-\lambda_{12} v_1^2 \left(\frac{-s_\alpha}{c_\beta} \right) - \lambda_2 v_2^2 \left(\frac{c_\alpha}{s_\beta} \right) + M_h^2 \left(\frac{c_\alpha}{s_\beta} \right) \right). \tag{2.5.14}$$

As the misalignment should be small, to estimate its size, we can assume that the mass eigenstates of the 2HDM are near alignment, which satisfy $(-s_\alpha, c_\alpha) \approx (c_\beta, s_\beta)$ approxi-

mately for the right-handed side. We then have

$$c_{\beta-\alpha} \approx \frac{1}{M_A^2 \tan\beta} \left(\lambda_1 v_1^2 + \lambda_{12} v_2^2 - M_h^2\right), \tag{2.5.15}$$

$$\approx \frac{1}{M_A^2 \cot\beta} \left(-\lambda_{12} v_1^2 - \lambda_2 v_2^2 + M_h^2\right). \tag{2.5.16}$$

Consider the benchmark values

$$\tan\beta \approx 3, \quad \lambda_{12} \approx 1, \quad \text{and} \quad M_A \approx 380 \text{ GeV}, \tag{2.5.17}$$

where the M_A value is chosen to keep the misalignment small and to evade the direct search in the $A^0 \to hZ$ decay channel at the LHC [24]. The equations for $c_{\beta-\alpha}$ becomes

$$c_{\beta-\alpha} \approx \ 0.014\lambda_1 + 0.090 \ \approx \ 0.199 - 1.132\lambda_2 \ . \tag{2.5.18}$$

Since λ_1 in this model is small, we have $c_{\beta-\alpha} \approx 0.090$ which parametrizes the deviation from the alignment. The misalignment will have a direct consequence on Higgs physics and will be discussed in the following sections. The most relevant deviation, the ratio of Higgs to vector bosons coupling to SM coupling, is proportional to $s_{\beta-\alpha} \approx \ 0.996$ and should still be safe.

Eq. (2.5.18) also implies that λ_2 needs to be ≈ 0.1, which is consistent with the estimate from the top quark loop contribution Eq. (2.5.10). To sum up, the three quartic couplings in our 2HDM potential take values

$$\lambda_{12} \approx 1 \quad \gg \quad \lambda_2 \approx 0.1 \quad \gg \quad \lambda_1 \ . \tag{2.5.19}$$

2.5.3 A Realistic Higgs Potential

So far, all numbers in the above discussion are estimations based on simplified approximations. In a realistic benchmark model, the exact values can be solved by directly diagonalizing the mass matrix. To reproduce the correct Higgs boson mass $M_h = 125$ GeV and small enough $c_{\beta-\alpha}$ with fixed $\tan\beta \approx 3$ and $\lambda_{12} \approx 1$, we choose the following values as a reference for our study:

$$\tan\beta \approx 3.0, \quad \lambda_{12} \approx 1.0, \quad \lambda_2 \approx 0.12, \quad \text{and} \quad M_A \approx 380 \text{ GeV} \ . \tag{2.5.20}$$

λ_1 is irrelevant as long as it is small so we don't set its value. The value of λ_2 is set by producing the correct Higgs boson mass.

With these numbers, we can diagonalize the mass matrix and get the mixing angle α and the misalignment $\beta - \alpha$ as

$$s_\alpha = -0.215, \quad c_\alpha = 0.977 \quad \Longrightarrow \quad c_{\beta-\alpha} = 0.1049, \quad s_{\beta-\alpha} = 0.9945 \ . \tag{2.5.21}$$

The eigenvalues of the matrix give the masses of the CP-even neutral scalar bosons as

$$M_h \approx 125 \text{ GeV} \quad \text{and} \quad M_H \approx 370 \text{ GeV} \ . \tag{2.5.22}$$

The complete spectrum will be discussed in the next section.

After we obtain the quartic couplings, we can go back to determine the mass terms. The value of M_A is chosen to satisfy the experimental constraint. It also gives the value of m_{12} based on the relation

$$m_{12}^2 = M_A^2 s_\beta c_\beta \sim (210 \text{ GeV})^2 \ . \tag{2.5.23}$$

Given the values of all the quartic couplings and m_{12}, we can obtain the other mass terms

$$m_1^2 = 3m_{12}^2 - \frac{1}{2}\lambda_1 v_1^2 - \frac{1}{2}\lambda_{12} v_2^2 \sim (320 \text{ GeV})^2 \,, \tag{2.5.24}$$

$$m_2^2 = \frac{1}{3}m_{12}^2 - \frac{1}{2}\lambda_2 v_2^2 - \frac{1}{2}\lambda_{12} v_1^2 \sim (90 \text{ GeV})^2 \ . \tag{2.5.25}$$

These numbers will serve as a benchmark for our phenomenological studies.

Assuming that these masses arise dominantly from the loop contributions discussed in the previous sections, we can also estimate the masses of the composite states in the CHM,

$$m_1^2 = \frac{3}{32\pi^2} g^2 M_\rho^2 \sim (320 \text{ GeV})^2 \,, \tag{2.5.26}$$

$$m_2^2 = \frac{3}{32\pi^2} g^2 M_\rho^2 - \frac{3}{8\pi^2} y_t^2 M_T^2 \sim (90 \text{ GeV})^2 \,, \tag{2.5.27}$$

$$m_{12}^2 = \frac{N_c}{8\pi^2} \lambda_L \lambda_L'' g_\psi^2 f^2 \sim (210 \text{ GeV})^2 \ , \tag{2.5.28}$$

where we have ignored the small $U(1)$ gauge contribution and taken $c_w \sim 1$. The m_1^2 equation gives the mass of the gauge boson partners $M_\rho \sim 5$ TeV. In the m_2^2 equation,

the top loop contribution needs to cancel the positive gauge contribution $(320\text{ GeV})^2$ to produce a $(90\text{ GeV})^2$ term. From that, the top partner is estimated to be around $M_T \sim 1.6$ TeV. This corresponds to an $\mathcal{O}(10\%)$ tuning between the gauge contribution and the top contribution, but it is hard to avoid given the experimental constraints on the top partner mass. The desired size of m_{12}^2 can be achieved by a suitable choice of the PQ-violating coupling λ_L'' which is a free parameter in this model.

2.6 The Spectrum of pNGBs

After discussing the Higgs potential from the naturalness consideration, we are ready to provide the estimates of masses of all other pNGBs, based on the benchmark point alluded in the previous section.

2.6.1 The Second Higgs Doublet

The 2HDM potential has been discussed in the previous section. In addition to the SM-like 125 GeV Higgs boson, there is one more CP-even neutral scalar H^0, a CP-odd neutral scalar A^0, and a complex charge scalar $H^\pm$. Their masses from the Higgs potential (2.5.1) are

$$\begin{aligned} M_A^2 &= \frac{m_{12}^2}{s_\beta c_\beta}\,, \qquad\qquad M_{H^\pm}^2 = M_A^2 - \frac{1}{2}\lambda_{12}v^2, \\ M_{h,H}^2 &= \frac{1}{2}\left(M_A^2 \pm \sqrt{M_A^4 - 8M_{H^\pm}^2\lambda_{12}v^2 s_\beta^2 c_\beta^2}\,\right), \end{aligned} \tag{2.6.1}$$

which results in a spectrum $M_A > M_H > M_{H^\pm}$. This is different from the 2HDM spectrum of the MSSM because the dominant quartic term is λ_{12}. For the benchmark point of the previous section, the three masses are estimated to be

$$M_A \sim 380\text{ GeV}, \quad M_H \sim 370\text{ GeV}, \quad \text{and} \quad M_{H^\pm} \sim 340\text{ GeV}. \tag{2.6.2}$$

2.6.2 Other pNGBs

In addition to the two doublets, the pNGBs also include a real triplet ϕ, a real singlet η, and a complex singlet s. The triplet obtains its mass from the gauge loop as shown in Eq. (2.3.14). For $M_\rho \sim 5$ TeV, it gives

$$M_\phi^2 = c_w \frac{1}{4\pi^2} g^2 M_\rho^2 \sim (500\text{ GeV})^2\,. \tag{2.6.3}$$

The singlets do not receive mass contributions from SM gauge interactions. The complex singlet s obtains its mass from the collective symmetry breaking mechanism (2.4.17),

$$M_s^2 = c_{k\ell}\frac{N_c}{4\pi^2}\lambda_{k_L}^2\lambda_{\ell_L}'^2 f^2 + c_{mn}\frac{N_c'}{4\pi^2}\lambda_{m_L}^2\lambda_{n_L}'^2 f^2 \geq 4\lambda_{12}f^2 \approx (2f)^2, \tag{2.6.4}$$

which is expected to be at the TeV scale. There is also a tadpole term from the PQ-violating potential, which will introduce a small VEV for s,

$$\langle s\rangle \sim \frac{m_{12}^2 f}{M_s^2} \leq \frac{(210\text{ GeV})^2}{4f} \sim \mathcal{O}(10\text{ GeV}). \tag{2.6.5}$$

It will have little effect on the mass of the singlet.

Finally, the real singlet η does not get a mass at the leading order but it couples quadratically to the Higgs doublets (e.g., from Eq. (3.7.8)), so it can still become massive after the Higgs doublets develop nonzero VEVs. Through Eq. (3.7.8), η receives a mass

$$M_\eta^2 \sim \frac{3}{8\pi^2}y_t^2 M_T^2 \cdot \left(\frac{v}{f}\right)^2 \implies M_\eta \sim \left(\frac{M_T}{f}\right) 48\text{ GeV}. \tag{2.6.6}$$

For naturalness, a relatively light top partner is preferred. On the other hand, the experimental constraints require η to be heavier than half of Higgs boson mass to avoid large Higgs decay rate to the $\eta\eta$ channel. We expect a light singlet scalar around 100 GeV, which can be the lightest composite state in the spectrum.

2.7 Collider Searches

In CHMs, there will be new composite states of scalars, fermions, and vectors near or below the compositeness scale. The detailed spectrum and quantum numbers depend on the specific realizations of the CHMs. In this section, we study the collider searches of and constraints on these new states in the $SU(6)/Sp(6)$ model discussed in this paper.

2.7.1 The Second Higgs Doublet

Under the requirement of naturalness, the second Higgs doublet is expected to be among the lightest states of the new resonances and could be the first sign of this model. In the Type-II 2HDM, the flavor-changing process $b \to s\gamma$ has put strong constraints on the charged Higgs mass to be above 600 GeV, which would require more tuning in the

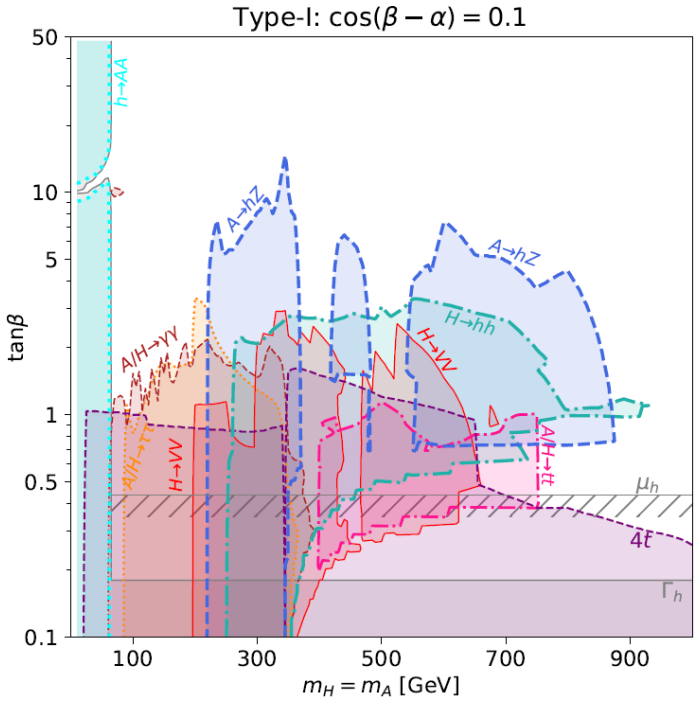

Fig. 2.1: Constraints on extra neutral Higgs bosons in a Type-I 2HDM with a small misalignment $c_{\beta-\alpha} = 0.1$. This summary plot is taken from Ref. [24].

Higgs potential. Therefore, we focus on the Type-I 2HDM scenario. As explained in the previous section, we will consider a relatively small $\tan\beta \sim 3$ with a small misalignment $c_{\beta-\alpha} \sim 0.1$.

The direct searches can be divided into two categories – charged Higgs bosons $H^{\pm}$ and neutral Higgs bosons H^0, A^0. In the Type-I 2HDM with a small misalignment, neutral Higgs bosons to fermion couplings are characterized by a factor $-s_\alpha/s_\beta \sim 1/4$ and the charged Higgs boson to fermion couplings are characterized by $c_\beta/s_\beta \sim 1/3$. Comparing to neutral Higgs bosons, the charged Higgs boson searches give a more reliable constraint on $\tan\beta$ because it doesn't depend on the mixing angle α.

The charged Higgs boson is searched by its decays to SM fermions. For $M_{H^\pm} \lesssim m_t$, the strongest constraint comes from decaying to $\tau\nu$ [37, 38]. Interpreted in the Type-I model, it excludes $\tan\beta < 14$ for $M_{H^\pm} \sim 100$ GeV and $\tan\beta < 3$ for $M_{H^\pm}$ up to 150 GeV [39]. For a heavier charged Higgs boson, the main constraint comes from the decay to tb, which rules out $\tan\beta \lesssim 2$ for $M_{H^\pm}$ in the range of 200-400 GeV, and becomes weaker for larger $M_{H^\pm}$ [31, 32].

For neutral Higgs bosons, there are multiple decay channels being searched. For light states below the $t\bar{t}$ threshold, they can be searched by $H/A \to \tau\tau$ [40, 41] and $H \to \gamma\gamma$ [42, 43] decays. For heavier states, the decay to $t\bar{t}$ becomes accessible and dominant. The searches of $H/A \to t\bar{t}$ has been done at CMS and ATLAS [44, 45]. These searches typically constrain $\tan\beta \gtrsim 1-2$ up to $M_{H/A} \sim 750$ GeV. When there is misalignment as expected in this model, there are also additional decay channels of these neutral scalars which give important constraints. These include $H/A \to WW$ [46, 47] and ZZ [48, 49], $H \to hh$ [50, 51], and $A \to hZ$ [52, 53]. The $A \to hZ$ and $H \to hh$ turn out to be most constraining for the region that we are interested in. The $A \to hZ$ can exclude $\tan\beta$ up to 10 below the $t\bar{t}$ threshold. Some higher mass ranges are also constrained due to data fluctuations. $H \to hh$ constrains $\tan\beta$ to be $\gtrsim 3$ for a wide mass range. Various constraints on the neutral scalars for 2HDMs are summarized in Ref. [24], and the relevant plot is reproduced in Fig. 2.1. We can see that the benchmark point chosen in the previous section,

$$M_A \sim 380 \text{ GeV}, \quad M_H \sim 370 \text{ GeV}, \quad \text{and} \quad M_{H^\pm} \sim 340 \text{ GeV}, \tag{2.7.1}$$

with $\tan\beta = 3$ is sitting in the gap of the constraints. It is still allowed by but very close to the current constraints, hence it will be tested in the near future.

For future searches, the most relevant channels for the more natural mass range are di-boson channels $H/A \to VV$, $H \to hh$, and $A \to hZ$. The current bounds are expected to be improved by ~ 10 times [54]. It will probe the parameter region that we are most interested in. If we can also find the charged Higgs with a slightly lighter mass, this particular spectrum can be an indication of the specific 2HDM Higgs potential (different from that of the MSSM) that arises from this type of CHMs.

2.7.2 Additional Scalar Bosons

Besides the second Higgs doublet, there are also several additional scalar bosons, which include a real triplet ϕ, a complex singlet s, and a real singlet η. At the leading order, they don't directly connect to the SM fermions. However, the couplings to SM fermions are induced through the mixing with Higgs bosons after EWSB, with a suppression factor

of $v/2f \sim 0.15$ (for $\xi \sim 0.1$).

Scalar triplet ϕ: The scalar triplet has unsuppressed gauge interactions with W and Z bosons, but only through four-point vertices. They can be paired produced through the vector boson fusion but the production is highly suppressed due to the large energy required. Therefore, here we only consider the single production through the interaction with SM fermions. The scalar triplet includes a complex charged scalar $\phi^\pm$ and a neutral scalar ϕ^0. The collider searches of the charged scalar are similar to those of $H^\pm$ of the second Higgs doublet but with the suppressed couplings. It can be produced in association with a top and a bottom. However, due to the suppressed coupling and the larger mass, the charged scalar $\phi^\pm$ is less constrained.

The neutral scalar ϕ^0 is searched in the same ways as the neutral scalars in 2HDMs. Guided by the benchmark scenario, we consider a scalar with mass $\sim$ 500 GeV, which gives a cross section 120 fb. The dominant decay mode will be $\phi^0 \to t\bar{t}$ with a branching ratio $\sim$ 75%. The current bound from the LHC searches [44, 45] on the cross section is $\sigma \times BR < 5$ pb, which is still loose for a neutral scalar with $\sigma \times BR \sim 90$ fb. The di-boson modes are also important with branching ratios $\sim$ 16% for WW and $\sim$ 8% for ZZ. The most stringent current upper bound comes from $\phi^0 \to ZZ$ channel, which ruled out $\sigma \times BR$ above 100 fb [48, 49]. It is also much larger than $\sim$ 10 fb for the benchmark point. In the future, around 3.6×10^5 ϕ^0 (at 500 GeV) would be produced in the HL-LHC era with an integrated luminosity of 3 ab^{-1}. The bound can be improved by 10 times [54]. And a 500 GeV ϕ^0 could be within reach in the HL-LHC era.

Scalar singlets: The complex scalar s is expected to be at TeV scale and the real singlet η is around 100 GeV. They both act like the neutral scalar ϕ^0 discussed above, but without the gauge interactions. They can be produced through the gluon fusion but the production cross sections will be suppressed by $\xi/4 \sim 0.025$.

For the heavy complex scalar s, The expectation of its mass in the benchmark point is above 1.5 TeV. The dominant decay channel will be a pair of neutral Higgs bosons $s \to h_1 h_2$ (hh, hH, HH) or charged Higgs bosons due to the large $s\tilde{H}_2{}^\dagger H_1$ coupling. It also connects to the fermions sector through the mixing with Higgs bosons. However,

the production is suppressed due to the large mass. Although it is an essential element of the collective Higgs quartic term, it is hard to detect even at the HL-LHC. It may be accessible in the next generation hadron collider.

The light real scalar η should be heavy enough so that $h \to \eta\eta$ is forbidden due to the constraint from the Higgs invisible decay measurement [55]. This requires $M_T/f \gtrsim 1.3$ for a realistic model, but it should remain relatively light if the top partner is not too heavy for the naturalness reason. Since the interactions between η and SM particles are all through the mixing with the Higgs boson, the search modes are similar but with the $\xi/4$ suppression on the production rate. The cross section is ~ 1.5 pb for a 100 GeV η. The dominant decay modes are $b\bar{b}\,(78.9\%)$, $\tau\tau\,(8.3\%)$ and $gg\,(7.4\%)$, but they all suffer from large backgrounds. On the other hand, the clean channel $\gamma\gamma$ suffers from a low branching ratio $\sim 0.16\%$. For the benchmark point, the diphoton channel has $\sigma \times BR \sim 3$ fb. The latest search from CMS [56] still has an uncertainty $\sim 20(10)$ fb for a diphoton invariant mass $\sim 80(110)$ GeV, much bigger than the cross section that we expect. With more data and improvements in the background determinations, it might be discoverable at future LHC runs.

2.7.3 Fermionic Top Partners

The top partners in the $SU(6)/Sp(6)$ CHM are vector-like fermionic resonances which form a sextet of the $Sp(6)$ global symmetry. Their quantum numbers under the SM gauge symmetry are $(3, 2, 1/6)[\times 2]$, $(3, 1, 2/3)$, and $(3, 1, -1/3)$, which are identical to those of SM quarks. There are no exotic states with higher or lower hypercharges. These states are degenerate in the limit of unbroken $Sp(6)$ global symmetry. (Small splittings arise from the explicit symmetry breaking effects and EWSB.) Their mass M_T plays the important role of cutting off the quadratic contribution from the top quark loop to the Higgs potential. Naturalness prefers M_T to be as low as possible allowed by the experimental constraints. The current bound on the top partner mass has reached ~ 1.2 TeV [27, 28]. The HL-LHC can further constrain the mass up to ~ 1.5 TeV [78]. The benchmark value of 1.6 TeV is close to but probably still beyond the reach of HL-LHC. A future 100 TeV collider will cover the entire interesting mass range of the top partners if no severe tuning conspires.

It may even be able to find the fermionic partners of the other SM quarks, which are expected to be much heavier.

2.7.4 Heavy Vector Bosons

Unlike the top partners, the partners of SM gauge bosons (spin-1 resonances) are not necessarily light because of the smallness of $SU(2)_W$, $U(1)_Y$ gauge couplings. In fact, their masses need to be large enough to give a sufficiently large mass to the second Higgs doublet and to cancel in a large part the negative contribution from the top sector to the quadratic Higgs potential. The largest couplings of these composite spin-1 resonances are to the composite states, including the pNGBs. Their mixings with SM gauge bosons are strongly suppressed by their multi-TeV masses, hence their couplings to SM light fermions are also suppressed, resulting in a small production rate as well as small decay branching ratios to SM elementary particles [58, 59]. The leading decay modes will be through the composite states, such as top partners or pNGBs which include the longitudinal modes of W and Z. The current searches of heavy vector triplets decaying into SM gauge bosons final states have reached a bound about 4 TeV [60, 61, 62, 63]. The bound is relieved for larger $g_\rho > 3$ with more suppression on the production rate. Besides, the model contains a richer sector of the pNGBs which will dilute the decay branching fractions to SM gauge bosons, further reducing the bound. If the vector resonances are heavier than twice the top partner mass, the decaying into top partners will dominate and it would require different search strategies. As the production rate quickly diminishes for heavier vector resonances, the typically expected masses of the vector resonances as in our benchmark will be out of reach even at the HL-LHC. A future higher energy machine will be needed to discover them.

2.8 Precision Tests

In this section, we discuss the indirect tests of this model from precision experimental measurements.

2.8.1 Higgs Coupling Measurements

The Higgs boson couplings to SM fields in the $SU(6)/Sp(6)$ CHM are modified by two effects: the nonlinear effect due to the pNGB nature of the Higgs boson and the misalignment from the mixing of the 2HDM. The deviation of the Higgs coupling to vector bosons is parameterized by

$$\kappa_V \equiv \frac{g_{hVV}}{g_{hVV}^{SM}} = \sin(\beta-\alpha)\ \cos\frac{\sqrt{V_1^2+V_2^2}}{\sqrt{2}f}\ , \tag{2.8.1}$$

where the first factor comes from the misalignment of the 2HDM and the second factor is the nonlinear effect of the pNGB. For the benchmark point in Sec. 2.5, $\sin(\beta-\alpha)\approx 0.995$, which gives

$$\kappa_V \approx (0.995)\sqrt{1-\frac{\xi}{2}} \approx 0.995 - 0.249\ \xi\ , \tag{2.8.2}$$

The deviation of the Higgs coupling to fermion is universal in Type-I 2HDMs because it couples to all fermions in the same way. The expression is somewhat more complicated in CHM, and here we only expand to $\mathcal{O}(\xi)$,

$$\kappa_f \equiv \frac{g_{hff}}{g_{hff}^{SM}} = \frac{1}{s_\beta}\left(c_\alpha - \xi\ \frac{1}{12}(3s_\beta^2 c_\alpha + c_\beta^2 c_\alpha - 2s_\beta c_\beta s_\alpha)\right) \approx 1.030 - 0.252\ \xi\ , \tag{2.8.3}$$

where the numerical value of the last expression is obtained for the benchmark point.

The current best-fit values of κ_V and κ_F from ATLAS [64] with an integrated luminosity of 80 fb^{-1} are

$$\kappa_V = 1.06 \pm 0.04\ , \tag{2.8.4}$$

$$\kappa_F = 1.05 \pm 0.09\ , \tag{2.8.5}$$

with a 45% correlation between the two quantities. The central values for both quantities are slightly above the SM value 1, but without significant deviations given the uncertainties. As shown in Fig. 2.2, within 95% CL level, $\xi \leq 0.12$ is still allowed (for the benchmark point), which gives a lower bound on the scale $f \sim 700$ GeV.

In the future, the uncertainties in κ_V and κ_F can be improved to 1% and 3% respectively at the HL-LHC, [65]. Assuming the central values of $(1,1)$, it can bound ξ down to 0.1 at 99% CL. The next generation Higgs factories, such as ILC, CEPC, and FCCee, will

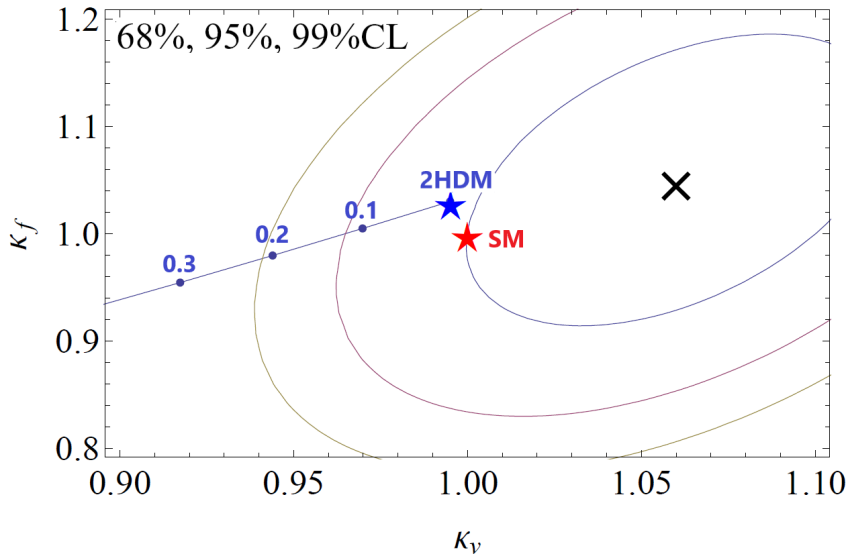

Fig. 2.2: The fit of the Higgs coupling strengths to the gauge bosons (κ_V) and fermions (κ_f) obtained by the ATLAS [64] from the 13 TeV LHC data. The cross is the observed central value. The circles from inside out represent the 68%, 95%, and 99% CL respectively. The red star shows the SM value $(1, 1)$. The blue star in the predicted value of the 2HDM benchmark of Sec. 2.5 with $\xi = 0$. Along the line, we show the predictions for the same benchmark with different ξ from 0 to 0.3.

have great sensitivities to the hZZ coupling and can measure κ_V with a precision $\approx 0.3\%$. It can test the scale f up to several TeV and hence cover the entire natural parameter region for the CHMs.

Another decay mode worth mentioning is $h \to \gamma\gamma$. The branching ratio of this decay mode will receive an additional contribution from charge Higgs bosons. But the current bound from this decay mode is still loose. It will improve at HL-LHC and future Higgs factories. It may provide a sign of the heavy charged Higgs bosons if they exist.

2.8.2 Flavor Changing Neutral Currents

New physics appearing near the TeV scale may introduce dangerously large flavor changing neutral currents (FCNCs), so the flavor-changing processes put strong constraints on the model constructions. The $SU(6)/Sp(6)$ model contains two light Higgs doublets. If general Yukawa couplings are allowed between them and SM fermions, large FCNCs will be induced. Therefore, it is desirable to impose the natural flavor conservation such that each type of Yukawa couplings only comes from one of the two Higgs doublets. Even so, a light charged Higgs boson can induce a significant contribution to the branching ratio

BR($B \to X_s\gamma$) [31, 32, 33, 34, 35, 36]. In the Type-II or flipped 2HDM, this gives a lower bound on the charged Higgs boson $M_{H^\pm} > 600$ GeV [37, 38], which would introduce more tuning in the Higgs potential. To have a more natural model, we therefore focus on the construction of the Type-I 2HDM. In a Type-I model, the $B \to X_s\gamma$ constraint rule out the region below $\tan\beta < 2$ [37, 38].

The partial compositeness couplings between the elementary fermions and the composite operators can potentially induce FCNCs. In our construction, the largest such couplings (for the top Yukawa and the collective Higgs quartic term) preserve a Peccei-Quinn symmetry with different PQ charges for different generations (see Appendix B). As a result, there is no FCNC induced by these large couplings in the leading order. Some FCNCs may be induced by other (smaller) couplings which are responsible for generating the complete SM fermion masses and mixings, but they are suppressed by the small couplings and depend on the details of their pattern.

2.8.3 Oblique Parameters

The electroweak oblique corrections provide important tests of new physics near the weak scale. They are usually expressed in terms of S, T, and U parameters [73, 74]. The current global fit gives [75]

$$S = -0.01 \pm 0.10, \quad T = 0.03 \pm 0.12, \quad U = 0.02 \pm 0.11. \tag{2.8.6}$$

For heavy new physics, U is typically small as it is suppressed by an additional factor $M_{\rm new}^2/m_Z^2$. If one fixes $U = 0$, then S and T constraints improve to

$$S = 0.0 \pm 0.07, \quad T = 0.05 \pm 0.06, \tag{2.8.7}$$

with a strong positive correlation (92%) between them. At 95% CL, one obtains $S < 0.14$ and $T < 0.22$.

There are several contributions to the oblique parameters in our model, with similarities and differences compared to the MCHM discussed in the literature. First, our model has two Higgs doublets. Their contributions to S and T can be found in Ref. [76, 77, 78]. To satisfy the other experimental constraints, the Higgs potential needs to be close to

the alignment limit and the heavy states are approximately degenerate. The contributions are expected to be small and do not provide a significant constraint [79]. The other contributions are discussed below.

The S parameter

The leading contribution to the S parameter comes from the mixing between the SM gauge bosons and the composite vector resonances. It is estimated to be [80, 81, 82]

$$\Delta S \sim c_S \; 4\pi \frac{v^2}{M_\rho^2} \sim c_S \; 0.03 \left(\frac{5 \text{ TeV}}{M_\rho}\right)^2 , \tag{2.8.8}$$

where c_S is an $\mathcal{O}(1)$ factor. It gives a lower bound of ~ 2.5 TeV on M_ρ for $c_S = 1$.

In CHMs, there is a contribution from the nonlinear Higgs dynamics due to the deviations of the Higgs couplings, which result in an incomplete cancellation of the electroweak loops [83, 84]. This contribution is proportional to ξ and depends logarithmically on M_ρ/M_h. For $M_\rho = 5$ TeV, it gives $\Delta S \sim 0.10 \; \xi$ which is well within the uncertainty.[5] In the MCHM, there is also a contribution due to loops of light fermionic resonances. It is logarithmically divergent and its coefficient depends on the UV physics [84]. This contribution can be significant, depending on the UV-sensitive coefficient. However, in our model, the fermionic resonances are complete multiplets of $SU(6)$ and their kinetic terms remain $SU(6)$ symmetric, so this divergent contribution is absent.

The T parameter

The T parameter parametrizes the amount of custodial $SU(2)$ breaking. There are also several potential contributions in our model. First, the pNGB spectrum contains a real $SU(2)_W$ triplet ϕ. If it obtains a VEV induced by the trilinear scalar couplings to a pair of Higgs doublets, $H_1^\dagger \phi H_1$, $H_2^\dagger \phi H_2$, or $(H_1 \phi H_2 + \text{h.c.})$, it will give a tree-level contribution to ΔT. Its VEV is bounded to be less than ~ 8 GeV, putting strong constraints on these couplings. However, if all the large couplings are real and the CP symmetry is (approximately) preserved, the real scalars ϕ and η are CP odd and the interactions $H_1^\dagger \phi H_1$, $H_2^\dagger \phi H_2$, and $(H_1 \phi H_2 + \text{h.c.})$ are forbidden by the CP symmetry. The η and ϕ fields need to couple quadratically to the Higgs fields. This also justifies the Higgs

[5] A factor of $1/2$ is included due to the normalization of f compared to Ref. [83, 84].

potential analysis based on the 2HDM potential. Of course, CP symmetry has to be broken in order to allow the nonzero phase in the CKM matrix. We assume that this is achieved with the small partial compositeness couplings so that the induced trilinear scalar couplings are kept small enough to satisfy the bound.

Apart from the potential triplet VEV contribution, the leading contribution to ΔT comes from fermion loops. For the partial compositeness couplings in this model, the custodial symmetry breaking comes from λ_R.[6] The dominant contribution comes from the light top partners and the corresponding mixing coupling λ_{t_R} The deviation is estimated to be [82][7]

$$\Delta T \sim \frac{N_c}{16\pi^2\alpha}\lambda_{t_R}^4\frac{v^2}{M_T^2} \sim 0.16\left(\frac{\lambda_{t_R}}{1.3}\right)^4\left(\frac{1.6\text{ TeV}}{M_T}\right)^2. \tag{2.8.9}$$

There is also a contribution from the modifications of the Higgs couplings to gauge bosons due to the nonlinear effects of the pNGB Higgs. The contribution to ΔT from the nonlinear effects again depends on ξ and is logarithmically sensitive to M_ρ. For $M_\rho = 5$ TeV, it gives $\Delta T \sim -0.28\ \xi$ [83, 84]. It is significant and can partially cancel the light top partner contribution. The contribution from the mixing of the hypercharge gauge boson and vector resonances is small due to the custodial symmetry. The tree-level contribution vanishes and the loop contribution is negligible. The overall ΔT correction is expected to be positive and could help to improve the electroweak precision fit in the presence of a positive ΔS.

In summary, among the various sources of the corrections to the electroweak observables, the contributions from the composite resonances are expected to be dominant. They give strong constraints on the masses of heavy resonances M_ρ and M_T as well as the relevant coupling like λ_{t_R}. Nevertheless, for natural parameter values as our benchmark, the corrections on (S, T) can still lie safely within the current uncertainty region. A future Z factory can greatly improve the precisions of the electroweak observables, which can provide a strong test of the model.

[6]The custodial symmetry of our model corresponds to the Case B in Ref. [17]

[7]The partial compositeness couplings are related to the top Yukawa coupling by $\lambda_{t_L}\lambda_{t_R} \sim y_t\, g_T$. For $y_t s_\beta \sim 0.85$ at 2 TeV and assuming $g_T \sim 2$, we need $\sqrt{\lambda_{t_L}\lambda_{t_R}} \sim 1.3$.

2.8.4 $Zf\bar{f}$ Couplings

The partial compositeness couplings generate mixings between elementary fermions and composite resonances. They can modify the $Zf\bar{f}$ couplings in the SM. This is a well-known problem in CHMs for the $Zb\bar{b}$ coupling in implementing the top partial compositeness. A solution based on an extended custodial symmetry $SU(2)_V \times P_{LR}$ on the top sector by embedding the left-handed top-bottom doublet into the $(2,2)$ representation of $SU(2)_L \times SU(2)_R$ was proposed in Ref. [85]. The top sector in our construction does not have this extended custodial symmetry. Furthermore, to obtain the collective quartic Higgs term, we need several large partial compositeness couplings involving other light SM fermions. As a consequence, we may expect significant deviations of the $Zf\bar{f}$ couplings for all fermions involved and they present important constraints on this model.

The third generation left-handed quark's partial compositeness couplings modify the $Zb_L\bar{b}_L$ coupling. Its deviation δg_{b_L} from the current experimental determination is constrained within 3×10^{-3} [86]. This deviation comes from mixings between the bottom quark b and the corresponding composite resonances B. Under our assignment in Appendix B, there are two terms that will have large positive contributions to δg_{b_L}. They are

$$\lambda_{t_L} \bar{q}_{3,L} H_1 B_R \quad \to \quad (\lambda_{t_L} v_1) \bar{b}_L B_R \ , \tag{2.8.10}$$

$$\lambda'_{b_L} \bar{q}_{3,L} \tilde{H}_2 B'_R \quad \to \quad (\lambda'_{b_L} v_2) \bar{b}_L B'_R \ . \tag{2.8.11}$$

The first one is responsible for generating the top Yukawa coupling and induces the mixing between b_L and the bottom partner B with PQ charge 0. The second introduces the bottom Yukawa coupling and the collective quartic term. It induces the mixing with another bottom partner B' with PQ charge 1. The deviations that they bring can be estimated as

$$\delta g_{b_L} \approx \frac{\lambda_{t_L}^2 c_\beta^2}{M_0^2(\text{TeV})} \times (30 \times 10^{-3}), \quad \delta g_{b_L} \approx \frac{\lambda_{b_L}'^2 s_\beta^2}{M_1^2(\text{TeV})} \times (30 \times 10^{-3}) \ , \tag{2.8.12}$$

where M_0 and M_1 are the masses of the fermions resonances B and B' respectively. Note that M_0 is also the top partner mass which is responsible to cut off the top loop

contribution to the quadratic Higgs potential so it should not be too large for naturalness. On the other hand M_1 is the bottom partner mass which can be much larger because of the small bottom Yukawa coupling. These corrections impose strong constraints on the couplings and masses of the composite fermion resonances. For the first term, taking $\lambda_{t_L} \approx 1.3$ and $c_\beta^2 \approx 0.1$ from the benchmark model, it requires $M_0 = M_T \gtrsim 1.3$ TeV, which is still in the range we expect. Compared to the other models without the $SU(2)_V \times P_{LR}$ custodial symmetry, such as the MCHM$_4$ [12], we are saved by the c_β^2 factor to allow a relatively light top partner. For the second one, taking $\lambda'_{b_L} \approx 1.9$ and $s_\beta \approx 1$ would require $M_1 \gtrsim 6$ TeV for the bottom partner. The bound on M_1 can be reduced for a smaller value of λ'_{b_L}, but at the cost of a larger λ_{c_L} if their combination is responsible for the collective Higgs quartic term, which increases the deviations for δg_{c_L} and δg_{s_L}.

The collective Higgs quartic term needs at least four large λ_L, λ'_L couplings. Each of them will induce two δg_L deviations from SM $Zf\bar{f}$ couplings and all of them reduce the magnitudes from the SM predicted values. Since the Z decay width and branching ratios are all well measured at $\mathcal{O}(10^{-3})$ precision, we also need to examine their observable consequences and the corresponding constraints.

It is harder to extract the constraints on individual couplings from the observables that depend on more complicated combinations of different couplings. Therefore we consider the constraints from Γ(hadron) and Γ(charged lepton) because they are directly proportional to the couplings instead of some ratios. We predict smaller values for both Γ(hadron) and Γ(charged lepton), but their observed central values are both larger than the SM predictions so the allowed parameter space is strongly restricted. At the 95% CL level, the allowed negative deviations are [75]

$$\Delta\Gamma(\text{had}) \sim -1.0 \text{ MeV} , \qquad \Delta\Gamma(\ell^+\ell^-) \sim -0.15 \text{ MeV} . \tag{2.8.13}$$

From these, we obtain the constraints on allowed negative deviations on the magnitude

of different left-handed fermion couplings (assuming only one term dominates) as follow,

$$|\delta g_{u_L}| < 0.7 \times 10^{-3} \quad \text{for up-type quarks,} \tag{2.8.14a}$$

$$|\delta g_{d_L}| < 0.6 \times 10^{-3} \quad \text{for down-type quarks,} \tag{2.8.14b}$$

$$|\delta g_{e_L}| < 0.4 \times 10^{-3} \quad \text{for charged leptons.} \tag{2.8.14c}$$

They strongly constrain the parameters of our model. To satisfy these constraints, the corresponding fermion partners need to be over 10 TeV if their couplings to the elementary fermions are large enough to be responsible for the collective Higgs quartic term.

These constraints can be relaxed somewhat if we use the neutrino couplings for the collective Higgs quartic term. The Γ(invisible) is smaller than the SM prediction. The allowed negative deviation is 4 MeV at the 95% CL level, which corresponds to

$$|\delta g_{\nu_L}| < 6 \times 10^{-3} \quad \text{for neutrinos.} \tag{2.8.14d}$$

The resulting constraints on the corresponding fermion resonances are milder.

The precision measurements of the Z couplings put strong constraints on our model because we predict a reduction of all $Zf_L\bar{f}_L$ couplings in the construction. A future Z factory may improve the coupling measurements by more than one order of magnitude. Consequently, it can either establish a deviation from the SM predictions which points to new physics in the nearby scales, or further affirm the SM predictions which will severely challenge this model or any other models with similar predictions. Nevertheless, we would like to emphasize that these constraints are indirect so it is quite possible that one can extend the model to introduce new contributions to cancel the deviations, at the expense of complexity and/or tuning.

2.9 Conclusions

Composite Higgs models remain an appealing solution to the hierarchy problem. However, in realistic models, some tuning in the Higgs potential is often required to obtain the correct EWSB and the observed Higgs boson mass. One source is from the mass splittings within the top partner multiplet of the composite resonances, which can generate a large quadratic Higgs potential through the partial compositeness couplings at the order

$\lambda^2_{L(R)}$. The other is to obtain the necessary relative size between the quartic term and the quadratic term of the Higgs potential in order to separate the EWSB scale and the compositeness scale. In this paper, we look for models that can address both problems. We show that a CHM based on the coset $SU(6)/Sp(6)$ can achieve the goals without introducing additional elementary fields beyond the SM and the composite sector, which otherwise will introduce a new coincidence problem that why the new elementary fields and the compositeness resonances are at the same mass scale.

A key part of the setup is to couple the elementary SM fermions to the composite operators of the fundamental representation of $SU(6)$. The composite resonances do not split after the symmetry is broken to $Sp(6)$ and hence do not induce any large potential from the UV dynamics for the pNGBs. The leading contribution to the Higgs quadratic term is reduced to the unavoidable top quark loop in the IR. In addition, the fundamental representation of $SU(6)$ contains two electroweak doublets of the same SM quantum numbers. This allows us to write down different ways of coupling between the elementary fermions and the composite resonances, each of which preserves a subset of the global symmetry. In this way, a quartic Higgs potential can be generated from the collective symmetry breaking of the little Higgs mechanism, without inducing the corresponding quadratic terms. This independent quartic term enables us to naturally separate the EWSB scale and the $SU(6)$ global symmetry breaking scale, reducing the tuning of the Higgs potential.

This model contains many more pNGBs than one Higgs double of the minimal model. In particular, there are two Higgs doublets and the second Higgs doublet should not be too heavy for naturalness considerations. The extra Higgs bosons are already subject to collider constraints and are the most likely new particles to be probed in the future LHC runs beside the top partners. The other pNGBs, having smaller couplings to SM particles, are more difficult to find. Together with the heavy vector and fermion resonances, they need higher energy machines with large integrated luminosities. The top partners in this model do not include new particles with exotic charges, e.g., 5/3, as in many other CHMs. The model also predicts deviations of the Higgs couplings and weak gauge boson

couplings. The current experimental data already provide substantial constraints on the model parameters in the most natural region. The Higgs coupling measurements will be greatly improved at the HL-LHC and future Higgs factories. A future Z factory can also further constrain the electroweak observables. Either the agreements with SM predictions with higher precisions will push the model completely out of the natural scale for the solution to the hierarchy problem, or some deviations will be discovered to point to the possible new physics, and if any of the CHMs can provide an explanation for them.

Acknowledgements

We thank Felix Kling, Shufang Su, and Wei Su for letting us use the figure in Ref. [24]. We also thank Da Liu, Matthew Low, and Ennio Salvioni for useful discussions. This work is supported by the Department of Energy Grant number DE-SC-0009999.

Appendix A: The $SU(5)/SO(5)$ Composite Higgs Model

The $SU(5)/SO(5)$ is also a possible coset that can naturally avoid large UV contributions to the Higgs potential. It was one of the cosets considered in early composite Higgs models of 1980s [87, 88]. It was also the coset of the littlest Higgs model [9] which was one of the pioneer models to realize the mechanism of the collective symmetry breaking for the Higgs quartic coupling. The symmetry breaking can be parametrized by a symmetric tensor field with a VEV

$$\langle \Sigma \rangle = \Sigma_0 = \begin{pmatrix} 0 & 0 & \mathbb{I} \\ 0 & 1 & 0 \\ \mathbb{I} & 0 & 0 \end{pmatrix}, \quad \text{where } \mathbb{I} \text{ is the } 2 \times 2 \text{ identity matrix.} \tag{2.9.1}$$

The SM $SU(2)_W$ and $U(1)_Y$ generators are embedded as

$$\frac{1}{2}\begin{pmatrix} \sigma^a & 0 & 0 \\ 0 & 0 & 0 \\ 0 & 0 & -\sigma^{a*} \end{pmatrix}, \quad \frac{1}{2}\begin{pmatrix} -\mathbb{I} & 0 & 0 \\ 0 & 0 & 0 \\ 0 & 0 & \mathbb{I} \end{pmatrix} + X\mathbf{I}\ , \tag{2.9.2}$$

where the extra $U(1)_X$ charge X accounts for the correct hypercharges of SM fermions.

There are 14 pNGBs, with a complex doublet (which is identified as the Higgs field H), a complex triplet ϕ, a real triplet ω, and a real singlet η. The partial compositeness couplings can go through the $\mathbf{5}$ and $\bar{\mathbf{5}}$ representations of $SU(5)$. They do not split under $SO(5)$ and hence do not give large UV contributions to the Higgs potential, just as in the $SU(6)/Sp(6)$ case. Under the SM $SU(2)_W \times U(1)_Y$, they decompose as

$$\mathbf{5}_x = \mathbf{2}_{x-1/2} \oplus \mathbf{1}_x \oplus \bar{\mathbf{2}}_{x+1/2}, \tag{2.9.3a}$$

$$\bar{\mathbf{5}}_x = \bar{\mathbf{2}}_{x+1/2} \oplus \mathbf{1}_x \oplus \mathbf{2}_{x-1/2}\ . \tag{2.9.3b}$$

To mix with elementary fermions, we need to choose $x = 2/3$ for the up-type quarks and $-1/3$ for the down-type quarks.

The Higgs quartic term arising from the collective symmetry breaking takes the form,

$$\kappa_1 f^2 \left| \phi_{ij} + \frac{i}{2f}(H_i H_j + H_j H_i) \right|^2 + \kappa_2 f^2 \left| \phi_{ij} - \frac{i}{2f}(H_i H_j + H_j H_i) \right|^2\ . \tag{2.9.4}$$

A drawback of this potential is that a nonzero VEV of the $SU(2)_W$ triplet ϕ will be induced after EWSB unless $\kappa_1 = \kappa_2$. The triplet VEV violates the custodial $SU(2)$ symmetry and is subject to the strong constraint of the T (or ρ) parameter. Even if we ignore that for a moment, it is also more challenging to generate the collective quartic potential (2.9.4) in this model. The two doublets in $\mathbf{5}$ or $\bar{\mathbf{5}}$ have different hypercharges if $x \neq 0$ and hence are not equivalent. We cannot couple the elementary SM fermion doublets to both $\mathbf{5}$ and $\bar{\mathbf{5}}$ in a way that preserves an $SU(3)$ global symmetry to protect the Higgs mass, so the mechanism introduced for the $SU(6)/Sp(6)$ model in Sec. 2.4 does not work here. One could add additional exotic vector-like elementary fermions (with hypercharge $7/6$ or $-5/6$) to couple to these composite operators for the purpose of generating the quartic term, but these exotic elementary fermions should have masses comparable to the compositeness scale, which requires some coincidence. Another possibility is to use the lepton partners that have $x = 0$, then the two doublets in $\mathbf{5}$, $\bar{\mathbf{5}}$ are equivalent representations. One can write down the partial compositeness couplings to generate Eq. (2.9.4), analogous to the $SU(6)/Sp(6)$ model. However, the same interactions will induce the Majorana mass terms for the left-handed neutrinos through the triplet ϕ VEV. The couplings need to be $\mathcal{O}(1)$ in order to produce a large enough quartic term. It means that unless the triplet VEV is tiny (which requires κ_1 and κ_2 to be equal to a very high accuracy), the induced neutrino masses will be too large. This constraint on the ϕ VEV is even much stronger than that from the custodial $SU(2)$ violation.

Appendix B: Couplings between SM Fermions and Composite Operators, and Their Peccei-Quinn Charges

Both SM Yukawa couplings and the Higgs quartic potential from collective symmetry breaking arise from the partial compositeness couplings between the elementary fermions and composite operators. The leading interactions (with $\mathcal{O}(1)$ coupling strength) should respect an approximate $U(1)_{PQ}$ symmetry to avoid a too large quadratic $\tilde{H}_2^\dagger H_1$ term and large FCNCs, so it is convenient to assign the PQ charges to the fermions in classifying the couplings. We will construct a Type-I 2HDM model because of the weaker constraint on

the heavy Higgs bosons, and produce both terms needed for the collective quartic Higgs potential.

For the quark sector, we include eight composite operators in **6** and $\bar{\mathbf{6}}$ representations of $SU(6)$ with overall PQ charges $r = 0, 1, 2, 3$,

$$\mathbf{6}_r = \mathbf{2}_{r+1/2} \oplus \mathbf{1}_r \oplus \bar{\mathbf{2}}_{r-1/2} \oplus \mathbf{1}_r \tag{2.9.5a}$$

$$\bar{\mathbf{6}}_r = \bar{\mathbf{2}}_{r-1/2} \oplus \mathbf{1}_r \oplus \mathbf{2}_{r+1/2} \oplus \mathbf{1}_r \tag{2.9.5b}$$

Here the subscript denotes the PQ charge instead of the hypercharge. The **6** and $\bar{\mathbf{6}}$ of the same PQ charges create the same resonances which become the quark partners of different flavors. The $U(1)_{PQ}$ charges of the three generations of elementary quarks are shown in Table 2.1. The lepton sector can be similarly assigned.

	$U(1)_{PQ}$		$U(1)_{PQ}$		$U(1)_{PQ}$
$q_{3,L} = (t_L, b_L)^T$	1/2	t_R	0	b_R	1
$q_{2,L} = (c_L, s_L)^T$	3/2	c_R	1	s_R	2
$q_{1,L} = (u_L, d_L)^T$	5/2	u_R	3	d_R	3

Table 2.1: PQ charges of elementary quarks. The PQ charge of u_R appears out of the pattern. As discussed in the text, the up quark Yukawa coupling comes from the $U(1)_{PQ}$ violating coupling, which also generates the required $\tilde{H}_2^\dagger H_1$ term.

There are some requirements for producing a Type-I 2HDM. First, to generate SM Yukawa couplings, we need to couple one of q_L and q_R to **6** and the other to $\bar{\mathbf{6}}$ of the same PQ charge. In addition, each q_L needs to couple to the composite operators at least in two ways in order to generate the up-type and down-type Yukawa couplings with the same Higgs doublet. If q_L had only one coupling to **6** (or $\bar{\mathbf{6}}$), the up- and down-type quarks would couple to different Higgs doublets as we discussed in Sec. 2.3.4. Once q_L couplings are fixed, the right-handed quark couplings follow directly from the PQ charges (except for the up quark). To generate the Higgs quartic term by collective symmetry breaking, we need to introduce two pairs of couplings between the elementary doublets and the (**6**, $\bar{\mathbf{6}}$) pairs, with each pair of couplings preserving a different $SU(4)$ symmetry. Finally, we add a $U(1)_{PQ}$ violating λ''_{u_L} which serves to generate the mixed Higgs quadratic term in Eq. (2.4.16), and also the up quark Yukawa coupling.

From these requirements, a possible set of couplings between elementary quarks and the composite operators is shown below (in the parentheses after the corresponding composite operators).

$$\mathbf{6}_0 = \mathbf{2}_{1/2}\ (\lambda_{t_L}) \oplus \mathbf{1}_0 \oplus \bar{\mathbf{2}}_{-1/2} \oplus \mathbf{1}_0 \tag{2.9.6a}$$

$$\bar{\mathbf{6}}_0 = \bar{\mathbf{2}}_{-1/2} \oplus \mathbf{1}_0 \oplus \mathbf{2}_{1/2} \oplus \mathbf{1}_0\ (\lambda_{t_R}) \tag{2.9.6b}$$

$$\mathbf{6}_1 = \mathbf{2}_{3/2}\ (\lambda_{c_L}) \oplus \mathbf{1}_1 \oplus \bar{\mathbf{2}}_{1/2} \oplus \mathbf{1}_1\ (\lambda'_{b_R}) \tag{2.9.6c}$$

$$\bar{\mathbf{6}}_1 = \bar{\mathbf{2}}_{1/2}\ (\lambda'_{b_L}) \oplus \mathbf{1}_1 \oplus \mathbf{2}_{3/2} \oplus \mathbf{1}_1\ (\lambda_{c_R}) \tag{2.9.6d}$$

$$\mathbf{6}_2 = \mathbf{2}_{5/2} \oplus \mathbf{1}_2 \oplus \bar{\mathbf{2}}_{3/2}\ (\tilde{\lambda}'_{s_L}) \oplus \mathbf{1}_2 \tag{2.9.6e}$$

$$\bar{\mathbf{6}}_2 = \bar{\mathbf{2}}_{3/2} \oplus \mathbf{1}_2\ (\tilde{\lambda}'_{s_R}) \oplus \mathbf{2}_{5/2}\ (\tilde{\lambda}_{u_L}) \oplus \mathbf{1}_2 \tag{2.9.6f}$$

$$\mathbf{6}_3 = \mathbf{2}_{7/2}\ (\lambda''_{u_L}) \oplus \mathbf{1}_3 \oplus \bar{\mathbf{2}}_{5/2} \oplus \mathbf{1}_3\ (\lambda'_{d_R}) \tag{2.9.6g}$$

$$\bar{\mathbf{6}}_3 = \bar{\mathbf{2}}_{5/2}\ (\lambda'_{d_L}) \oplus \mathbf{1}_3 \oplus \mathbf{2}_{7/2} \oplus \mathbf{1}_3\ (\lambda_{u_R}) \tag{2.9.6h}$$

where the subscript of the coupling tells which elementary quark it is coupled to. (The left-handed couplings couple to the whole doublets despite the quark labels.) The SM quark Yukawa couplings are given by

$$y_t \sim \frac{\lambda_{t_L}\lambda_{t_R}}{g_{\psi_0}}, \qquad y_b \sim \frac{\lambda'_{b_L}\lambda'_{b_R}}{g_{\psi_1}}, \tag{2.9.7}$$

$$y_c \sim \frac{\lambda_{c_L}\lambda_{c_R}}{g_{\psi_1}}, \qquad y_s \sim \frac{\tilde{\lambda}'_{s_L}\tilde{\lambda}'_{s_R}}{g_{\psi_2}} \tag{2.9.8}$$

$$y_u \sim \frac{\lambda''_{u_L}\lambda_{u_R}}{g_{\psi_3}}, \qquad y_d \sim \frac{\lambda'_{d_L}\lambda'_{d_R}}{g_{\psi_3}}, \tag{2.9.9}$$

where g_{ψ_r} is the coupling of the strong resonances in $\mathbf{6}_r, \bar{\mathbf{6}}_r$, with their masses given by $\sim g_{\psi_r} f$. To have a relatively light top partner, we should have $g_{\psi_0} \sim 2$, while all other g_{ψ_r}'s are expected to be large. The quark flavor mixings (CKM matrix) can be generated by additional $U(1)_{PQ}$ violating couplings which are not shown. These couplings are expected to be small and will not significantly affect the Higgs potential.

For the Higgs quartic term, the combination of λ_{c_L} and λ'_{b_L} generates one term of the collective symmetry breaking, while the combination of $\tilde{\lambda}'_{s_L}$ and $\tilde{\lambda}_{u_L}$ generates the other. Alternatively, we could also use the lepton sector to generate one of the collective

symmetry breaking terms. The quartic coupling is estimated to be

$$\lambda_{12} = \frac{3}{4\pi^2}\frac{c_{cb}c_{us}\lambda^2_{c_L}\lambda'^2_{b_L}\tilde{\lambda}^2_{u_L}\tilde{\lambda}'^2_{s_L}}{c_{cb}\lambda^2_{c_L}\lambda'^2_{b_L} + c_{us}\tilde{\lambda}^2_{u_L}\tilde{\lambda}'^2_{s_L}} \sim \frac{3}{4\pi^2}\lambda^2_{c_L}\lambda'^2_{b_L} \quad (\text{if } \lambda_{c_L}\lambda'_{b_L} \sim \tilde{\lambda}_{u_L}\tilde{\lambda}'_{s_L},\ c_{cb} \sim c_{us} \sim 2). \tag{2.9.10}$$

To get a large enough λ_{12}, these couplings should be quite large ($\gtrsim 1$). The correct SM Yukawa couplings can still be obtained by suitable choices of λ_R couplings and g_{ψ_r}. The λ''_{u_L} coupling violates the $U(1)_{PQ}$ symmetry as it mixes the $q_{1,L}$ with charge 5/2 with the composite doublet of charge 7/2. By combining with λ'_{d_L}, it will generate a mixing mass term for the two Higgs doublets,

$$m^2_{12} \sim \frac{3}{8\pi^2}\lambda'_{d_L}\lambda''_{u_L}g^2_{\psi_3}f^2\ . \tag{2.9.11}$$

In this way, all terms required in the Higgs potential for a realistic model can be generated without introducing additional elementary fermions.

References

[1] **CMS** Collaboration, S. Chatrchyan *et al.*, "Observation of a new boson at a mass of 125 GeV with the CMS experiment at the LHC," *Phys. Lett.* **B716** (2012) 30–61, [arXiv:1207.7235].

[2] **ATLAS** Collaboration, G. Aad *et al.*, "Observation of a new particle in the search for the Standard Model Higgs boson with the ATLAS detector at the LHC," *Phys. Lett.* **B716** (2012) 1–29, [arXiv:1207.7214].

[3] D. B. Kaplan and H. Georgi, "SU(2) x U(1) Breaking by Vacuum Misalignment," *Phys. Lett.* **136B** (1984) 183–186.

[4] D. B. Kaplan, H. Georgi, and S. Dimopoulos, "Composite Higgs Scalars," *Phys. Lett.* **136B** (1984) 187–190.

[5] **CMS** Collaboration, A. M. Sirunyan *et al.*, "Search for vector-like T and B quark pairs in final states with leptons at $\sqrt{s} = 13$ TeV," *JHEP* **08** (2018) 177, [arXiv:1805.04758].

[6] **ATLAS** Collaboration, M. Aaboud *et al.*, "Combination of the searches for pair-produced vector-like partners of the third-generation quarks at $\sqrt{s} = 13$ TeV with the ATLAS detector," *Phys. Rev. Lett.* **121** no. 21, (2018) 211801, [arXiv:1808.02343].

[7] N. Arkani-Hamed, A. G. Cohen, and H. Georgi, "Electroweak symmetry breaking from dimensional deconstruction," *Phys. Lett.* **B513** (2001) 232–240, [hep-ph/0105239].

[8] N. Arkani-Hamed, A. G. Cohen, E. Katz, A. E. Nelson, T. Gregoire, and J. G. Wacker, "The Minimal moose for a little Higgs," *JHEP* **08** (2002) 021, [hep-ph/0206020].

[9] N. Arkani-Hamed, A. G. Cohen, E. Katz, and A. E. Nelson, "The Littlest Higgs," *JHEP* **07** (2002) 034, [hep-ph/0206021].

[10] G. Panico, M. Redi, A. Tesi, and A. Wulzer, "On the Tuning and the Mass of the Composite Higgs," *JHEP* **03** (2013) 051, [arXiv:1210.7114].

[11] G. Panico and A. Wulzer, "The Composite Nambu-Goldstone Higgs," *Lect. Notes Phys.* **913** (2016) pp.1–316, [arXiv:1506.01961].

[12] K. Agashe, R. Contino, and A. Pomarol, "The Minimal composite Higgs model," *Nucl. Phys.* **B719** (2005) 165–187, [hep-ph/0412089].

[13] D. B. Kaplan, "Flavor at SSC energies: A New mechanism for dynamically generated fermion masses," *Nucl. Phys.* **B365** (1991) 259–278.

[14] C. Csaki, T. Ma, and J. Shu, "Maximally Symmetric Composite Higgs Models," *Phys. Rev. Lett.* **119** no. 13, (2017) 131803, [arXiv:1702.00405].

[15] C. Csáki, T. Ma, J. Shu, and J.-H. Yu, "Emergence of Maximal Symmetry," *Phys. Rev. Lett.* **124** no. 24, (2020) 241801, [arXiv:1810.07704].

[16] S. Blasi, C. Csaki, and F. Goertz, "A Natural Composite Higgs via Universal Boundary Conditions," arXiv:2004.06120.

[17] L. Vecchi, "The Natural Composite Higgs," , (2013) , [arXiv:1304.4579].

[18] C. Csaki, M. Geller, and O. Telem, "Tree-level Quartic for a Holographic Composite Higgs," *JHEP* **05** (2018) 134, [arXiv:1710.08921].

[19] C. Csáki, C.-s. Guan, T. Ma, and J. Shu, "Generating a Higgs Quartic," *Phys. Rev. Lett.* **124** no. 25, (2020) 251801, [arXiv:1904.03191].

[20] I. Low, W. Skiba, and D. Tucker-Smith, "Little Higgses from an antisymmetric condensate," *Phys. Rev.* **D66** (2002) 072001, [hep-ph/0207243].

[21] C. Cai, G. Cacciapaglia, and H.-H. Zhang, "Vacuum alignment in a composite 2HDM," *JHEP* **01** (2019) 130, [arXiv:1805.07619].

[22] S. L. Glashow and S. Weinberg, "Natural Conservation Laws for Neutral Currents," *Phys. Rev. D* **15** (1977) 1958.

[23] E. Paschos, "Diagonal Neutral Currents," *Phys. Rev. D* **15** (1977) 1966.

[24] M. Misiak and M. Steinhauser, "Weak radiative decays of the B meson and bounds on $M_{H^\pm}$ in the Two-Higgs-Doublet Model," *Eur. Phys. J.* **C77** no. 3, (2017) 201, [arXiv:1702.04571].

[25] R. Peccei and H. R. Quinn, "Constraints Imposed by CP Conservation in the Presence of Instantons," *Phys. Rev. D* **16** (1977) 1791–1797.

[26] O. Matsedonskyi, G. Panico, and A. Wulzer, "Light Top Partners for a Light Composite Higgs," *JHEP* **01** (2013) 164, [arXiv:1204.6333].

[27] D. Marzocca, M. Serone, and J. Shu, "General Composite Higgs Models," *JHEP* **08** (2012) 013, [arXiv:1205.0770].

[28] A. Pomarol and F. Riva, "The Composite Higgs and Light Resonance Connection," *JHEP* **08** (2012) 135, [arXiv:1205.6434].

[29] G. C. Branco, P. M. Ferreira, L. Lavoura, M. N. Rebelo, M. Sher, and J. P. Silva, "Theory and phenomenology of two-Higgs-doublet models," *Phys. Rept.* **516** (2012) 1–102, [arXiv:1106.0034].

[30] F. Kling, S. Su, and W. Su, "2HDM Neutral Scalars under the LHC," arXiv:2004.04172.

[31] **CMS** Collaboration, A. M. Sirunyan *et al.*, "Search for a charged Higgs boson decaying into top and bottom quarks in events with electrons or muons in proton-proton collisions at $\sqrt{s} = 13$ TeV," *JHEP* **01** (2020) 096, [arXiv:1908.09206].

[32] **ATLAS** Collaboration, M. Aaboud *et al.*, "Search for charged Higgs bosons decaying into top and bottom quarks at $\sqrt{s} = 13$ TeV with the ATLAS detector," *JHEP* **11** (2018) 085, [arXiv:1808.03599].

[33] J. F. Gunion and H. E. Haber, "The CP conserving two Higgs doublet model: The Approach to the decoupling limit," *Phys. Rev. D* **67** (2003) 075019, [hep-ph/0207010].

[34] N. Craig and S. Thomas, "Exclusive Signals of an Extended Higgs Sector," *JHEP* **11** (2012) 083, [arXiv:1207.4835].

[35] N. Craig, J. Galloway, and S. Thomas, "Searching for Signs of the Second Higgs Doublet," arXiv:1305.2424.

[36] M. Carena, I. Low, N. R. Shah, and C. E. M. Wagner, "Impersonating the Standard Model Higgs Boson: Alignment without Decoupling," *JHEP* **04** (2014) 015, [arXiv:1310.2248].

[37] **ATLAS** Collaboration, M. Aaboud *et al.*, "Search for charged Higgs bosons decaying via $H^{\pm} \to \tau^{\pm}\nu_{\tau}$ in the τ+jets and τ+lepton final states with 36 fb^{-1} of pp collision data recorded at $\sqrt{s} = 13$ TeV with the ATLAS experiment," *JHEP* **09** (2018) 139, [arXiv:1807.07915].

[38] **CMS** Collaboration, A. M. Sirunyan *et al.*, "Search for charged Higgs bosons in the $\mathrm{H}^{\pm} \to \tau^{\pm}\nu_{\tau}$ decay channel in proton-proton collisions at $\sqrt{s} = 13$ TeV," *JHEP* **07** (2019) 142, [arXiv:1903.04560].

[39] P. Sanyal, "Limits on the Charged Higgs Parameters in the Two Higgs Doublet Model using CMS $\sqrt{s} = 13$ TeV Results," *Eur. Phys. J. C* **79** no. 11, (2019) 913, [arXiv:1906.02520].

[40] **CMS** Collaboration, A. M. Sirunyan *et al.*, "Search for additional neutral MSSM Higgs bosons in the $\tau\tau$ final state in proton-proton collisions at $\sqrt{s} = 13$ TeV," *JHEP* **09** (2018) 007, [arXiv:1803.06553].

[41] **ATLAS** Collaboration, G. Aad *et al.*, "Search for heavy Higgs bosons decaying into two tau leptons with the ATLAS detector using pp collisions at $\sqrt{s} = 13$ TeV," arXiv:2002.12223.

[42] **CMS** Collaboration, A. M. Sirunyan *et al.*, "Search for physics beyond the standard model in high-mass diphoton events from proton-proton collisions at $\sqrt{s} = 13$ TeV," *Phys. Rev. D* **98** no. 9, (2018) 092001, [arXiv:1809.00327].

[43] **ATLAS** Collaboration, M. Aaboud *et al.*, "Search for new phenomena in high-mass diphoton final states using 37 fb^{-1} of proton–proton collisions collected at $\sqrt{s} = 13$ TeV with the ATLAS detector," *Phys. Lett. B* **775** (2017) 105–125, [arXiv:1707.04147].

[44] **CMS** Collaboration, A. M. Sirunyan *et al.*, "Search for heavy Higgs bosons decaying to a top quark pair in proton-proton collisions at $\sqrt{s} = 13$ TeV," arXiv:1908.01115.

[45] **ATLAS** Collaboration, M. Aaboud *et al.*, "Search for heavy particles decaying into top-quark pairs using lepton-plus-jets events in proton–proton collisions at $\sqrt{s} = 13$ TeV with the ATLAS detector," *Eur. Phys. J. C* **78** no. 7, (2018) 565, [arXiv:1804.10823].

[46] **CMS** Collaboration, A. M. Sirunyan *et al.*, "Search for a heavy Higgs boson decaying to a pair of W bosons in proton-proton collisions at $\sqrt{s} = 13$ TeV," arXiv:1912.01594.

[47] **ATLAS** Collaboration, M. Aaboud *et al.*, "Search for heavy resonances decaying into WW in the $e\nu\mu\nu$ final state in pp collisions at $\sqrt{s} = 13$ TeV with the ATLAS detector," *Eur. Phys. J. C* **78** no. 1, (2018) 24, [arXiv:1710.01123].

[48] **CMS** Collaboration, A. M. Sirunyan *et al.*, "Search for a new scalar resonance decaying to a pair of Z bosons in proton-proton collisions at $\sqrt{s} = 13$ TeV," *JHEP* **06** (2018) 127, [arXiv:1804.01939]. [Erratum: JHEP 03, 128 (2019)].

[49] **ATLAS** Collaboration, M. Aaboud *et al.*, "Search for heavy ZZ resonances in the $\ell^+\ell^-\ell^+\ell^-$ and $\ell^+\ell^-\nu\bar{\nu}$ final states using proton–proton collisions at $\sqrt{s} = 13$ TeV with the ATLAS detector," *Eur. Phys. J. C* **78** no. 4, (2018) 293, [arXiv:1712.06386].

[50] **CMS** Collaboration, A. M. Sirunyan *et al.*, "Combination of searches for Higgs boson pair production in proton-proton collisions at $\sqrt{s} = 13$ TeV," *Phys. Rev. Lett.* **122** no. 12, (2019) 121803, [arXiv:1811.09689].

[51] **ATLAS** Collaboration, G. Aad *et al.*, "Combination of searches for Higgs boson pairs in pp collisions at $\sqrt{s}$ =13 TeV with the ATLAS detector," *Phys. Lett. B* **800** (2020) 135103, [arXiv:1906.02025].

[52] **CMS** Collaboration, A. M. Sirunyan *et al.*, "Search for a heavy pseudoscalar boson decaying to a Z and a Higgs boson at $\sqrt{s} = 13$ TeV," *Eur. Phys. J. C* **79** no. 7, (2019) 564, [arXiv:1903.00941].

[53] **ATLAS** Collaboration, M. Aaboud *et al.*, "Search for heavy resonances decaying into a W or Z boson and a Higgs boson in final states with leptons and b-jets in 36 fb^{-1} of $\sqrt{s} = 13$ TeV pp collisions with the ATLAS detector," *JHEP* **03** (2018) 174, [arXiv:1712.06518]. [Erratum: JHEP 11, 051 (2018)].

[54] M. Cepeda *et al.*, *Report from Working Group 2: Higgs Physics at the HL-LHC and HE-LHC*, vol. 7, pp. 221–584. 12, 2019. arXiv:1902.00134.

[55] **CMS** Collaboration, V. Khachatryan *et al.*, "Searches for invisible decays of the Higgs boson in pp collisions at $\sqrt{s} = 7$, 8, and 13 TeV," *JHEP* **02** (2017) 135, [arXiv:1610.09218].

[56] **CMS** Collaboration, CMS Collaboration, "Search for new resonances in the diphoton final state in the mass range between 70 and 110 GeV in pp collisions at $\sqrt{s} = 8$ and 13 TeV,".

[57] X. Cid Vidal *et al.*, "Report from Working Group 3," *CERN Yellow Rep. Monogr.* **7** (2019) 585–865, [arXiv:1812.07831].

[58] D. Pappadopulo, A. Thamm, R. Torre, and A. Wulzer, "Heavy Vector Triplets: Bridging Theory and Data," *JHEP* **09** (2014) 060, [arXiv:1402.4431].

[59] D. Greco and D. Liu, "Hunting composite vector resonances at the LHC: naturalness facing data," *JHEP* **12** (2014) 126, [arXiv:1410.2883].

[60] **ATLAS** Collaboration, G. Aad *et al.*, "Search for heavy diboson resonances in semileptonic final states in pp collisions at $\sqrt{s} = 13$ TeV with the ATLAS detector," arXiv:2004.14636.

[61] **ATLAS** Collaboration, G. Aad *et al.*, "Search for diboson resonances in hadronic final states in 139 fb^{-1} of pp collisions at $\sqrt{s} = 13$ TeV with the ATLAS detector," *JHEP* **09** (2019) 091, [arXiv:1906.08589]. [Erratum: JHEP 06, 042 (2020)].

[62] **CMS** Collaboration, A. M. Sirunyan *et al.*, "Combination of CMS searches for heavy resonances decaying to pairs of bosons or leptons," *Phys. Lett. B* **798** (2019) 134952, [arXiv:1906.00057].

[63] **CMS** Collaboration, A. M. Sirunyan *et al.*, "A multi-dimensional search for new heavy resonances decaying to boosted WW, WZ, or ZZ boson pairs in the dijet final state at 13 TeV," *Eur. Phys. J. C* **80** no. 3, (2020) 237, [arXiv:1906.05977].

[64] **ATLAS** Collaboration, G. Aad *et al.*, "Combined measurements of Higgs boson production and decay using up to 80 fb^{-1} of proton-proton collision data at $\sqrt{s} =$ 13 TeV collected with the ATLAS experiment," *Phys. Rev.* **D101** no. 1, (2020) 012002, [arXiv:1909.02845].

[65] J. de Blas *et al.*, "Higgs Boson Studies at Future Particle Colliders," *JHEP* **01** (2020) 139, [arXiv:1905.03764].

[66] B. Grinstein and M. B. Wise, "Weak Radiative B Meson Decay as a Probe of the Higgs Sector," *Phys. Lett. B* **201** (1988) 274–278.

[67] W.-S. Hou and R. Willey, "Effects of Charged Higgs Bosons on the Processes b —¿ s Gamma, b —¿ s g* and b —¿ s Lepton+ Lepton-," *Phys. Lett. B* **202** (1988) 591–595.

[68] T. G. Rizzo, "$b \to s\gamma$ in the Two Higgs Doublet Model," *Phys. Rev. D* **38** (1988) 820.

[69] C. Geng and J. N. Ng, "Charged Higgs Effect in $B)d)0$ - $\bar{B}(d)0$ Mixing, $K \to \pi$ Neutrino Anti-neutrino Decay and Rare Decays of B Mesons," *Phys. Rev. D* **38** (1988) 2857. [Erratum: Phys.Rev.D 41, 1715 (1990)].

[70] V. D. Barger, J. Hewett, and R. Phillips, "New Constraints on the Charged Higgs Sector in Two Higgs Doublet Models," *Phys. Rev. D* **41** (1990) 3421–3441.

[71] B. Grinstein, R. P. Springer, and M. B. Wise, "Strong Interaction Effects in Weak Radiative $\bar{B}$ Meson Decay," *Nucl. Phys. B* **339** (1990) 269–309.

[72] A. Arbey, F. Mahmoudi, O. Stal, and T. Stefaniak, "Status of the Charged Higgs Boson in Two Higgs Doublet Models," *Eur. Phys. J.* **C78** no. 3, (2018) 182, [arXiv:1706.07414].

[73] M. E. Peskin and T. Takeuchi, "A New constraint on a strongly interacting Higgs sector," *Phys. Rev. Lett.* **65** (1990) 964–967.

[74] M. E. Peskin and T. Takeuchi, "Estimation of oblique electroweak corrections," *Phys. Rev. D* **46** (1992) 381–409.

[75] **Particle Data Group** Collaboration, M. Tanabashi *et al.*, "Review of Particle Physics," *Phys. Rev.* **D98** no. 3, (2018) 030001.

[76] H. E. Haber, "Introductory low-energy supersymmetry," in *Theoretical Advanced Study Institute (TASI 92): From Black Holes and Strings to Particles*, pp. 589–686. 4, 1993. hep-ph/9306207.

[77] H. E. Haber and H. E. Logan, "Radiative corrections to the Z b anti-b vertex and constraints on extended Higgs sectors," *Phys. Rev. D* **62** (2000) 015011, [hep-ph/9909335].

[78] C. Froggatt, R. Moorhouse, and I. Knowles, "Leading radiative corrections in two scalar doublet models," *Phys. Rev. D* **45** (1992) 2471–2481.

[79] J. Haller, A. Hoecker, R. Kogler, K. Moenig, T. Peiffer, and J. Stelzer, "Update of the global electroweak fit and constraints on two-Higgs-doublet models," *Eur. Phys. J. C* **78** no. 8, (2018) 675, [arXiv:1803.01853].

[80] K. Agashe, A. Delgado, M. J. May, and R. Sundrum, "RS1, custodial isospin and precision tests," *JHEP* **08** (2003) 050, [hep-ph/0308036].

[81] K. Agashe and R. Contino, "The Minimal composite Higgs model and electroweak precision tests," *Nucl. Phys. B* **742** (2006) 59–85, [hep-ph/0510164].

[82] G. Giudice, C. Grojean, A. Pomarol, and R. Rattazzi, "The Strongly-Interacting Light Higgs," *JHEP* **06** (2007) 045, [hep-ph/0703164].

[83] R. Barbieri, B. Bellazzini, V. S. Rychkov, and A. Varagnolo, "The Higgs boson from an extended symmetry," *Phys. Rev. D* **76** (2007) 115008, [arXiv:0706.0432].

[84] C. Grojean, O. Matsedonskyi, and G. Panico, "Light top partners and precision physics," *JHEP* **10** (2013) 160, [arXiv:1306.4655].

[85] K. Agashe, R. Contino, L. Da Rold, and A. Pomarol, "A Custodial symmetry for $Zb\bar{b}$," *Phys. Lett.* **B641** (2006) 62–66, [hep-ph/0605341].

[86] B. Batell, S. Gori, and L.-T. Wang, "Higgs Couplings and Precision Electroweak Data," *JHEP* **01** (2013) 139, [arXiv:1209.6382].

[87] H. Georgi and D. B. Kaplan, "Composite Higgs and Custodial SU(2)," *Phys. Lett.* **145B** (1984) 216–220.

[88] M. J. Dugan, H. Georgi, and D. B. Kaplan, "Anatomy of a Composite Higgs Model," *Nucl. Phys.* **B254** (1985) 299–326.

Chapter 3

Composite Flavon-Higgs Models

Yi Chung

Center for Quantum Mathematics and Physics (QMAP), Department of Physics, University of California, Davis, CA 95616, U.S.A.

We consider a composite Higgs model based on the $SU(6)/Sp(6)$ coset, where an $U(1)$ subgroup of $Sp(6)$ is identified as the flavor symmetry. A complex scalar field s, which is a pseudo-Nambu-Goldstone boson of the broken symmetry, carries a flavor charge and plays the role of a flavon field. The $U(1)_F$ flavor symmetry is then broken by a VEV of the flavon field, which leads to a small parameter and generates the mass hierarchy between the top and bottom quarks. A light flavon below the TeV scale can be naturally introduced, which provides a fully testable model for the origin of flavor hierarchy. A light flavon also leads to substantial flavor changing neutral currents, which are strongly constrained by the flavor experiments. The direct search of additional scalar bosons can also be conducted in HL-LHC and future hadron colliders.

3.1 Introduction

The Standard Model (SM) of particle physics successfully describes all known elementary particles and their interactions. However, there are still a few puzzles that have yet to be understood, including two mysterious hierarchies. One is the well-known **hierarchy problem**. With the discovery of light Higgs bosons in 2012 [1, 2], the last missing piece

of the SM seemed to be filled, but SM does not address the UV-sensitive nature of scalar bosons. The Higgs mass-squared receives quadratically divergent radiative corrections from the interactions with SM fields, which require an extremely sensitive cancellation to have a 125 GeV Higgs boson. The other puzzle is related to the large hierarchies in the masses and mixings of the SM fermions. Even within the quark sector, the masses of quarks span over six orders of magnitude. The mixing angles also show a hierarchical structure. The problem is known as the **flavor puzzle** [3], which represents the mysterious structure of SM Yukawa couplings.

One such appealing solution to the hierarchy problem is the composite Higgs model (CHM), where the Higgs doublet is the pseudo-Nambu-Goldstone bosons (pNGB) of a spontaneously broken global symmetry of the underlying strong dynamics [3, 4]. Through the analogy of the chiral symmetry breaking in quantum chromodynamics (QCD), which naturally introduces light scalar fields, i.e., pions, we can construct models with light Higgs bosons. In a CHM, an approximate global symmetry G is spontaneously broken by some strong dynamics down to a subgroup H with a symmetry breaking scale f. The heavy resonances of the strong dynamics are expected to be around the compositeness scale $\sim 4\pi f$. The pNGBs of the symmetry breaking, on the other hand, can naturally be light with masses $< f$ as they are protected by the shift symmetry.

For the flavor puzzle, the hierarchy in the masses and mixings of the SM fermions can be achieved by assuming an abelian $U(1)_F$ flavor symmetry [6], where different SM fermions carry different charges. The low-energy effective Yukawa coupling terms require the insertion of additional scalar fields as

$$\mathcal{L}_{\text{Yukawa}} = y_{ij} \left(\frac{s}{\Lambda_F} \right)^{a_{ij}} \bar{q}_{L,i} H q_{R,j}, \tag{3.1.1}$$

where y_{ij} is a $\mathcal{O}(1)$ coupling, the complex scalar field s is called flavon field, and Λ_F is the scale of flavor dynamics. After the flavon field acquires a VEV, it will lead to a small parameter $\epsilon = \langle s \rangle / \Lambda_F$ and result in the hierarchy of SM Yukawa couplings. It is known as the Froggatt-Nielsen (FN) mechanism. Despite the success in explaining the flavor structure, the scale of flavor dynamics is not predicted and can be arbitrarily high. Also, the flavon as a scalar boson receives large radiative corrections from the interactions with

SM fields and is expected to be well beyond the collider search.

In this paper, we explore models that can address these two problems at once and provide predictive experimental signatures which can be probed by colliders. We choose the specific CHMs with the unbroken subgroup large enough to include the $U(1)_F$ symmetry. That is, the flavor symmetry arises as part of the accidental global symmetry of the strong dynamics. Under this construction, the Higgs doublet and the flavon are pNGBs of the spontaneously broken global symmetries. In this case, the hierarchy problem is relieved, and a light flavon is naturally introduced, which provides a testable theory for the origin of flavor hierarchy.

Efforts to generate flavons as pNGBs have been implemented in the little flavon model [7, 8], which is aimed at realizing collective symmetry breaking on the flavon field. Versions combined with Higgs doublet were also studied [9, 10], but the large symmetry group makes them uncompelling. They also failed to treat the generation of Yukawa coupling carefully. Other attempts aiming at generating the Higgs and flavon from a common source have been studied recently [11], inspired by axiflavon models [12, 13]. However, the scalar flavon in the model is not the pNGB mode but the heavy unstable radial mode, which is hard to be detected, and the FN fields are elementary vector-like fermions added by hands. There are also other efforts to relate the flavor breaking scale to the electroweak scale but within the framework of 2HDM [14, 15].

For a concrete model, we consider a composite Higgs model based on the $SU(6)/Sp(6)$ coset, where the unbroken $Sp(6)$ is large enough to include both the SM gauge group and the global flavor symmetry group $SU(2)_W \times U(1)_Y \times U(1)_F$. The flavons as well as two Higgs doublets are the pNGBs of the coset. We then show how a suppressed Yukawa coupling can be generated through partial compositeness with specific flavor charge assignments. We discuss different scenarios to realize the Froggatt-Nielsen mechanism and generate the top-bottom mass hierarchy. The experimental constraints of different cases will also be discussed.

3.2 The $SU(6)/Sp(6)$ CHM

The $SU(6)/Sp(6)$ coset is one of the earliest cosets employed in little Higgs models [16] where the collective symmetry breaking for the quartic term was realized. Recently, it was considered for dark matter study [17] and natural Higgs potential [18]. It was pointed out in [18] that there is a $U(1)$ Peccei-Quinn like subgroup [19], which protects the theory from dangerous tadpole terms and flavor changing neutral currents. In this paper, this subgroup is identified as $U(1)_F$ flavor symmetry to realize the Froggatt-Nielsen mechanism. For our purpose, we will focus on the fermion sector and Yukawa couplings in the main text. The gauge sector and the pNGB potential are discussed in the Appendix. A more comprehensive discussion on these topics can also be found in [18].

3.2.1 Basics of $SU(6)/Sp(6)$

The $SU(6)/Sp(6)$ non-linear sigma model can be parametrized by a sigma field Σ^{ij}, which transforms as an anti-symmetric tensor representation **15** of $SU(6)$, where $i, j = 1, \ldots 6$ are $SU(6)$ indices. The transformation under $SU(6)$ can be expressed as $\Sigma \to g\,\Sigma\,g^T$ with $g \in SU(6)$ or as $\Sigma^{ij} \to g^i{}_k g^j{}_\ell \Sigma^{k\ell}$ with indices explicitly written out. The scalar field Σ has an anti-symmetric VEV $\langle\Sigma\rangle = \Sigma_0^{\alpha\beta}$ (with α, β representing $Sp(6)$ indices), where

$$\Sigma_0 = \begin{pmatrix} 0 & -\mathbb{I}_{3\times 3} \\ \mathbb{I}_{3\times 3} & 0 \end{pmatrix}. \tag{3.2.1}$$

The Σ VEV breaks $SU(6)$ down to $Sp(6)$, producing 14 Nambu-Goldstone bosons.

The 35 $SU(6)$ generators can be divided into unbroken ones and broken ones with each type satisfying

$$\begin{cases} \text{unbroken generators} & T_a : T_a\Sigma_0 + \Sigma_0 T_a^T = 0\ , \\ \text{broken generators} & X_a : X_a\Sigma_0 - \Sigma_0 X_a^T = 0\ . \end{cases} \tag{3.2.2}$$

The Nambu-Goldstone fields can be written as a matrix with the broken generators:

$$\xi(x) = \xi^i{}_\alpha(x) \equiv e^{\frac{i\pi_a(x)X_a}{2f}}. \tag{3.2.3}$$

Under $SU(6)$, the ξ field transforms as $\xi \to g\,\xi\,h^\dagger$ where $g \in SU(6)$ and $h \in Sp(6)$, so ξ carries one $SU(6)$ index and one $Sp(6)$ index. The relation between ξ and Σ field is given

by

$$\Sigma(x) = \Sigma^{ij}(x) \equiv \xi\,\Sigma_0\,\xi^T = e^{\frac{i\pi_a(x)X_a}{f}}\Sigma_0\ . \tag{3.2.4}$$

The complex conjugation raises or lowers the indices. The fundamental representation of $Sp(6)$ is (pseudo-)real and the $Sp(6)$ index can be raised or lowered by $\Sigma_0^{\alpha\beta}$ or $\Sigma_{0,\alpha\beta}$.

The broken generators and the corresponding fields in the matrix can be organized as follows ($\epsilon = i\sigma^2$):

$$\pi_a X_a = \begin{pmatrix} \frac{\phi_a}{\sqrt{2}}\sigma^a - \frac{\eta}{\sqrt{6}}\mathbf{1} & H_2 & \epsilon s & H_1 \\ H_2^\dagger & \frac{2\eta}{\sqrt{6}} & -H_1^T & 0 \\ \epsilon^T s^* & -H_1^* & \frac{\phi_a}{\sqrt{2}}\sigma^{a*} - \frac{\eta}{\sqrt{6}}\mathbf{1} & H_2^* \\ H_1^\dagger & 0 & H_2^T & \frac{2\eta}{\sqrt{6}} \end{pmatrix}. \tag{3.2.5}$$

In this matrix, there are 14 independent fields. They are (under $SU(2)_W$): a real triplet ϕ_a, a real singlet η, a complex singlet s (as the flavon field), and two Higgs (complex) doublets H_1 and H_2. We effectively end up with a two-Higgs-doublet model (2HDM). The observed Higgs boson will correspond to a mixture of h_1 and h_2 inside two Higgs doublets $H_1 = H_{1/2} \supset \frac{1}{\sqrt{2}}\binom{0}{h_1}$ and $H_2 = H_{-1/2} \supset \frac{1}{\sqrt{2}}\binom{h_2}{0}$. Using the ξ and Σ matrices, we can construct the low energy effective Lagrangian for the flavon field, the Higgs fields, and all the other pNGBs.

3.2.2 Unbroken subgroups of $Sp(6)$

To realize the FN mechanism, we need a global symmetry with scalars and fermions charged under it. Within the $Sp(6)$ symmetry, there are several unbroken $U(1)$ symmetries. The symmetries with generators

$$\frac{1}{2}\begin{pmatrix} \sigma^a & 0 & 0 & 0 \\ 0 & 0 & 0 & 0 \\ 0 & 0 & -\sigma^{a*} & 0 \\ 0 & 0 & 0 & 0 \end{pmatrix} \quad \text{and} \quad \frac{1}{2}\begin{pmatrix} 0_{2\times2} & 0 & 0 & 0 \\ 0 & 1 & 0 & 0 \\ 0 & 0 & 0_{2\times2} & 0 \\ 0 & 0 & 0 & -1 \end{pmatrix} + X\mathbf{I}$$

are identified as the SM gauge group $SU(2)_W$ and $U(1)_Y$, which are discussed in Appendix A.

Besides the SM gauge group, there is one more $U(1)_F$ global symmetry with the generator

$$U(1)_F : \frac{1}{2}\begin{pmatrix} \mathbb{I}_{2\times 2} & 0 & 0 & 0 \\ 0 & 0 & 0 & 0 \\ 0 & 0 & -\mathbb{I}_{2\times 2} & 0 \\ 0 & 0 & 0 & 0 \end{pmatrix}.$$

Under $U(1)_F$, the complex scalar field s has charge 1, both Higgs doublets H have charge 1/2, and other pNGB fields have charge 0. The complex singlet s can then be identified as the composite flavon field. We then get the charge assignment for all pNGBs as

$$s : 1, \quad H_1,\ H_2 : 1/2, \quad \phi,\ \eta : 0\ , \tag{3.2.6}$$

which is a little different from the normal FN mechanism since Higgs also carries flavor charges [1]. So far, we get the desired scalar sector with the flavon and Higgs doublets. We can then move on to the fermion sector.

3.3 Yukawa coupling

In CHMs, the SM Yukawa couplings can arise from the partial compositeness mechanism [20]. That is, elementary fermions mix with composite operators of the same SM quantum numbers from the strong dynamics,

$$\mathcal{L} = \lambda_L \bar{q}_L O_R + \lambda_R \bar{q}_R O_L, \tag{3.3.1}$$

where q_L, q_R are elementary fermions and O_L, O_R are composite operators of some representations of $SU(6)$.

To be able to mix with the elementary fermions, the representations of the composite operators must contain states with the same SM quantum numbers as the SM fermions. To account for the correct hypercharge, e.g., $q_L = 2_{1/6}$ for left-handed quarks, $q_R = 1_{2/3}$ for right-handed up-type quarks, and $q_R = 1_{-1/3}$ for right-handed down-type quarks, the composite operators need to carry additional charges under the $U(1)_X$ outside $SU(6)$, and the

[1] In fact, this global symmetry is more similar to the $U(1)$ Peccei-Quinn (PQ) symmetry [19]. Models that identify $U(1)_{PQ}$ as flavor symmetry had been studied in axiflavon models [12, 13]. However, in this paper, we will not deal with the strong CP problem and axions, so we would like to call it $U(1)_F$ flavor symmetry.

SM hypercharge is a linear combination of the $SU(6)$ generator $\mathrm{Diag}(0,0,1/2,0,0,-1/2)$ and X.

Let us start with the top quark. To get the top Yukawa coupling, the suitable and economical choice of composite operators is $\mathbf{6}$ with $X = 1/6$. The composite operator as a $\mathbf{6}_{1/6}$ of $SU(6)$ (where the subscript 1/6 denotes its $U(1)_X$ charge) can be decomposed under the SM gauge group as

$$O^i_{L,R} \sim \xi^i{}_\alpha Q^\alpha_{L,R} \sim \mathbf{6}_{1/6} = \mathbf{2}_{1/6} \oplus \mathbf{1}_{2/3} \oplus \bar{\mathbf{2}}_{1/6} \oplus \mathbf{1}_{-1/3}, \tag{3.3.2}$$

where $Q_{L,R}$ are the corresponding composite resonances. The composite states $Q_{L,R}$ belong to the $\mathbf{6}$ representations of $Sp(6)$ and play the roles of SM fermion composite partners. For $SU(2)$, $\mathbf{2}$ and $\bar{\mathbf{2}}$ are equivalent and related by the ϵ tensor. We make the distinction to keep track of the order of the fermions in a doublet. We see that the composite states have the appropriate quantum numbers to mix with the SM quarks.

The left-handed top quark can mix with the first two components of the sextet. The mixing term can be express as

$$\lambda_L \bar{q}_{La} \Lambda^a{}_i O^i_R = \lambda_L \bar{q}_{La} \Lambda^a{}_i \left(\xi^i{}_\alpha Q^\alpha_R\right), \tag{3.3.3}$$

where a represents an $SU(2)_W$ index, and

$$(\Lambda)^a{}_i = \Lambda = \begin{pmatrix} 1 & 0 & 0 & 0 & 0 & 0 \\ 0 & 1 & 0 & 0 & 0 & 0 \end{pmatrix} \tag{3.3.4}$$

is the spurion which keeps track of the symmetry breaking.

To get the complete top Yukawa coupling, we couple the elementary right-handed top quark to the $\bar{\mathbf{6}}_{1/6}$, which decomposes under $SU(2)_W \times U(1)_Y$ as

$$O'_{L,Rj} \sim \xi^*{}_j{}^\beta \Sigma_{0\beta\alpha} Q^\alpha_{L,R} \sim \bar{\mathbf{6}}_{1/6} = \bar{\mathbf{2}}_{1/6} \oplus \mathbf{1}_{-1/3} \oplus \mathbf{2}_{1/6} \oplus \mathbf{1}_{2/3}\ . \tag{3.3.5}$$

The right-handed top quark mixes with the last component of the $\bar{\mathbf{6}}_{1/6}$, which can be written as

$$\lambda_{t_R} \bar{t}_R \Gamma_{t_R}{}^j O'_{Lj} = \lambda_{t_R} \bar{t}_R \Gamma_{t_R}{}^j \left(\xi^*{}_j{}^\beta \Sigma_{0\beta\alpha} Q^\alpha_L\right), \tag{3.3.6}$$

where $\Gamma_{t_R} = (0\ 0\ 0\ 0\ 0\ 1)$ is the corresponding spurion.

Combining λ_L and λ_{t_R} couplings, we can generate the SM Yukawa coupling for the top quark

$$\sim \lambda_L \lambda_{t_R} \bar{q}_{La} \Lambda^a{}_i \xi^i{}_\alpha \Sigma_0^{\alpha\beta} \xi^T{}_\beta{}^j \Gamma^\dagger_{t_R j} t_R \supset \lambda_L \lambda_{t_R} (\bar{q}_L H_2 t_R) \ . \tag{3.3.7}$$

The top quark gets its mass from the vacuum of H_2 as

$$m_t = \frac{\lambda_L \lambda_{t_R}}{g_T} \frac{v_2}{\sqrt{2}} \ , \tag{3.3.8}$$

where g_T is a coupling of the composite top partners.

Similarly, for the bottom quark, we can couple b_R to the third component of $\bar{\mathbf{6}}_{1/6}$ with the coupling λ_{b_R} and spurion $\Gamma_{b_R} = (0\ 0\ 1\ 0\ 0\ 0)$. This generates a bottom Yukawa coupling

$$\sim \lambda_L \lambda_{b_R} \bar{q}_{La} \Lambda^a{}_i \xi^i{}_\alpha \Sigma_0^{\alpha\beta} \xi^T{}_\beta{}^j \Gamma^\dagger_{b_R j} b_R \supset \lambda_L \lambda_{b_R} (\bar{q}_L H_1 b_R) \ , \tag{3.3.9}$$

where the bottom quark gets its mass from the vacuum of H_1 instead.

In this paper, we will not address the lepton sector, so there are only two types of 2HDMs satisfying the natural flavor conservation [21, 22]. They are categorized by Type-I and Type-II based on the Yukawa couplings of the quarks. So far, the Yukawa couplings of the third generation quarks come from different Higgs doublets, which implies a **Type-II 2HDM**. The smallness of the bottom quark mass can be achieved by a small VEV of H_1, i.e. a large tanβ Type-II 2HDM. However, the parameter space with a large tanβ is strongly constrained by direct searches, and it is also not what we want. To get mass hierarchy between the top and bottom through the FN mechanism, we want an insertion of the flavon field s in these Yukawa coupling terms.

3.4 Froggatt-Nielsen mechanism

3.4.1 FN mechanism: The first taste

Before we move on to the correct FN mechanism setup, let us first look at the flavor charges of quarks. In the previous section, all the quarks are embedded in $\mathbf{6}_{1/6}$ and $\bar{\mathbf{6}}_{1/6}$ of $SU(6)$ without additional flavor charges, which are decomposed under $SU(2)_W \times U(1)_F$

as

$$\mathbf{6}_0 = \mathbf{2}_{1/2} \oplus \mathbf{1}_0 \oplus \bar{\mathbf{2}}_{-1/2} \oplus \mathbf{1}_0 \ , \tag{3.4.1}$$

$$\bar{\mathbf{6}}_0 = \bar{\mathbf{2}}_{-1/2} \oplus \mathbf{1}_0 \oplus \mathbf{2}_{1/2} \oplus \mathbf{1}_0 \ . \tag{3.4.2}$$

It means that the flavor charges of fermions are set as

$$q_L = (t_L,\ b_L)^T : 1/2, \quad t_R,\ b_R : 0 \ , \tag{3.4.3}$$

where both right-handed quarks have no flavor charge.

Within this assignment, we can already write down a suppressed bottom quark mass through the FN mechanism by the term like

$$\frac{1}{f}\left(\bar{q}_L s\tilde{H}_2 b_R\right) \sim \left(\frac{v_s v_2}{2f}\right)\bar{b}_L b_R \ , \tag{3.4.4}$$

where v_s is the VEV of the flavon field. The term satisfies the flavor symmetry. The reason it is possible is that the top quark gets mass from H with flavor charge $1/2$, but the bottom quark can get mass from $\tilde{H}$ with flavor charge $-1/2$. However, it turns out that this term can not successfully realize the FN mechanism in this model.

To see that, we can go back to the term we derived for the bottom quark mass in Eq. (3.3.9). In the non-linear Sigma model, if we expand the Σ field to the next order, it becomes

$$\bar{q}_L(H_1 + \frac{i}{2f}s\tilde{H}_2)b_R \supset \frac{i}{2f}\left(\bar{q}_L s\tilde{H}_2 b_R\right) \ , \tag{3.4.5}$$

which already contains the term in Eq. (3.4.4). That means, due to the shift symmetry of pNGBs, the term $s\tilde{H}_2$ can only show up following H_1. That also means we can always transfer the nontrivial vacuum of $\langle s\tilde{H}_2\rangle$ to the leading order $\langle H_1\rangle$ by shift symmetry. Therefore, the bottom quark mass still comes from $\langle H_1\rangle$, and it is equivalent to the Type-II 2HDM we have already gotten.

If we define $\Delta_f \equiv [f_L] - [f_R]$ as the difference between flavor charges of left-handed and right-handed fermions. Fixing the top quark charge as in Eq. (3.4.3) with $\Delta_t = 1/2$, we find that $\Delta_b = 1/2$ gives us the bottom quark mass through H_1, which leads to a Type-II

2HDM. $\Delta_b = -1/2$, instead, generates the bottom quark mass through $\tilde{H}_2$ and makes it a Type-I 2HDM. Either case is just normal 2HDM. To realize the FN mechanism, we need to have a larger $|\Delta_b|$, which would allow us to generate the bottom Yukawa coupling term with the insertion of two pNGBs, s and H, at the same time. That also requires us to embed the bottom quark into a larger representation, which will generate a term with the insertion of two Σ fields.

3.4.2 Antisymmetric tensor representation 15 and $\bar{15}$

The minimal choice is to have a bit larger $|\Delta_b| = 3/2$. There are two cases, case (1) with $\Delta_b = 3/2$ and case (2) with $\Delta_b = -3/2$. By analyzing the quantum numbers, we expect to generate bottom Yukawa coupling terms as

$$(1)\ \bar{q}_L s H_1 b_R \quad \text{and} \quad (2)\ \bar{q}_L s^* \tilde{H}_2 b_R. \tag{3.4.6}$$

To realize such $|\Delta_b|$, the minimal choice is to use antisymmetric tensor representation **15** and $\bar{\mathbf{15}}$. To mix the SM quarks with composite operators, we first analyze their SM quantum numbers. To have operators sharing the same quantum numbers with the SM quarks, additional gauge $U(1)_X$ and global $U(1)_R$ are required. With additional x and r charges, the representation $\mathbf{15}_{x,r}$ can be decomposed under $SU(2)_W \times U(1)_Y \times U(1)_F$ as

$$\begin{aligned}\mathbf{15}_{x,r} =& (\mathbf{3} \oplus \mathbf{1})_{x,r} \oplus \mathbf{2}_{x+\frac{1}{2},r+\frac{1}{2}} \oplus \mathbf{2}_{x-\frac{1}{2},r+\frac{1}{2}} \oplus \bar{\mathbf{2}}_{x+\frac{1}{2},r-\frac{1}{2}} \\ & \oplus \bar{\mathbf{2}}_{x-\frac{1}{2},r-\frac{1}{2}} \oplus \mathbf{1}_{x,r+1} \oplus \mathbf{1}_{x,r} \oplus \mathbf{1}_{x,r-1},\end{aligned} \tag{3.4.7}$$

where the first subscript denotes its hypercharge and the second subscript denotes its flavor charge. Or we can write them in matrix form as

$$\mathbf{15}_{x,r} = \begin{pmatrix} 1_{x,r+1} & 2_{x+\frac{1}{2},r+\frac{1}{2}} & (3 \oplus 1)_{x,r} & 2_{x-\frac{1}{2},r+\frac{1}{2}} \\ \cdot & 0 & \bar{2}_{x+\frac{1}{2},r-\frac{1}{2}} & 1_{x,r} \\ \cdot & \cdot & 1_{x,r-1} & \bar{2}_{x-\frac{1}{2},r-\frac{1}{2}} \\ \cdot & \cdot & \cdot & 0 \end{pmatrix}, \tag{3.4.8}$$

and also for it complex conjugate $\bar{\mathbf{15}}_{x,r}$ as

$$\bar{\mathbf{15}}_{x,r} = \begin{pmatrix} 1_{x,r-1} & \bar{2}_{x-\frac{1}{2},r-\frac{1}{2}} & (3\oplus 1)_{x,r} & \bar{2}_{x+\frac{1}{2},r-\frac{1}{2}} \\ \cdot & 0 & 2_{x-\frac{1}{2},r+\frac{1}{2}} & 1_{x,r} \\ \cdot & \cdot & 1_{x,r+1} & 2_{x+\frac{1}{2},r+\frac{1}{2}} \\ \cdot & \cdot & \cdot & 0 \end{pmatrix}. \tag{3.4.9}$$

Since they are antisymmetric, we only put the numbers on the up-right triangle for simplicity.

3.4.3 Two ways to embed the bottom quark

Next, we want to mix the left-handed bottom quark with **15** and the right-handed bottom quark with $\bar{\mathbf{15}}$. The goal is to find a pair with $|\Delta_b| = 3/2$. From the previous decomposition, we found two pairs that satisfy our requirement:

$$\left(2_{x+\frac{1}{2},r+\frac{1}{2}}, 1_{x,r-1}\right) \quad \text{and} \quad \left(\bar{2}_{x+\frac{1}{2},r-\frac{1}{2}}, 1_{x,r+1}\right),$$

which correspond to case (1) with $\Delta_b = 3/2$ and case (2) with $\Delta_b = -3/2$ respectively.

Let us start with case (1) by taking the first pair with $x = -1/3$ and $r = 0$. Just as we have done before, we first write down the composite operators and the corresponding composite resonances as

$$O^{ij}_{L,R} \sim \xi^i{}_\alpha \xi^j{}_\beta Q^{\alpha\beta}_{L,R} \sim \mathbf{15}_{-\frac{1}{3},0} = \mathbf{14}_{-\frac{1}{3},0} \oplus \mathbf{1}_{-\frac{1}{3},0}, \tag{3.4.10}$$

where $Q_{L,R}$ are the corresponding composite resonances. $Q_{L,R}$ are **14** and **1** of $Sp(6)$ and play the roles of the SM fermion composite partners.

The mixing term for the left-handed quark can be expressed as

$$\lambda_{b_L} \bar{q}_{La} \Lambda^a{}_{ij} O^{ij}_R = \lambda_{b_L} \bar{q}_{La} \Lambda^a{}_{ij} \left(\xi^i{}_\alpha \xi^j{}_\beta Q^{\alpha\beta}_{L,R}\right), \tag{3.4.11}$$

where

$$(\Lambda)^a{}_{ij} = \left(\begin{pmatrix} 0 & 0 & 1 & 0 & 0 & 0 \\ 0 & 0 & 0 & 0 & 0 & 0 \\ -1 & 0 & 0 & 0 & 0 & 0 \\ 0 & 0 & 0 & 0 & 0 & 0 \\ 0 & 0 & 0 & 0 & 0 & 0 \\ 0 & 0 & 0 & 0 & 0 & 0 \end{pmatrix}, \begin{pmatrix} 0 & 0 & 0 & 0 & 0 & 0 \\ 0 & 0 & 1 & 0 & 0 & 0 \\ 0 & -1 & 0 & 0 & 0 & 0 \\ 0 & 0 & 0 & 0 & 0 & 0 \\ 0 & 0 & 0 & 0 & 0 & 0 \\ 0 & 0 & 0 & 0 & 0 & 0 \end{pmatrix} \right) \tag{3.4.12}$$

is the spurion that can help us keep track of symmetry breaking.

We still need to mix the right-handed bottom quark with the composite operators and the corresponding composite resonances as $O'_{L,Rij} \sim \xi^*{}_i{}^\alpha \xi^*{}_j{}^\beta \Sigma_{0\alpha\rho}\Sigma_{0\beta\sigma} Q^{\rho\sigma}_{L,R} \sim \bar{\mathbf{15}}_{-\frac{1}{3},0}$. The right-handed bottom quark need to mix with the $\mathbf{1}_{-\frac{1}{3},-1}$ of the $\bar{\mathbf{15}}_{-\frac{1}{3},0}$, which can be written as

$$\lambda_{b_R} \bar{b}_R \Gamma^{ij} O'_{Lij} = \lambda_{b_R} \bar{b}_R \Gamma^{ij} \left(\xi_i^{*\alpha} \xi_j^{*\beta} \Sigma_{0\alpha\rho}\Sigma_{0\beta\sigma} Q^{\rho\sigma}_{L,R} \right), \tag{3.4.13}$$

where

$$(\Gamma)^{ij} = \begin{pmatrix} 0 & 1 & 0 & 0 & 0 & 0 \\ -1 & 0 & 0 & 0 & 0 & 0 \\ 0 & 0 & 0 & 0 & 0 & 0 \\ 0 & 0 & 0 & 0 & 0 & 0 \\ 0 & 0 & 0 & 0 & 0 & 0 \\ 0 & 0 & 0 & 0 & 0 & 0 \end{pmatrix} \tag{3.4.14}$$

is the corresponding spurion.

Combining λ_{b_L} and λ_{b_R} couplings, we can generate the bottom quark Yukawa coupling as

$$\begin{aligned} &\sim \lambda_{b_L}\lambda_{b_R} \bar{q}_{La} \Lambda^a{}_{ij} \xi^i{}_\alpha \xi^j{}_\beta \Sigma_0^{\alpha\rho}\Sigma_0^{\beta\sigma} \xi^T{}_\rho{}^k \xi^T{}_\sigma{}^l \Gamma^\dagger{}_{kl} b_R \\ &= \lambda_{b_L}\lambda_{b_R} \bar{q}_{La} \Lambda^a{}_{ij} \Sigma^{ik}\Sigma^{jl}\Gamma^\dagger{}_{kl} b_R \supset \lambda_{b_L}\lambda_{b_R} \left(\bar{q}_L s H_1 b_R\right) \ , \end{aligned} \tag{3.4.15}$$

which is exactly what we expect in Eq. (3.4.6). The bottom quark gets mass from H_1 but with additional suppression from the FN mechanism as

$$m_b = \frac{\langle is \rangle}{f} \frac{\lambda_{b_L}\lambda_{b_R}}{g_B} \frac{v_1}{\sqrt{2}} = \frac{\lambda_{b_L}\lambda_{b_R}}{g_B} \frac{v_s v_1}{2f}, \tag{3.4.16}$$

where g_B is a coupling of the composite bottom partners. This is like a Type-II 2HDM but with smaller $\tan\beta$ due to the suppression by small v_s/f.

Therefore, for case (1), we can get the top-bottom mass hierarchy. Assuming all the λ and g are $\mathcal{O}(1)$ couplings, the mass ratio becomes [2]

$$\frac{m_b}{m_t} \sim \frac{v_s}{\sqrt{2}f} \frac{v_1}{v_2} = \frac{\epsilon}{\tan\beta} \sim \frac{1}{60} \ , \tag{3.4.17}$$

[2]We consider the running of quark masses up to 1 TeV [23], which gives $m_b/m_t \sim 2.43$ GeV/150 GeV $\sim 1/60$. The ratio might be larger because the VEV of the flavon field is below the TeV scale.

where $\epsilon \equiv v_s/\sqrt{2}f$. The hierarchy comes from both ϵ and $\tan\beta$. Taking the symmetry breaking scale $f \sim 1$ TeV, we get

$$v_s \sim 25 \tan\beta \text{ GeV}, \tag{3.4.18}$$

If ϵ (namely v_s) is small, we can get a Type-II 2HDM with a smaller $\tan\beta$.

Similarly, consider case (2) by taking the second pair with $x = -1/3$ and $r = 1$, i.e. $\left(\bar{2}_{\frac{1}{6},\frac{1}{2}}, 1_{-\frac{1}{3},2}\right)$. The spurion for the left-handed quark becomes

$$(\Lambda)^a{}_{ij} = \left(\begin{pmatrix} 0&0&0&0&0&0\\ 0&0&0&0&0&0\\ 0&0&0&0&1&0\\ 0&0&0&0&0&0\\ 0&0&-1&0&0&0\\ 0&0&0&0&0&0 \end{pmatrix}, \begin{pmatrix} 0&0&0&0&0&0\\ 0&0&0&0&0&0\\ 0&0&0&1&0&0\\ 0&0&-1&0&0&0\\ 0&0&0&0&0&0\\ 0&0&0&0&0&0 \end{pmatrix} \right), \tag{3.4.19}$$

and for the right-handed bottom quark is

$$(\Gamma)^{ij} = \begin{pmatrix} 0&0&0&0&0&0\\ 0&0&0&0&0&0\\ 0&0&0&0&0&0\\ 0&0&0&0&1&0\\ 0&0&0&-1&0&0\\ 0&0&0&0&0&0 \end{pmatrix}. \tag{3.4.20}$$

Combining λ_{b_L} and λ_{b_R} couplings in case (2), we get the bottom Yukawa coupling as

$$\begin{aligned} &\sim \lambda_{b_L}\lambda_{b_R}\bar{q}_{La}\Lambda^a{}_{ij}\xi^i{}_\alpha\xi^j{}_\beta\Sigma_0^{\alpha\rho}\Sigma_0^{\beta\sigma}\xi^T{}_\rho{}^k\xi^T{}_\sigma{}^l\Gamma^\dagger{}_{kl}b_R \\ &= \lambda_{b_L}\lambda_{b_R}\bar{q}_{La}\Lambda^a{}_{ij}\Sigma^{ik}\Sigma^{jl}\Gamma^\dagger{}_{kl}b_R \supset \lambda_{b_L}\lambda_{b_R}\left(\bar{q}_L s^* \tilde{H}_2 b_R\right) . \end{aligned} \tag{3.4.21}$$

Again it is what we expect in Eq. (3.4.6). This case will lead to a Type-I 2HDM with the small bottom Yukawa coupling merely due to the FN mechanism as

$$m_b = \frac{\langle is\rangle}{f}\frac{\lambda_{b_L}\lambda_{b_R}}{g_B}\frac{v_2}{\sqrt{2}} = \frac{\lambda_{b_L}\lambda_{b_R}}{g_B}\frac{v_s v_2}{2f}. \tag{3.4.22}$$

Assuming all the λ are $\mathcal{O}(1)$ couplings. The mass ratio

$$\frac{m_b}{m_t} \sim \frac{v_s}{\sqrt{2}f} = \epsilon \sim \frac{1}{60} \quad \Longrightarrow \quad v_s \sim 25 \text{ GeV}, \tag{3.4.23}$$

if the symmetry breaking scale $f \sim 1$ TeV.

3.4.4 Composite resonances and spaghetti diagrams

In the last section, we see how the FN mechanism can be realized and create the hierarchy between the top and bottom mass. The composite resonances, which carry the same quantum number but different flavor charges, play the role of the Froggatt-Nielsen fields in the FN mechanism. We can write down all the composite resonances in matrix form as

$$\mathbf{15}_{-\frac{1}{3},0} = \mathbf{14}_{-\frac{1}{3},0} \oplus \mathbf{1}_{-\frac{1}{3},0} = \begin{pmatrix} 0 & \tilde{B}_1 & T_{\frac{1}{2}} & \tilde{B}'_0 & \tilde{T}_0 & \tilde{B}_{\frac{1}{2}} \\ \cdot & 0 & B_{\frac{1}{2}} & Y_0 & \tilde{B}''_0 & Y_{\frac{1}{2}} \\ \cdot & \cdot & 0 & B_{-\frac{1}{2}} & T_{-\frac{1}{2}} & 0 \\ \cdot & \cdot & \cdot & 0 & \tilde{B}_{-1} & Y_{-\frac{1}{2}} \\ \cdot & \cdot & \cdot & \cdot & 0 & \tilde{B}_{-\frac{1}{2}} \\ \cdot & \cdot & \cdot & \cdot & \cdot & 0 \end{pmatrix} \oplus \tilde{B}_0, \tag{3.4.24}$$

where T and B are composite resonances with the same quantum numbers as the SM top and bottom quarks but with different flavor charges as labeled in the subscript, $\tilde{T}$ and $\tilde{B}$ are resonances with the same hypercharges as the SM top and bottom quarks but under different $SU(2)_W$ representations, and Y are exotic resonances with hypercharge $-4/3$.

The FN mechanism can also be expressed through the "spaghetti diagrams", which looks like a 2 to 2 scattering in this case with only one flavon inserted. Spaghetti diagrams that generate the suppressed bottom quark mass are shown in Fig. 3.1. These diagrams give us the bottom mass we expect after integrating out the heavy Froggatt-Nielsen fields, which are composite fermionic resonances in this model, and replacing the scalar fields with their VEVs.

3.4.5 Comparison between two cases

So far, we see two different flavor charge assignments for the right-handed bottom quark, which lead to two different bottom Yukawa coupling terms. Both of them successfully gen-

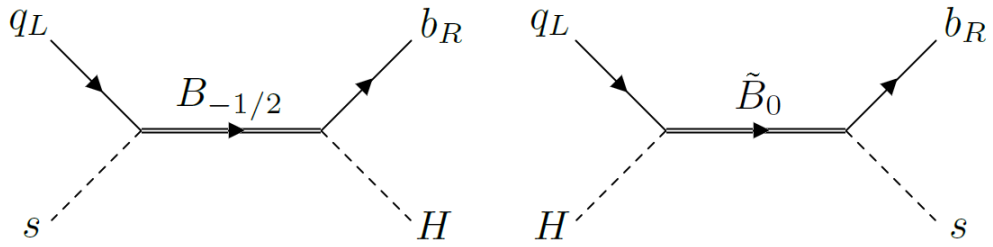

Fig. 3.1: Spaghetti diagrams that generate the bottom Yukawa coupling through the Froggatt-Nielsen mechanism in case (1). Diagrams for case (2) are similar.

erate a suppressed bottom Yukawa coupling through the FN mechanism. The difference between these two cases is listed in Table 3.1.

	Case (0)	Case (1)	Case (2)
$\Delta_b \equiv [q_L] - [b_R]$	1/2	3/2	$-3/2$
Flavor charge of b_R	0	-1	2
Coupling term	$\bar{q}_L H_1 b_R$	$\bar{q}_L s H_1 b_R$	$\bar{q}_L s^* \tilde{H}_2 b_R$
Type of 2HDM	Type-II	Type-II	Type-I
Suppression of m_b/m_t	$1/\tan\beta$	$\epsilon/\tan\beta$	ϵ

Table 3.1: The comparison between two cases with suppressed bottom Yukawa couplings through the FN mechanism. Case (0) for the unsuccessful first taste is also shown. In the last row, $\epsilon \equiv v_s/\sqrt{2}f$ is the suppression by the FN mechanism.

Here we assume the flavor charge of q_L is 1/2 and t_R is 0, such that the top quark mass comes from H_2. We can see the two cases represent different signs of Δ_b. It will affect the way we extend our model to include lighter quarks, which will be discussed next. The difference between the types of 2HDM results in different Higgs phenomenology. The second Higgs doublet is expected to be the main target among the exotic states in the model. The results of the direct searches will be shown in the next section. The factor of suppression is also related to the experimental constraint. The smaller ϵ required for the correct mass ratio implies a smaller VEV v_s of the flavon field, which will end up with a larger deviation in flavor observables and thus is strongly constrained.

3.4.6 Include all the generations

As yet, we only get the hierarchy between the top and bottom quarks, which belong to the third generation. To include the lighter quarks, more suppression is needed, which means more insertion of the flavon field s and a larger difference in flavor charges. This will require the lighter quarks to be embedded in even larger representations.

Take case (1) for example. We have already gotten the flavor charges of the third generation quarks. To extend to the first and the second generations, one possible flavor charges assignment [3] is listed in Table 3.2. It implies that we need even larger representations to have flavor charges different by 7/2. That would require representations with more than 4 indices for the quark sector.

	$U(1)_F$		$U(1)_F$		$U(1)_F$
$q_{3,L} = (t_L, b_L)^T$	1/2	t_R	0	b_R	-1
$q_{2,L} = (c_L, s_L)^T$	3/2	c_R	0	s_R	-1
$q_{1,L} = (u_L, d_L)^T$	3/2	u_R	-2	d_R	-2

Table 3.2: A possible flavor charge assignment of all elementary quarks for case (1) setup.

For case (2), it is more difficult to get a consistent flavor charges assignment for the desired CKM matrix. For the flavor charge of the third generation quarks, we find that they follow the order $[b_R] > [q_L] > [t_R]$, which is also applied to the extension. From the relation, the left-handed quarks should always sit in the middle. This requirement restricts the flavor charge difference we can have. For example, $q_{1,L}$ and $q_{2,L}$ can only be either 1/2 or 3/2, which will lead to unsuppressed entries in the CKM matrix. Therefore, considering the flavor charge assignment for the light quarks, case (1) is preferred over case (2). However, we will still discuss the constraints on parameter space of case (2) assuming that it can generate a similar Yukawa matrix as case (1).

The exact embedding will be explored in future work. To discuss the experimental constraints of flavons in the following section, we will assume this mechanism can be extended to all the generations and is responsible for all the light quark masses in both cases.

[3] The assignment is borrowed from Eq. (2.15) of [14]. The resulting mass ratios and CKM matrix can partially reproduce observed values with $\mathcal{O}(1)$ correction.

Also, for flavon phenomenology, the results are mainly determined by two parameters, the flavon mass M_s and the flavon VEV v_s.

3.5 Collider Signature

The phenomenology of this model is similar to other CHMs based on $SU(6)/Sp(6)$ coset with partial compositeness [18], which includes 14 pNGBs and composite partners of the SM particles. The main targets would be on the particles that couple to SM particles at leading order. In our setup, the most important search modes include the second Higgs doublet, flavons, and fermionic composite resonances.

3.5.1 The second Higgs Doublet

The phenomenology of 2HDM has been well-studied, and we can directly borrow the results from [24]. For case (2) as a Type-I 2HDM, there is no further constraint since the second Higgs doublet is decoupled from the fermion sector. But for case (1), a Type-II 2HDM, the constraints are important because the suppression of the bottom mass comes partially from the FN mechanism and partially from $\tan\beta$. Therefore, the value of $\tan\beta$ will decide the ϵ we need from the FN mechanism. The strongest constraint for a Type-II 2HDM comes from the $\tau\tau$ search, which restricts $\tan\beta < 6 - 10$ for a wide mass scale. If we make it a Flipped 2HDM instead, where the charged leptons get masses from H_2 instead of H_1, the coupling between heavy Higgs and $\tau\tau$ will become much smaller. Then the main constraint comes from $\bar{b}b$ search, and $\tan\beta \sim 20$ is still allowed. However, we would like to stick to a normal Type-II 2HDM for case (1) and set the benchmark with

$$\tan\beta \sim 6 \quad \Longrightarrow \quad v_s \sim 150 \text{ GeV} \tag{3.5.1}$$

for the following discussion.

3.5.2 Flavons

The physical flavon fields include a scalar component s and a pseudoscalar component a. The masses of two types of flavons depend on the complete flavon potential, which is discussed in the Appendix B. If flavor symmetry is exact and spontaneously broken by flavor symmetry conserving potential, then the pseudoscalar flavon should be massless,

which is not acceptable. Therefore, the explicit breaking of flavor symmetry in the flavon potential is needed. For simplicity, we will assume the mass of scalar, M_s, and the mass of pseudoscalar, M_a, are the same. This spectrum can be achieved if flavor symmetry is broken by a tadpole term in the flavon potential as shown in Appendix B. Therefore, from now on, we will use flavon s for both the scalar and pseudoscalar components and M_s for the flavon mass, which is expected to be at the sub-TeV scale.

The production and decay of flavons have already been comprehensively discussed in [25, 26]. Although the flavon coupling terms in these papers might look different from ours, the exact values are determined by the observed quark masses and the CKM matrix. Therefore, the flavon couplings with the form m/v_s should have similar values in all kinds of flavon models up to an $\mathcal{O}(1)$ factor. The numerical values in these two sections are derived based on their analysis with additional adjustments from our setup.

The main production for sub-TeV flavons come from the single production process $b\bar{b} \to s$. The cross section for flavons with $M_s = 500$ GeV is

$$\sigma(b\bar{b} \to s) \sim 9.8 \times 10^{-3} \left(\frac{150 \text{ GeV}}{v_s}\right)^2 \text{ pb} \tag{3.5.2}$$

in 14 TeV LHC. Taking $v_s = 150$ GeV, around 2.2×10^4 flavons will be produced in the HL-LHC era with an integrated luminosity of 3 ab^{-1}. In case (2) with smaller v_s, the number is multiplied by a factor of 36.

The decay branching ratios for flavons are independent of v_s but only depend on the flavor structure. If flavons only couple to the third generation, the dominate decay channel will be $b\bar{b}$ channel and $\tau\tau$ channel with roughly $\sim 85\%$ and $\sim 15\%$ branching ratio. If the FN mechanism is extended to all SM particles and responsible for the full Yukawa matrix, then there will be exotic final states like tc and tu. It turns out that the tc channel will be the dominant one due to the large mixing required to reproduce the desired CKM matrix. The ratios depend on $\tan\beta$, too. Under the benchmark values, we get the branching ratios for each channels as tc (96.8%), $b\bar{b}$ (2.7%), and $\tau\tau$ (0.5%). However, the hadronic channels suffer from large backgrounds. The leptonic channel can reach $\sigma \times BR \sim 10^{-3}$ pb for sub-TeV flavon in HL-LHC, but it is still above the benchmark value. The discovery can be made in a future 100 TeV collider, where the cross section is expected to be ~ 100

times larger, and the integrated luminosity is also higher. In that case, the distinct tc channel search will provide strong evidence for the origin of the Yukawa matrix.

3.5.3 Fermionic Resonances

The top partners in the $SU(6)/Sp(6)$ CHM are vector-like fermionic resonances that form a sextet of the $Sp(6)$ global symmetry. Their quantum numbers under the SM gauge symmetry are $(3, 2, 1/6)[\times 2]$, $(3, 1, 2/3)$, and $(3, 1, -1/3)$, which are identical to those of the SM quarks. There are no exotic states with higher or lower hypercharges. These states are degenerate in the limit of unbroken $Sp(6)$ global symmetry. Only small splittings arise from the explicit symmetry breaking effects. Their mass $M_T \sim g_T f$ plays the important role of cutting off the quadratic contribution from the top quark loop to the Higgs potential. The generic expectation of the composite fermionic resonances is $M_F = 5 - 10$ TeV with $g_F = 5 - 10$. However, naturalness prefers a smaller M_T to minimize the required fine-tuning, which usually requires $g_T \gtrsim 1$. The current bound on the top partner mass has reached ~ 1.2 TeV [27, 28]. The HL-LHC can further constrain the mass up to ~ 1.5 TeV [78]. A future 100 TeV collider will cover the entire interesting mass range of the top partners if no severe tuning conspires.

For the bottom partners, they form a $\mathbf{14}_{-1/3} \oplus \mathbf{1}_{-1/3}$ under $Sp(6)$ global symmetry. The quantum numbers for the total of 15 fields under the SM gauge group are $(3, 2, 1/6)[\times 2]$, $(3, 2, -5/6)[\times 2]$, $(3, 1, -1/3)[\times 4]$, and $(3, 3, -1/3)$, which include exotic resonances with EM charge $-4/3$. The states are not degenerate, and the singlet is expected to be lighter. The masses of the bottom partners $M_B \sim g_B f$, unlike the top partners, do not have a large effect on the fine-tuning due to the small bottom Yukawa coupling. Therefore, they could be around the compositeness scale with $M_B = 5 - 10$ TeV, which is beyond the LHC searches. The heavier $M_B \sim g_B f$ also leads to additional suppression g_T/g_B on the mass ratio between the top and bottom quarks, which can relieve the required ϵ we need.

If we extend the FN mechanism to the light generations, a larger representation is required to get a larger flavor charge difference, which also implies a larger EM charge difference within the multiplet. Therefore, there could be more exotic resonances with EM charges like $-7/3$ or $5/3$, which are important in identifying the correct representation.

These heavy fermionic resonances can be found in a future 100 TeV collider. If the exotic spectrum corresponding to the large representation shows up, it might unveil the nature of SM fermion partners and the origin of Yukawa couplings.

3.6 Flavor constraints

Compared to the collider signatures, the flavor constraints usually probe a higher scale and place stronger bounds on the models. Assume that the FN mechanism can be extended to all elementary quarks and leptons with suitable Yukawa coupling matrices. Then we can discuss the flavor constraints through a similar analysis as in [26].

The new flavor processes can be mediated through flavons or the second Higgs doublet. The flavon contributions strongly depend on the couplings and spectrum of flavons. As we mention above, there are a scalar component and a pseudoscalar component. We will assume the scalar and pseudoscalar components share the same mass M_s. This assumption will give us the weakest flavor constraints because, for some flavor processes, the contributions from a scalar and a pseudoscalar will cancel exactly if they are degenerate. It can also be understood that the assumption raises an $U(1)$ symmetry for the flavon field around the vacuum, which forbids these flavor processes. However, we will see even the weakest constraints from flavor are much stronger than the direct searches.

3.6.1 Meson Decay

The new particles might enhance some rare processes that are suppressed within SM. The measurements of rare decays of neutral mesons can give strong constraints on the new physics scale. In this model, flavons can mediate some rare decays of neutral mesons. For example, the branching ratio of $B_s \to \mu^+\mu^-$ provides a constraint on dimension-6 operators induced by flavons, which include

$$C_S^{ij}(\bar{q}_i P_L q_j)(\bar{\ell}\ell) \quad \text{and} \quad \tilde{C}_S^{ij}(\bar{q}_i P_R q_j)(\bar{\ell}\ell) \tag{3.6.1}$$

from a scalar flavon with coefficient

$$C_S^{ij} = g_{\ell\ell} g_{ji} \left(\frac{1}{M_s^2}\right) \quad \text{and} \quad \tilde{C}_S^{ij} = g_{\ell\ell} g_{ij} \left(\frac{1}{M_s^2}\right) \tag{3.6.2}$$

and

$$C_P^{ij}(\bar{q}_i P_L q_j)(\bar{\ell}\gamma_5\ell) \quad \text{and} \quad \tilde{C}_P^{ij}(\bar{q}_i P_R q_j)(\bar{\ell}\gamma_5\ell) \tag{3.6.3}$$

from a pseudoscalar flavon with coefficient

$$C_P^{ij} = g_{\ell\ell} g_{ji} \left(\frac{1}{M_a^2}\right) \quad \text{and} \quad \tilde{C}_P^{ij} = g_{\ell\ell} g_{ij} \left(\frac{1}{M_a^2}\right). \tag{3.6.4}$$

The difference between C and $\tilde{C}$ will modify the predicted SM values. The leading order deviation comes from the pseudoscalar flavon exchange, which interferes with the SM contribution. The coupling g_{ij} is determined by the observed fermion masses over the flavon VEV v_s. Therefore, once we take the mass $M_s = M_a$, the measurement can put a constraint on the $C_P^{ij} - \tilde{C}_P^{ij}$ and thus the product of $v_s M_s$. Later we will find that most of the flavor constraints can be transferred into the constraint on the value of $v_s M_s$.

The latest result of $B_s \to \mu^+\mu^-$ measurement by LHCb [30] requires $v_s M_s \geq 5 \times 10^4$ $(\text{GeV})^2$, which give a M_s lower bound under the benchmark value as

$$\text{case (1) } M_s \geq 400 \text{ (GeV)}, \quad \text{case (2) } M_s \geq 2000 \text{ (GeV)}.$$

There is a stronger constraint for case (2) flavon model with smaller v_s. The reason is, though we want to have a small v_s to generate the hierarchy, a small v_s also implies a larger coupling between flavons and the SM quarks, which is disfavored by flavor physics. We also find that case (1) as a Type-II 2HDM has a looser bound due to the assistance from $\tan\beta$. The improvement in the measurement of $\text{BR}(B_s \to \mu^+\mu^-)$ will further constraints the allowed values in the future. The interesting parameter space might be ruled out by LHCb and Belle-II.

Meson decays also put strong constraints on the second Higgs doublet. A light charged Higgs boson can induce a significant contribution to the branching ratio $\text{BR}(B \to X_s\gamma)$ [31, 32, 33, 34, 35, 36]. In the Type-II or flipped 2HDM, this gives a strong lower bound on the charged Higgs boson mass $M_{H^\pm} > 600$ GeV [37, 38], which would require a tuning or an additional symmetry in the 2HDM potential in case (1) model.

3.6.2 Neutral Meson Mixing

The strongest bounds for flavons come from the neutral meson mixing, especially from the light mesons. The relevant $\Delta F = 2$ interaction terms include

$$C_2^{ij}(\bar{q}_R^i q_L^j)^2, \quad \tilde{C}_2^{ij}(\bar{q}_L^i q_R^j)^2, \quad \text{and} \quad C_4^{ij}(\bar{q}_R^i q_L^j)(\bar{q}_L^i q_R^j).$$

In this paper, since we assume that the scalar and pseudoscalar flavons share the same mass M_s, there is an $U(1)$ symmetry that forbids C_2^{ij} and $\tilde{C}_2^{ij}$ terms. That is, the contributions from scalars and pseudoscalars will cancel exactly. The only relevant dimension-6 operator is

$$C_4^{ij}(\bar{q}_R^i q_L^j)(\bar{q}_L^i q_R^j) \quad \text{with} \quad C_4^{ij} = -g_{ij} g_{ji}^* \left(\frac{1}{M_s^2}\right). \tag{3.6.5}$$

The coefficients as a function of $v_s M_s$ are strongly constrained by experiments.

In Table 3.3, we conclude the flavor constraints on the product $v_s M_s$ from all neutral meson systems, including those with the first generation quarks. The numbers are extracted from [26]. The corresponding lower bounds on flavon mass M_s are also shown based on the benchmark value of each case.

	$v_s M_s$ (GeV^2)	Case (1) (GeV)	Case (2) (GeV)
C_{B_s}	32000	210	1280
φ_{B_s}	128000	850	5120
C_{B_d}	183000	1220	7320
φ_{B_d}	250000	1670	10000
Δm_K	255000	1700	10200
ϵ_K	2550000	17000	102000

Table 3.3: Flavor constraints from all kinds of neutral meson mixing observables, including the lower bounds on the value of $v_s M_s$ and flavon mass M_s of each case.

From the constraints of neutral meson mixing, we again find that case (1) is preferred because case (2) has a smaller v_s and thus larger couplings to the SM fermions. The lower bounds for case (2) have reached multi-TeV, which might be too heavy to be treated as pNGBs. The flavor symmetry is hardly broken, and the sigma model might not be

an appropriate way to describe it. Even for case (1) with milder bounds, constraints from the CP phases are also high. If we assume that the flavon preserves CP-symmetry and ignore the constraints from the CP phase, the current bounds for case (1) become $M_s \geq 1.2 - 1.7$ TeV, and the future experiments will raise the bounds by a factor of 2. If the FN mechanism is not responsible for the first generation quarks, then the only constraint is from C_{B_s}, and a sub-TeV flavon is still allowed. The bounds can also be relieved if the bottom partner is heavier than the top partner, where $g_B > g_T$ can give another suppression, and the required v_s can be larger. Nevertheless, the most interesting mass region for flavons as pNGBs of the TeV scale confinement will be covered in the near future by LHCb and Belle-II.

3.7 Conclusions

The Froggatt-Nielsen mechanism is an appealing solution to the Flavor Puzzle. However, the scale of flavor dynamics and the flavon field can be arbitrarily high. The predictive flavon models require the dynamics to stabilize the flavon potential. One way, analogous to the composite Higgs models, is to introduce the flavon field as a pseudo-Nambu-Goldstone boson. In this paper, we construct a non-linear sigma model with pNGBs, including both the Higgs doublets and the flavon field.

The flavon field as a pNGB provides a possibility to have the origin of flavor hierarchy at the TeV scale. The shift symmetry is slightly broken, which leads to the flavon mass and VEV. The non-linear nature of the flavon also constraints the interactions we can write down. In this paper, we show two possible ways to generate suppressed bottom Yukawa coupling terms through the Froggatt-Nielsen mechanism, where the composite resonances play the role of the FN fields. The derivation and explanation of the process are presented in detail.

Two cases lead to different phenomenology and receive different constraints. Case (1) as a Type-II 2HDM with small $\tan\beta$ has a larger v_s and smaller couplings to the SM fermions. Some parameter space with the sub-TeV flavon is still allowed if the constraints from the neutral meson of the first generation quarks are not taken into account. Case (2)

as a Type-I 2HDM has a weaker bound on the Higgs sector. However, the requirements of small v_s and the strong couplings with the SM particles are disfavored. Future measurements of neutral meson systems by LHCb and Belle-II will keep probing the scenario with the light flavon. Either push the mass bound to a much higher scale or find the existence of the pNGB flavon.

Acknowledgements

We thank Hsin-Chia Cheng for useful discussions. This work is supported by the Department of Energy Grant number DE-SC-0009999.

Appendix A: The SM gauge sector

The SM electroweak gauge group $SU(2)_W \times U(1)_Y$ is embedded in $SU(6) \times U(1)_X$ with generators given by

$$\frac{1}{2}\begin{pmatrix} \sigma^a & 0 & 0 & 0 \\ 0 & 0 & 0 & 0 \\ 0 & 0 & -\sigma^{a*} & 0 \\ 0 & 0 & 0 & 0 \end{pmatrix} \quad \text{and} \quad \frac{1}{2}\begin{pmatrix} 0_{2\times 2} & 0 & 0 & 0 \\ 0 & 1 & 0 & 0 \\ 0 & 0 & 0_{2\times 2} & 0 \\ 0 & 0 & 0 & -1 \end{pmatrix} + X\mathbf{I} \ .$$

The extra $U(1)_X$ factor accounts for the different hypercharges of the SM fermions but is not relevant for the bosonic fields. These generators belong to $Sp(6) \times U(1)_X$ and are not broken by Σ_0.

Using the Σ field, the Lagrangian for kinetic terms of Higgs boson is given by

$$\mathcal{L}_h = \frac{f^2}{4}\mathrm{tr}\left[(D_\mu \Sigma)(D^\mu \Sigma)^\dagger\right] + \cdots \ , \tag{3.7.1}$$

where D_μ is the electroweak covariant derivative. Expanding this term, we get

$$\mathcal{L}_h = \frac{1}{2}(\partial_\mu h_1)(\partial^\mu h_1) + \frac{1}{2}(\partial_\mu h_2)(\partial^\mu h_2) + \frac{f^2}{2} g_W^2 \left(\sin^2 \frac{\sqrt{h_1^2 + h_2^2}}{\sqrt{2} f}\right)\left[W_\mu^+ W^{-\mu} + \frac{Z_\mu Z^\mu}{2\cos\theta_W}\right] \ . \tag{3.7.2}$$

The non-linear behavior of the Higgs boson in CHMs is apparent from the dependence of trigonometric functions.

The W boson acquires a mass when h_1 and h_2 obtain nonzero VEVs V_1 and V_2 of

$$m_W^2 = \frac{f^2}{2} g_W^2 \left(\sin^2 \frac{\sqrt{V_1^2 + V_2^2}}{\sqrt{2} f}\right) = \frac{1}{4} g_W^2 (v_1^2 + v_2^2), \tag{3.7.3}$$

where

$$v_i \equiv \sqrt{2} f \frac{V_i}{\sqrt{V_1^2 + V_2^2}} \sin \frac{\sqrt{V_1^2 + V_2^2}}{\sqrt{2} f} \approx V_i = \langle h_i \rangle \ . \tag{3.7.4}$$

The parameter that parametrizes the nonlinearity of the CHM is given by

$$\xi \equiv \frac{v^2}{f^2} = 2 \sin^2 \frac{\sqrt{V_1^2 + V_2^2}}{\sqrt{2} f} \ , \tag{3.7.5}$$

where the VEV $v^2 = v_1^2 + v_2^2 = (246 \text{ GeV})^2$. The ξ plays an important role in the phenomenology of CHMs, but it is not of interest in this study.

Appendix B: The pNGB potential

The pNGB potential comes from the explicit breaking of $SU(6)$ global symmetry. Within SM, there are symmetry-breaking sources like the gauge couplings and Yukawa couplings. Additional sources are also needed to introduce the flavon potential. Here we will briefly list their contributions to the pNGB potential one by one.

Starting with the SM gauge interactions, we can derive the pNGB potential by the generators listed in Appendix A. Both $SU(2)_W$ and $U(1)_Y$ only break the global symmetry partially and generate the potential for the pNGBs which are charged. The two Higgs doublets are charged under both gauge interactions and get

$$\Delta V_H = \frac{3}{16\pi^2}\left(\frac{3}{4}c_w g^2 + \frac{1}{4}c' g'^2\right) M_\rho^2 |H|^2, \tag{3.7.6}$$

where $M_\rho \sim g_\rho f$ is the mass of the vector resonances ρ, which act as the gauge boson partners to cut off the gauge loop contribution to the pNGB masses, and c_w and c' are $\mathcal{O}(1)$ constants. The scalar triplet ϕ also gets a potential

$$\Delta V_\phi = \frac{3}{16\pi^2}\left(2c_w g^2\right) M_\rho^2 (\phi^a \phi_a), \tag{3.7.7}$$

The $SU(2)_W \times U(1)_Y$ singlets s and η do not receive potentials from the gauge interactions at this order, but they will obtain potentials elsewhere.

Next, the Yukawa coupling also breaks the $SU(6)$ global symmetry. Take the top quark loop-induced potential for example, where the required spurions are already written in section 3.3. We can estimate

$$\Delta V_H \sim -\frac{N_c}{8\pi^2}\lambda_L^2 \lambda_R^2 f^4 \left|(\Lambda)^a{}_i (\Gamma^*)_j \Sigma^{ij}\right|^2 \supset -\frac{N_c}{8\pi^2}\lambda_L^2 \lambda_R^2 f^2 |H|^2 = -\frac{N_c}{8\pi^2} y_t^2 M_T^2 |H|^2. \tag{3.7.8}$$

The dominant quartic term is also from the top loop as

$$\Delta V_H \sim \frac{N_c}{4\pi^2} y_t^4 |H|^4. \tag{3.7.9}$$

Similar potentials also arise for other SM Yukawa interactions.

The real singlet η does not get a potential at the leading order, but it couples quadratically to the Higgs doublets (e.g., from Eq. (3.7.8)), so it can still obtain a potential after

the Higgs doublets develop nonzero VEVs. Through Eq. (3.7.8), η gets a quadratic potential

$$\Delta V_\eta \sim \frac{3}{8\pi^2} y_t^2 M_T^2 \cdot \left(\frac{v}{f}\right)^2 \eta^2. \tag{3.7.10}$$

So far, we have not gotten any potential for the flavon field s. Although the flavon field in our model couples to the bottom quark, which will lead to a loop-induced pNGB potential. However, we would like to have the potential from a separate source, so they are independent of the FN mechanism. A nontrivial potential for the flavon field s is common in models with collective symmetry breaking [16, 18], where the potential

$$\Delta V \sim M_s^2 \left| s \pm \frac{i}{2f} \tilde{H}_2{}^\dagger H_1 \right|^2 \supset M_s^2 |s|^2 \tag{3.7.11}$$

is introduced. For example, in the $SU(6)/Sp(6)$ little Higgs model [16], the term can be generated by gauging two copies of $SU(2)$. However, it introduces new heavy gauge bosons W' and Z', which are strongly constrained.

Another way, following [18], is using the interactions between the elementary fermions and the resonances of the strong dynamics. In the section 3.3, we see that the elementary quark doublets can couple to composite operators of $SU(6)$ representations $\mathbf{6}$ and $\bar{\mathbf{6}}$ with $x = 1/6$ and $r = 0$, which are decomposed under $SU(2)_W \times U(1)_Y \times U(1)_F$ as

$$\mathbf{6}_{1/6,0} = \mathbf{2}_{1/6,1/2} \oplus \mathbf{1}_{2/3,0} \oplus \bar{\mathbf{2}}_{1/6,-1/2} \oplus \mathbf{1}_{-1/3,0}, \tag{3.7.12a}$$

$$\bar{\mathbf{6}}_{1/6,0} = \bar{\mathbf{2}}_{1/6,-1/2} \oplus \mathbf{1}_{-1/3,0} \oplus \mathbf{2}_{1/6,1/2} \oplus \mathbf{1}_{2/3,0}. \tag{3.7.12b}$$

Both operators create the same resonances, which belong to $\mathbf{6}$ of the $Sp(6)$ group.

Now consider two elementary quark doublets, q_L and q'_L, couple to the first two components of the composite operators of $\mathbf{6}$ and $\bar{\mathbf{6}}$ respectively, while both representations contain the same resonances:

$$\lambda_L \bar{q}_{La} \Lambda^a{}_i O_R^i = \lambda_L \bar{q}_{La} \Lambda^a{}_i \left(\xi^i{}_\alpha Q_R^\alpha\right), \tag{3.7.13}$$

where

$$(\Lambda)^a{}_i = \Lambda = \begin{pmatrix} 1 & 0 & 0 & 0 & 0 & 0 \\ 0 & 1 & 0 & 0 & 0 & 0 \end{pmatrix}, \tag{3.7.14}$$

and

$$\lambda'_L \vec{q}'_{La} \epsilon^{ab} \Omega_b{}^i O'_{Ri} = \lambda'_L \vec{q}'_{La} \epsilon^{ab} \Omega_b{}^i \left(\xi_i^{*\beta} \Sigma_{0\beta\alpha} Q_R^\alpha \right), \tag{3.7.15}$$

where

$$(\Omega)_a{}^i = \Omega = \begin{pmatrix} 1 & 0 & 0 & 0 & 0 & 0 \\ 0 & 1 & 0 & 0 & 0 & 0 \end{pmatrix} . \tag{3.7.16}$$

The combination of the two interactions breaks the $SU(6)$ global symmetry explicitly. It leads to a potential for the pNGBs at $\mathcal{O}(\lambda_L^2 \lambda_L'^2)$ of the form

$$\Delta V_s \propto [(\Lambda)^a{}_i (\Omega^*)^b{}_j \Sigma^{ij}][(\Omega)_b{}^m (\Lambda^*)_a{}^n \Sigma^*_{mn}] , \tag{3.7.17}$$

which can easily be checked by drawing a one-loop diagram, with q_L, q'_L, Q_R running in the loop. After expanding it, we obtain a flavon potential

$$\Delta V_s \sim \frac{N_c}{8\pi^2} \lambda_L^2 \lambda_L'^2 f^4 \left| (\Lambda)^a{}_i (\Omega^*)^b{}_j \Sigma^{ij} \right|^2 \supset M_s^2 |s|^2, \tag{3.7.18}$$

where

$$M_s^2 \sim \frac{N_c}{8\pi^2} \lambda_L^2 \lambda_L'^2 f^2 . \tag{3.7.19}$$

Notice that we have chosen different (generations of) elementary quark doublets, q_L and q'_L, in the two couplings such that the leading order potential is the quadratic term $|s|^2$.

To have a nontrivial flavon VEV, we want to introduce interactions that explicitly break the $U(1)_F$ symmetry. It can be achieved by mixing q_L to both resonances, which have the quantum number $\mathbf{2}_{1/6,1/2}$ and $\mathbf{2}_{1/6,-1/2}$, with coupling λ_L and λ''_L. In this way, the loop can be closed at $\mathcal{O}(\lambda_L \lambda''_L)$ and generate a s tadpole term

$$\Delta V_s \sim \frac{N_c}{8\pi^2} \lambda_L \lambda''_L f^4 \left(\epsilon_{ab} (\Lambda)^a{}_i (\Omega^*)^b{}_j \Sigma^{ij} \right) \sim \kappa\, s , \tag{3.7.20}$$

where

$$\kappa \sim \frac{N_c}{8\pi^2} \lambda_L \lambda''_L g_\psi^2 f^3. \tag{3.7.21}$$

Combining the two potentials we got, the flavon VEV is given by

$$v_s \sim \frac{\kappa}{M_s^2} \sim \frac{\lambda_L \lambda''_L g_\psi^2}{\lambda_L^2 \lambda_L'^2} f \propto \lambda''_L f, \tag{3.7.22}$$

which is controlled by the explicit breaking coupling λ_L''. If λ_L'' is small, we can have $v_s \ll f$ with the desired value. Although the tadpole term shifts the vacuum, it preserves the shape of the potential. That is, the masses of the two flavon degrees of freedom, a scalar component s and a pseudoscalar component a, are the same with

$$M_s = M_a \sim \sqrt{\frac{N_c}{8\pi^2}} \lambda_L \lambda_L' f. \tag{3.7.23}$$

The value is controlled by λ_L and λ_L', which can be large and lead to a heavy flavon.

References

[1] **CMS** Collaboration, S. Chatrchyan *et al.*, "Observation of a new boson at a mass of 125 GeV with the CMS experiment at the LHC," *Phys. Lett.* **B716** (2012) 30–61, [arXiv:1207.7235].

[2] **ATLAS** Collaboration, G. Aad *et al.*, "Observation of a new particle in the search for the Standard Model Higgs boson with the ATLAS detector at the LHC," *Phys. Lett.* **B716** (2012) 1–29, [arXiv:1207.7214].

[3] K. Babu, "TASI Lectures on Flavor Physics," in *Theoretical Advanced Study Institute in Elementary Particle Physics: The Dawn of the LHC Era*, pp. 49–123. 2010. arXiv:0910.2948.

[4] D. B. Kaplan and H. Georgi, "SU(2) x U(1) Breaking by Vacuum Misalignment," *Phys. Lett.* **136B** (1984) 183–186.

[5] D. B. Kaplan, H. Georgi, and S. Dimopoulos, "Composite Higgs Scalars," *Phys. Lett.* **136B** (1984) 187–190.

[6] C. Froggatt and H. B. Nielsen, "Hierarchy of Quark Masses, Cabibbo Angles and CP Violation," *Nucl. Phys. B* **147** (1979) 277–298.

[7] F. Bazzocchi, S. Bertolini, M. Fabbrichesi, and M. Piai, "The Little flavons," *Phys. Rev. D* **68** (2003) 096007, [hep-ph/0306184].

[8] F. Bazzocchi, S. Bertolini, M. Fabbrichesi, and M. Piai, "Fermion masses and mixings in the little flavon model," *Phys. Rev. D* **69** (2004) 036002, [hep-ph/0309182].

[9] F. Bazzocchi and M. Fabbrichesi, "A Heavy Higgs boson from flavor and electroweak symmetry breaking unification," *Phys. Rev. D* **70** (2004) 115008, [hep-ph/0407358].

[10] F. Bazzocchi and M. Fabbrichesi, "Flavor and electroweak symmetry breaking at the TeV scale," *Nucl. Phys. B* **715** (2005) 372–412, [hep-ph/0410107].

[11] T. Alanne, S. Blasi, and F. Goertz, "Common source for scalars: Flavored axion-Higgs unification," *Phys. Rev. D* **99** no. 1, (2019) 015028, [arXiv:1807.10156].

[12] L. Calibbi, F. Goertz, D. Redigolo, R. Ziegler, and J. Zupan, "Minimal axion model from flavor," *Phys. Rev. D* **95** no. 9, (2017) 095009, [arXiv:1612.08040].

[13] Y. Ema, K. Hamaguchi, T. Moroi, and K. Nakayama, "Flaxion: a minimal extension to solve puzzles in the standard model," *JHEP* **01** (2017) 096, [arXiv:1612.05492].

[14] M. Bauer, M. Carena, and K. Gemmler, "Flavor from the Electroweak Scale," *JHEP* **11** (2015) 016, [arXiv:1506.01719].

[15] M. Bauer, M. Carena, and K. Gemmler, "Creating the fermion mass hierarchies with multiple Higgs bosons," *Phys. Rev. D* **94** no. 11, (2016) 115030, [arXiv:1512.03458].

[16] I. Low, W. Skiba, and D. Tucker-Smith, "Little Higgses from an antisymmetric condensate," *Phys. Rev.* **D66** (2002) 072001, [hep-ph/0207243].

[17] C. Cai, G. Cacciapaglia, and H.-H. Zhang, "Vacuum alignment in a composite 2HDM," *JHEP* **01** (2019) 130, [arXiv:1805.07619].

[18] H.-C. Cheng and Y. Chung, "A More Natural Composite Higgs Model," *JHEP* **10** (2020) 175, [arXiv:2007.11780].

[19] R. Peccei and H. R. Quinn, "Constraints Imposed by CP Conservation in the Presence of Instantons," *Phys. Rev. D* **16** (1977) 1791–1797.

[20] D. B. Kaplan, "Flavor at SSC energies: A New mechanism for dynamically generated fermion masses," *Nucl. Phys.* **B365** (1991) 259–278.

[21] S. L. Glashow and S. Weinberg, "Natural Conservation Laws for Neutral Currents," *Phys. Rev. D* **15** (1977) 1958.

[22] E. Paschos, "Diagonal Neutral Currents," *Phys. Rev. D* **15** (1977) 1966.

[23] Z.-z. Xing, H. Zhang, and S. Zhou, "Updated Values of Running Quark and Lepton Masses," *Phys. Rev. D* **77** (2008) 113016, [arXiv:0712.1419].

[24] F. Kling, S. Su, and W. Su, "2HDM Neutral Scalars under the LHC," *JHEP* **06** (2020) 163, [arXiv:2004.04172].

[25] K. Tsumura and L. Velasco-Sevilla, "Phenomenology of flavon fields at the LHC," *Phys. Rev. D* **81** (2010) 036012, [arXiv:0911.2149].

[26] M. Bauer, T. Schell, and T. Plehn, "Hunting the Flavon," *Phys. Rev. D* **94** no. 5, (2016) 056003, [arXiv:1603.06950].

[27] **CMS** Collaboration, A. M. Sirunyan *et al.*, "Search for vector-like T and B quark pairs in final states with leptons at $\sqrt{s} = 13$ TeV," *JHEP* **08** (2018) 177, [arXiv:1805.04758].

[28] **ATLAS** Collaboration, M. Aaboud *et al.*, "Combination of the searches for pair-produced vector-like partners of the third-generation quarks at $\sqrt{s} = 13$ TeV with the ATLAS detector," *Phys. Rev. Lett.* **121** no. 21, (2018) 211801, [arXiv:1808.02343].

[29] X. Cid Vidal *et al.*, "Report from Working Group 3," *CERN Yellow Rep. Monogr.* **7** (2019) 585–865, [arXiv:1812.07831].

[30] LHCb-Collaboration, "New results on theoretically clean observables in rare B-meson decays from LHCb,".

[31] B. Grinstein and M. B. Wise, "Weak Radiative B Meson Decay as a Probe of the Higgs Sector," *Phys. Lett. B* **201** (1988) 274–278.

[32] W.-S. Hou and R. S. Willey, "Effects of Charged Higgs Bosons on the Processes $b \to s\gamma$, $b \to sg^*$ and $b \to s\ell^+\ell^-$," *Phys. Lett. B* **202** (1988) 591–595.

[33] T. G. Rizzo, "$b \to s\gamma$ in the Two Higgs Doublet Model," *Phys. Rev. D* **38** (1988) 820.

[34] C. Geng and J. N. Ng, "Charged Higgs Effect in $B^0_d - \bar{B}^0_d$ Mixing, $K \to \pi$ Neutrino Anti-neutrino Decay and Rare Decays of B Mesons," *Phys. Rev. D* **38** (1988) 2857. [Erratum: Phys.Rev.D 41, 1715 (1990)].

[35] V. D. Barger, J. Hewett, and R. Phillips, "New Constraints on the Charged Higgs Sector in Two Higgs Doublet Models," *Phys. Rev. D* **41** (1990) 3421–3441.

[36] B. Grinstein, R. P. Springer, and M. B. Wise, "Strong Interaction Effects in Weak Radiative $\bar{B}$ Meson Decay," *Nucl. Phys. B* **339** (1990) 269–309.

[37] A. Arbey, F. Mahmoudi, O. Stal, and T. Stefaniak, "Status of the Charged Higgs Boson in Two Higgs Doublet Models," *Eur. Phys. J.* **C78** no. 3, (2018) 182, [arXiv:1706.07414].

[38] M. Misiak and M. Steinhauser, "Weak radiative decays of the B meson and bounds on $M_{H^\pm}$ in the Two-Higgs-Doublet Model," *Eur. Phys. J.* **C77** no. 3, (2017) 201, [arXiv:1702.04571].

Chapter 4

A Flavorful Composite Higgs Model: Connecting the B anomalies with the hierarchy problem

Yi Chung

Center for Quantum Mathematics and Physics (QMAP), Department of Physics, University of California, Davis, CA 95616, U.S.A.

We present a model which connects the neutral current B anomalies with composite Higgs models. The model is based on the minimal fundamental composite Higgs model with $SU(4)/Sp(4)$ coset. The strong dynamics spontaneously break the symmetry and introduce five Nambu-Goldstone bosons. Four of them become the Standard Model Higgs doublet and the last one, corresponding to the broken local $U(1)'$ symmetry, is eaten by the gauge boson. This leads to an additional TeV-scale Z' boson, which can explain the recent B anomalies. The experimental constraints and allowed parameter space are discussed in detail.

4.1 Introduction

The Standard Model (SM) of particle physics successfully describes all known elementary particles and their interactions. However, there are still a few puzzles that have yet to be understood. One of them is the well-known hierarchy problem. With the discovery of light

Higgs bosons in 2012 [1, 2], the last missing piece of the SM seemed to be filled. However, SM does not address the UV-sensitive nature of scalar bosons. The Higgs mass-squared receives quadratically divergent radiative corrections from the interactions with SM fields, which require an extremely sensitive cancellation to get a 125 GeV Higgs boson. To avoid the large quadratic corrections, the most natural way is to invoke some new symmetry such that the quadratic contributions cancel in the symmetric limit. This requires the presence of new particles related to SM particles by the new symmetry.

One appealing solution to the hierarchy problem is the composite Higgs model (CHM), where the Higgs doublet is the pseudo-Nambu-Goldstone boson (pNGB) of a spontaneously broken global symmetry of the underlying strong dynamics [3, 4]. Through the analogy to the chiral symmetry breaking in quantum chromodynamics (QCD), which naturally introduces light scalar fields, i.e., pions, we can construct models with light Higgs bosons in a similar way. In a CHM, an approximate global symmetry G is spontaneously broken by some strong dynamics down to a subgroup H at a symmetry breaking scale f. The heavy resonances of the strong dynamics are expected to be around the compositeness scale $\sim 4\pi f$ generically. The pNGBs of the symmetry breaking, on the other hand, can naturally be light with masses $< f$ as they are protected by the shift symmetry.

Among all types of CHMs with different cosets, the CHMs with fundamental gauge dynamics featuring only fermionic matter fields are of interest in many studies [5, 6, 7, 8], which is known as the fundamental composite Higgs model (FCHM). In this type of CHMs, hyperfermions ψ are introduced as the representation of hypercolor (HC) group G_{HC}. Once the HC group becomes strongly coupled, hyperfermions form a condensate, which breaks the global symmetry. However, they always introduce more than four pNGBs, which means more light states are expected to be found. The minimal FCHM, which is based on the $SU(4)/Sp(4)$ coset [9, 10, 11], contains five pNGBs. The four of them formes the SM Higgs doublet, and the fifth one, as a SM singlet, could be a light scalar boson (if the symmetry is global) or a TeV-scale Z' boson (if the symmetry is local). No matter which, it should lead to some deviations in low energy phenomenology.

Although the direct searches by ATLAS and CMS haven't got any evidence of new

particles, LHCb, which does the precise measurement of B meson properties, shows interesting hints of new physics. There are discrepancies in several measurements of semileptonic B meson decays, especially the tests of lepton flavor universality (LFU), which are so-called the neutral current B anomalies [12, 13, 14, 15, 16, 17, 18]. Each anomaly is not statistically significant enough to reach the discovery level, but the combined analysis shows a consistent deviation from the SM prediction [19, 20, 21, 22, 23, 24]. These anomalies might be the deviation we are looking for.

One of the popular explanations is through a new Z' vector boson which has flavor-dependent interactions with SM fermions. Many different types of Z' models with diverse origins of $U(1)'$ gauge symmetry have been proposed [25, 26, 27, 28, 29, 30, 31, 32, 33, 34, 35, 36, 37, 38, 39, 40, 41, 42, 43, 44, 45, 46, 47, 48, 49, 50, 51, 52]. Depending on its couplings with fermions, the mass of the Z' can range from sub-TeV to multi-TeV. For a Z' boson at the TeV scale, it is natural to try to connect it with the hierarchy problem [1].

In this paper, we realize this idea using a $SU(4)/Sp(4)$ FCHM, where an $U(1)'$ subgroup within $SU(4)$ is gauged. The corresponding Z' boson only couples to the third generation SM fermions F_3 and the hyperfermions ψ through the terms

$$\mathcal{L}_{\rm int} = g_{Z'} Z'_\mu \left(\bar{F}_3 \gamma^\mu F_3 + Q_{HC} \bar{\psi} \gamma^\mu \psi \right), \tag{4.1.1}$$

where $g_{Z'}$ was normalized such that SM fermions F_3 carry a unit charge and hyperfermions carry charge Q_{HC}. When the hypercolor group becomes strongly coupled, the global symmetry $SU(4)$ and its gauged $U(1)'$ subgroup are broken. The 5^{th} pNGB is eaten by the $U(1)'$ gauge boson, which results in a TeV-scale Z' boson. We will test the potential for this Z' boson to explain the neutral current B anomalies. The parameter space allowed by different experimental constraints, mainly from neutral meson mixings and lepton flavor violation decays, will be discussed. The bounds on $M_{Z'}$ from the LHC direct searches are also shown.

[1] For our interest, we would like to mention some researches aiming at explaining the B anomalies within composite Higgs models. Different studies using different features of composite theory to address the problem, such as additional composite leptoquarks [53, 54, 55, 56] or composite vector resonances [57, 58, 59, 60, 61, 62, 63]. However, they are all different from this study, where we introduce a new Z' boson.

This paper is organized as follows. In section 4.2, we introduce the $SU(4)/Sp(4)$ FCHM. The calculations of the gauge sector, including SM gauge group and $U(1)'$ gauge symmetry, are presented. To study its phenomenology, we specify the transformation between flavor basis and mass basis in section 4.3. The resulting low energy phenomenology is discussed in section 4.4, including the B anomalies and other experimental constraints. Section 4.5 focuses on the direct searches, which play an important role in constraining a TeV-scale Z' boson. Section 4.6 and Section 4.7 contains our discussions and conclusions.

4.2 The $SU(4)/Sp(4)$ FCHM

In fundamental composite Higgs models, additional hyperfermions ψ are added to generate composite Higgs. The hyperfermions are representations of hypercolor group G_{HC}, whose coupling becomes strong around the TeV scale. The hyperfermions then form a condensate, which breaks the global symmetry and results in the pNGBs as the Higgs doublet. In this paper, we study the minimal fundamental composite Higgs model based on the global symmetry breaking $SU(4) \to Sp(4)$. The fermionic UV completion of a $SU(4)/Sp(4)$ FCHM only require four Weyl fermions in the fundamental representation of the $SU(2) = Sp(2)$ hypercolor group [7, 8]. The four Weyl fermions transform under $G_{SM} = SU(3)_C \times SU(2)_L \times U(1)_Y$ as

$$\psi_L = (U_L, D_L) = (1, 2, 0), \quad U_R = (1, 1, 1/2), \quad D_R = (1, 1, -1/2). \tag{4.2.1}$$

Next, we rewrite the two right-handed hyperfermions as $\tilde{U}_L = -i\sigma^2 C\bar{U}_R^T$ and $\tilde{D}_L = -i\sigma^2 C\bar{D}_R^T$. Since all the four Weyl fermions are according to the same representation of the hypercolor group, we can recast them together as

$$\psi = (U_L, D_L, \tilde{U}_L, \tilde{D}_L)^T \ , \tag{4.2.2}$$

which has a $SU(4)$ global symmetry (partially gauged). The hypercolor group becomes strongly coupled at the TeV scale, which forms a non-perturbative vacuum and breaks the $SU(4)$ down to $Sp(4)$. In CHMs, the condensate $\langle\psi\psi\rangle \propto \Sigma_0$ is chosen such that electroweak symmetry is preserved. It will be broken after the Higgs interactions and loop-induced potentials are taken into account. However, we will only focus on some key ingredients here and leave the complete analysis to the future.

4.2.1 Basics of $SU(4)/Sp(4)$

To study the $SU(4)/Sp(4)$ symmetry breaking, we can parametrize it by a non-linear sigma model. Consider a sigma field Σ, which transforms as an anti-symmetric tensor representation **6** of $SU(4)$. The transformation can be expressed as $\Sigma \to g\,\Sigma\,g^T$ with $g \in SU(4)$. The scalar field Σ has an anti-symmetric VEV $\langle\Sigma\rangle$, where

$$\langle\Sigma\rangle = \Sigma_0 = \begin{pmatrix} i\sigma_2 & 0 \\ 0 & i\sigma_2 \end{pmatrix}. \tag{4.2.3}$$

The Σ VEV breaks $SU(4)$ down to $Sp(4)$, producing five Nambu-Goldstone bosons.

The 15 $SU(4)$ generators can be divided into the unbroken ones and broken ones with each type satisfying

$$\begin{cases} \text{unbroken generators} & T_a : T_a\Sigma_0 + \Sigma_0 T_a^T = 0\ , \\ \text{broken generators} & X_a : X_a\Sigma_0 - \Sigma_0 X_a^T = 0\ . \end{cases} \tag{4.2.4}$$

The Nambu-Goldstone fields can be written as a matrix with the broken generator:

$$\xi(x) \equiv e^{\frac{i\pi_a(x)X_a}{2f}}. \tag{4.2.5}$$

Under $SU(4)$, the ξ field transforms as $\xi \to g\,\xi\,h^\dagger$ where $g \in SU(4)$ and $h \in Sp(4)$. The relation between ξ and Σ field is given by

$$\Sigma(x) = \xi\,\Sigma_0\,\xi^T = e^{\frac{i\pi_a(x)X_a}{f}}\Sigma_0\ . \tag{4.2.6}$$

The broken generators and the corresponding fields in the matrix can be organized as follows:

$$i\pi_a X_a = \begin{pmatrix} ia\,\mathbb{I} & \sqrt{2}\left(\tilde{H}H\right) \\ -\sqrt{2}\left(\tilde{H}H\right)^\dagger & -ia\,\mathbb{I} \end{pmatrix} \tag{4.2.7}$$

In this matrix, there are five independent fields. The four of them form the Higgs (complex) doublet H. Besides, there is one more singlet a, which will turn out to be the longitudinal part of the Z' boson. By these matrices, we can construct the low energy effective Lagrangian for these pNGB fields.

4.2.2 The SM gauge sector

The SM electroweak gauge group $SU(2)_W \times U(1)_Y$ is embedded in $SU(4) \times U(1)_X$ with generators given by

$$SU(2)_W : \frac{1}{2}\begin{pmatrix} \sigma^a & 0 \\ 0 & 0 \end{pmatrix}, \quad U(1)_Y : \frac{1}{2}\begin{pmatrix} 0 & 0 & 0 & 0 \\ 0 & 0 & 0 & 0 \\ 0 & 0 & -1 & 0 \\ 0 & 0 & 0 & 1 \end{pmatrix} + X\mathbf{I} \, . \tag{4.2.8}$$

The extra $U(1)_X$ factor accounts for the different hypercharges of the fermion representations but is not relevant for the bosonic fields. These generators belong to $Sp(4) \times U(1)_X$ and are not broken by Σ_0. Using the Σ field, the Lagrangian for kinetic terms of Higgs boson comes from

$$\mathcal{L}_h = \frac{f^2}{8}\mathrm{tr}\left[(D_\mu \Sigma)(D^\mu \Sigma)^\dagger\right] + \cdots \, , \tag{4.2.9}$$

where D_μ is the electroweak covariant derivative. Expanding this, we get

$$\mathcal{L}_h = \frac{1}{2}(\partial_\mu h)^2 + \frac{f^2}{8} g_W^2 \sin^2\left(\frac{h}{f}\right)\left[2W_\mu^+ W^{-\mu} + \frac{Z_\mu Z^\mu}{\cos\theta_W}\right] . \tag{4.2.10}$$

The non-linear behavior of the Higgs boson in the CHM is apparent from the dependence of trigonometric functions. When h obtains a nonzero VEV $\langle h \rangle = V$, the W boson acquires a mass of

$$m_W^2 = \frac{f^2}{4} g_W^2 \sin^2\left(\frac{V}{f}\right) = \frac{1}{4} g_W^2 v^2, \tag{4.2.11}$$

where $v \equiv f \sin(V/f) \approx V$. The non-linearity of the CHM is parametrized by

$$\xi \equiv \frac{v^2}{f^2} = \sin^2\left(\frac{V}{f}\right) \, . \tag{4.2.12}$$

The Higgs boson couplings to SM fields in the $SU(4)/Sp(4)$ CHM are modified by the non-linear effect due to the pNGB nature of the Higgs boson. For example, the deviation of the Higgs coupling to vector bosons is parameterized by

$$\kappa_V \equiv \frac{g_{hVV}}{g_{hVV}^{SM}} = \cos\left(\frac{V}{f}\right) = \sqrt{1-\xi} \approx 1 - \frac{\xi}{2} \, . \tag{4.2.13}$$

To decide the bound on the parameter ξ, we also need to determine the Yukawa coupling in the model, which is beyond the scope of the present work. The most conservative bound requires $\xi \lesssim 0.06$ [64, 65], which implies the symmetry breaking scale $f \gtrsim 1$ TeV.

4.2.3 $U(1)'$ gauge symmetry

Besides the SM gauge symmetry, we also gauge the $U(1)'$ subgroup of $SU(4)$ with the generator given by

$$U(1)' : \ Q_{HC} \begin{pmatrix} \mathbb{I} & 0 \\ 0 & -\mathbb{I} \end{pmatrix}. \tag{4.2.14}$$

The $U(1)'$ behaves like the lepton number of hyperfermions, where a hyperfermion carry charge Q_{HC} and an anti-hyperfermion carry charge $-Q_{HC}$. To explain the neutral current B anomalies without violating the experimental constraints, we assume SM fermions (but only the third generation) also carry a nonzero, universal charge, which is set to 1 for simplicity as mentioned in Eq. (4.1.1). To make the $U(1)'$ gauge symmetry anomaly-free, we need to take $Q_{HC} = -2$ in the minimal FCHM. Now the $U(1)'$ gauge symmetry becomes the difference between the third generation SM number and the hyperfermion number, or written as $SM_3 - HF$, which is like the hyper version of anomaly-free $B - L$ symmetry.

When $SU(4)$ global symmetry is broken down by the Σ VEV to $Sp(4)$ at the symmetry breaking scale, the $U(1)'$ subgroup is also broken down. It results in a massive Z' gauge boson with

$$M_{Z'} = g_{Z'} \left(2 \left|Q_{HC}\right| f\right) \equiv g_{Z'} f', \tag{4.2.15}$$

where we define the scale

$$f' \equiv 2 \left|Q_{HC}\right| f = 4f, \tag{4.2.16}$$

which is relevant in the study of Z' phenomenology.

To sum up, in this flavorful $SU(4)/Sp(4)$ FCHM, five pNGBs are generated below the compositeness scale. The four of them become the SM Higgs doublet we observed but with non-linear nature, which will be tested in the future Higgs measurements. The 5^{th} one is eaten by the $U(1)'$ gauge boson and results in a heavy Z' boson around the TeV scale. Other model construction issues and phenomenology of $SU(4)/Sp(4)$ CHM have been studied comprehensively in [7, 8]. In the following sections, we will focus on the Z' phenomenology and the connection with the B anomalies.

4.3 Specify the mixing matrices for phenomenology

To discuss the phenomenology, we need to first rewrite the Z' interaction terms in Eq. (4.1.1) to cover all generations and separate different chirality as

$$\mathcal{L}_{\text{int}} = g_{Z'} Z'_\mu \left(\bar{F}_L^f \gamma^\mu Q_{F_L}^f F_L^f + \bar{F}_R^f \gamma^\mu Q_{F_R}^f F_R^f \right), \tag{4.3.1}$$

where $F = (F_1, F_2, F_3)$ includes SM fermions of all the three generations with superscript f for flavor basis. The 3×3 charge matrices in the flavor basis look like

$$Q_{F_{L/R}}^f = \begin{pmatrix} 0 & 0 & 0 \\ 0 & 0 & 0 \\ 0 & 0 & 1 \end{pmatrix}. \tag{4.3.2}$$

However, to study phenomenology, we need to transform them to the mass basis $F_{L/R}^m$ through the mixing matrices as $F_{L/R}^f = U_{F_{L/R}} F_{L/R}^m$. After the transformation, we get

$$\mathcal{L}_{\text{int}} = g_{Z'} Z'_\mu \left(\bar{F}_L^m \gamma^\mu Q_{F_L}^m F_L^m + \bar{F}_R^m \gamma^\mu Q_{F_R}^m F_R^m \right), \tag{4.3.3}$$

where the charge matrices becomes

$$Q_{F_{L/R}}^m = U_{F_{L/R}}^\dagger Q_{F_{L/R}}^f U_{F_{L/R}}. \tag{4.3.4}$$

Therefore, we need to know all the $U_{F_{L/R}}$ to determine the magnitude of each interaction. However, The only information about these unitary transformation matrices is the CKM matrix for quarks and PMNS matrix for leptons. The two relations that need to be satisfied are

$$V_{CKM} \equiv U_{u_L}^\dagger U_{d_L} \quad \text{and} \quad V_{PMNS} \equiv U_{\nu_L}^\dagger U_{e_L}, \tag{4.3.5}$$

which only tells us about the left-handed part with no information about the right-handed part. Even with these two constraints, they only give the difference between two unitary transformations, but not the individual one. Therefore, we need to make some assumptions about the matrices so there won't be too many parameters.

To simplify the analysis, we assume all the U_{F_R} are identity matrices. Therefore, for right-handed fermions, only the third generation joins in the interaction with no flavor

changing at all. The couplings are the same for all the right-handed fermions it couples to with coupling strength $g_{Z'}$.

For the left-handed side, due to the observation of V_{CKM} and V_{PMNS}, there is a guarantee minimal transformation for U_{F_L}. Because we only care about the transition between the second and third generation down-type quarks and charged leptons, we will only specify the rotation θ_{23} between the second and third generation of U_{d_L} and U_{e_L} as

$$U_{F_L} = \begin{pmatrix} 1 & 0 & 0 \\ 0 & \cos\theta_F & \sin\theta_F \\ 0 & -\sin\theta_F & \cos\theta_F \end{pmatrix} \tag{4.3.6}$$

where $F = d,\, e$. Keeping only the angle θ_{23} is a strong assumption but a good example case for phenomenological study because it avoids some of the most stringent flavor constraints from light fermions and leaves a simple parameter space for analysis. Following this assumption, the rest of the matrices are fixed as $U_{u_L} = V_{CKM}^\dagger U_{d_L}$ and $U_{\nu_L} = V_{PMNS}^\dagger U_{e_L}$. Notice that, although they looks similar, the magnitude we expect for the two angles are quite different. For θ_d, we expect it to be CKM-like, i.e. $\sin\theta_d \sim \mathcal{O}(0.01)$. However, for θ_e, it could be as large as $\sin\theta_e \sim 1$.

We can then calculate the charge matrices as

$$Q^m_{F_L} = \begin{pmatrix} 0 & 0 & 0 \\ 0 & \sin^2\theta_F & -\frac{1}{2}\sin 2\theta_F \\ 0 & -\frac{1}{2}\sin 2\theta_F & \cos^2\theta_F \end{pmatrix}, \tag{4.3.7}$$

where $F = d,\, e$, and write down all the coupling for left-handed fermions. To study the B anomalies, two of them, g_{sb} and $g_{\mu\mu}$, are especially important, so we further define

$$g_{sb} \equiv -g_{Z'}\epsilon_{sb} \quad \text{with} \quad \epsilon_{sb} = \frac{1}{2}\sin 2\theta_d, \tag{4.3.8}$$

$$g_{\mu\mu} \equiv g_{Z'}\epsilon_{\mu\mu} \quad \text{with} \quad \epsilon_{\mu\mu} = \sin^2\theta_e. \tag{4.3.9}$$

We will see later that constraints will be put on the three key parameters: the scale f', the mixings ϵ_{sb}, and $\epsilon_{\mu\mu}$.

4.4 Low Energy Phenomenology

With the specified mixing matrices, we can then discuss the parameter space allowed to explain the B anomalies. Also, the constraints from other low energy experiments are presented in this section.

4.4.1 Neutral Current B Anomalies

To explain the observed neutral current B anomalies, an additional negative contribution on $b \to s\mu^+\mu^-$ is required. Based on the assumption we make, after integrating out the Z' boson, we can get the operator

$$\Delta\mathcal{L} = \frac{4G_F}{\sqrt{2}} V_{tb}V_{ts}^* \frac{e^2}{16\pi^2} C_{LL}(\bar{s}_L\gamma^\rho b_L)(\bar{\mu}_L\gamma_\rho\mu_L) \tag{4.4.1}$$

in the low energy effective Lagrangian with coefficient

$$C_{LL} = \frac{g_{sb}g_{\mu\mu}}{M_{Z'}^2}\ (35\ \text{TeV})^2 = -\frac{\epsilon_{sb}\epsilon_{\mu\mu}}{f'^2}\ (35\ \text{TeV})^2. \tag{4.4.2}$$

The global fit value for the Wilson coefficient, considering all rare B decays [19], gives

$$C_{LL} = -0.82 \pm 0.14\ , \tag{4.4.3}$$

which requires

$$\frac{\epsilon_{sb}\epsilon_{\mu\mu}}{f'^2} = \frac{1}{(39\ \text{TeV})^2} \implies f' \sim \sqrt{\epsilon_{sb}\epsilon_{\mu\mu}}\ (39\ \text{TeV}). \tag{4.4.4}$$

The generic scale with large mixing angles is $f' \sim 40$ TeV. However, as we mentioned, the value $\epsilon_{sb} \sim \mathcal{O}(0.01)$, which will bring it down to the TeV scale.

4.4.2 Neutral Meson Mixing

The measurement of neutral meson mixing put strong constraints on the Z' solution. Based on our specified mixing matrices, which have suppressed mixings between the first two generations, the $B_s - \bar{B}_s$ mixing turns out to be the strongest constraint. The measurement of mixing parameter [66] compared with SM prediction by recent lattice data [67] gives the bound on the $\bar{s}bZ'$ vertex as

$$\frac{g_{Z'}}{M_{Z'}}\epsilon_{sb} \leq \frac{1}{194\ \text{TeV}} \implies f' \geq \epsilon_{sb} \cdot 194\ (\text{TeV}). \tag{4.4.5}$$

Combining with the requirement from Eq. (4.4.4), we can rewrite the constraint as

$$f' \leq \epsilon_{\mu\mu} \cdot 7.7 \text{ (TeV)} \ . \tag{4.4.6}$$

The constraint can be understood as that, in the $b \to s\mu^+\mu^-$ process, the bs side, which is constrained by the $B_s - \bar{B}_s$ mixing measurement, should be extremely suppressed. Therefore, the $\mu\mu$ side needs to be large enough to generate the observed B anomalies. We can also find a hierarchy $\epsilon_{\mu\mu}/\epsilon_{sb} \geq 25$, which leads to the bound $\epsilon_{sb} \leq 0.04$, which is consistent with what we expected.

4.4.3 Lepton Flavor Violation Decay

In the lepton sector, there is also a strong constraint from the flavor changing neutral currents (FCNCs). The off-diagonal term in the charge matrix of charged lepton will introduce lepton flavor violation decay, in particular, $\tau \to 3\mu$, from the effective term

$$\mathcal{L}_{LFV} = \frac{g_{Z'}^2}{M_{Z'}^2} s_e^3 c_e (\bar{\tau}_L \gamma^\rho \mu_L)(\bar{\mu}_L \gamma_\rho \mu_L) \ , \tag{4.4.7}$$

where $s_e = \sin\theta_e$ and $c_e = \cos\theta_e$. The resulting branching ratio can be expressed as

$$BR(\tau \to 3\mu) = \frac{2m_\tau^5}{1536\pi^3\Gamma_\tau} \left(\frac{g_{Z'}^2}{M_{Z'}^2} s_e^3 c_e \right)^2 = 3.28 \times 10^{-4} \left(\frac{1 \text{ TeV}}{f'} \right)^4 \epsilon_{\mu\mu}^3 (1 - \epsilon_{\mu\mu}) \ . \tag{4.4.8}$$

The value should be $< 2.1 \times 10^{-8}$ at 90% CL by the measurement [68]. It also puts a strong constraint on the available parameter space. The exclusion plot combining the constraint from $B_s - \bar{B}_s$ mixing on the parameter space f' v.s. $\epsilon_{\mu\mu}$ is shown in Fig. 4.1.

The small $\epsilon_{\mu\mu}$ region is excluded, which give a minimal value $\epsilon_{\mu\mu} \geq 0.82$. It implies the angle θ_e is quite large. The value of f' is bounded from above as shown in Eq. (4.4.6) but not from below as it could be small in the $\epsilon_{\mu\mu} = 1$ limit. However, due to the connection with symmetry breaking scale $f \gtrsim 1$ TeV, we are interested in $f' \gtrsim 4$ TeV, which corresponds to the upper region of the parameter space. In this region, the Z' contributions to neutrino trident production [69, 70] and muon $(g-2)$ [71, 72] are negligible, so we will only focus on the experimental constraints we mention in this section.

4.5 Direct Z' Searches

The measurements from flavor physics in the last section can only put the constraints on the mixings and the scale $f' = M_{Z'}/g_{Z'}$. The direct searches, on the other hand, can

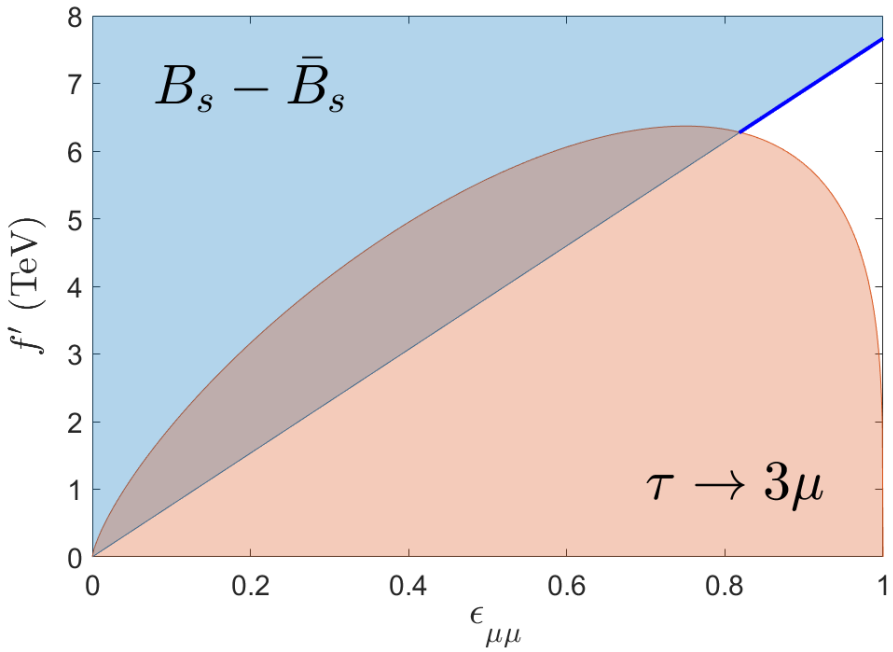

Fig. 4.1: The viable parameter space from the experimental constraints. The shaded region is excluded by the corresponding measurements. The bright blue line labels the upper edge of the available parameter space.

give the lower bound on the mass of $M_{Z'}$ directly. A general Z' collider search has been discussed in [73]. In this section, we will focus on the scenario determined by our model.

4.5.1 Decay width and branching ratios

The partial width of the Z' boson decaying into Weyl fermion pairs $\bar{f}_i f_j$ is

$$\Gamma_{ij} = \frac{C}{24\pi} g_{ij}^2 M_{Z'}, \tag{4.5.1}$$

where g_{ij} is the coupling of $\bar{f}_i f_j Z'$ vertex and C counts the color degree of freedom. In the limit that all m_f are negligible, we get the total relative width as

$$\frac{\Gamma_{Z'}}{M_{Z'}} = \frac{16}{24\pi} g_{Z'}^2 \sim 0.2\ g_{Z'}^2\ . \tag{4.5.2}$$

The value is important when we try to pick up the bound from the LHC searches.

The dominant decay channels are the diquarks channel of the third generation quarks as

$$Br(t\bar{t}) \sim Br(b\bar{b}) \sim 37.5\%. \tag{4.5.3}$$

Decays to the light quarks and exotic decays like tc and bs are also allowed but strongly suppressed due to the small rotational angles.

The main constraint is expected to come from the clear dilepton channels. Based on the specified mixing matrices we gave, the branching ratios are

$$Br(\tau\tau) \sim 6.25\ (1 + (1 - \epsilon_{\mu\mu})^2)\ \%, \tag{4.5.4}$$

$$Br(\tau\mu) \sim 12.5\ \epsilon_{\mu\mu}(1 - \epsilon_{\mu\mu})\ \%, \tag{4.5.5}$$

$$Br(\mu\mu) \sim 6.25\ \epsilon_{\mu\mu}^2\ \%. \tag{4.5.6}$$

We already get $\epsilon_{\mu\mu} \geq 0.82$ from the flavor constraints, which implies $Br(\mu\mu) \geq 4.2\%$. Therefore, the $\mu\mu$ final state is the most promising channel but also puts the stringent constraint on the $M_{Z'}$.

4.5.2 Production cross section

In the model, the Z' boson only couples to the third generation quarks in the flavor basis. Even after rotating to the mass basis, the couplings to the first and second generation quarks are still suppressed due to the small mixing angles. Therefore, the dominant production come from the process $b\bar{b} \to Z'$. In the following discussion, we will ignore all the other production processes and the small mixing angle θ_d. In this way, the cross section can be written as

$$\sigma(b\bar{b} \to Z') \equiv g_{Z'}^2 \cdot \sigma_{bb}(M_{Z'}) \tag{4.5.7}$$

where the coupling dependence is taken out. The σ_{bb} is determined by the bottom-quark parton distribution functions [74, 75], which is a function of $M_{Z'}$.

4.5.3 The $\mu\mu$ channel search

From the branching ratios and the production cross section we got, we can calculate the cross section for dimuon final state

$$\sigma_{\mu\mu} \equiv \sigma \times Br(\mu\mu) = \frac{1}{16}\,\sigma_{bb} \cdot g_{Z'}^2\ \epsilon_{\mu\mu}^2. \tag{4.5.8}$$

Moreover, from the $B_s - \bar{B}_s$ constraint, we get the lower bound on $\epsilon_{\mu\mu}$ as a function of f' in (4.4.6), which gives

$$\sigma_{\mu\mu} \geq \frac{1}{16}\,\sigma_{bb} \cdot g_{Z'}^2 \left(\frac{f'}{7.7\ \text{TeV}}\right)^2 = \sigma_{bb} \left(\frac{M_{Z'}}{31\ \text{TeV}}\right)^2. \tag{4.5.9}$$

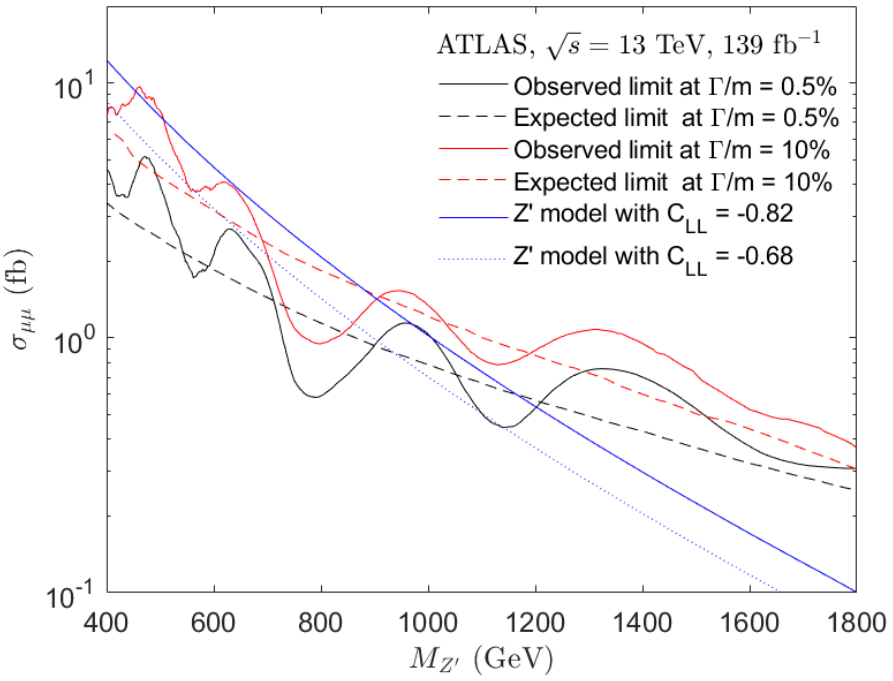

Fig. 4.2: Upper limits at 95% CL on the cross section times branching ratio $\sigma_{\mu\mu}$ as a function of $M_{Z'}$ for 10% (red) and 0.5% (black) relative width signals for the dimuon channel. Observed limits are shown as a solid line and expected limits as a dashed line. Also shown are theoretical predictions of the minimal cross section for Z' in the model (blue) assuming $C_{LL} = -0.82$ (solid) and -0.68 (dotted).

The equality holds when $\epsilon_{\mu\mu} = f'/7.7$ TeV, which corresponds to the blue line in Fig. 4.1. It gives the minimal cross section as a function of $M_{Z'}$ that allows us to compare with the experimental results. The current best search comes from the ATLAS [76] with an integrated luminosity of 139 fb^{-1}. The result is shown in Fig. 4.2.

Notice that, the bound by collider searches depends on the width. In Fig. 4.2, we show relative width of 10%(red) and 0.5%(black). The wider one gives a weaker bound. However, it require a larger $g_{Z'} \sim 0.7$ and thus a smaller $f' \sim 1.7$ TeV, which is excluded as shown in Fig. 4.1. The bright blue segment in Fig. 4.1 is the available parameter space with the minimal cross section. In this region, the value $f' \sim 7$ TeV, which implies a smaller $g_{Z'} \sim 0.17$. Therefore, we should use the black line with 0.5% width in the plot, which requires $M_{Z'} \gtrsim 1200$ GeV. If we relax the best-fit value in the Eq. (4.4.3) to one sigma region, we get a weaker bound as $M_{Z'} \gtrsim 900$ GeV.

4.5.4 Other decay channels

To looks for other decay channels, we need to first set up benchmark points. From the previous discussion, we choose the value $M_{Z'} = 1.4$ TeV, which is right above the current bound. For simplicity, we set $\epsilon_{\mu\mu} = 1$, which makes $\sigma_{\tau\tau} = \sigma_{\mu\mu}$ and $\sigma_{\tau\mu} = 0$. Once we pick up a value for f', other parameters are automatically set. We can then calculate all the cross sections we are interested in. The results are listed in table 4.1. For a fixed $M_{Z'}$, a larger f' implies a smaller $g_{Z'}$ and thus smaller cross sections. We can check that the $\sigma_{\mu\mu}$ for these benchmark points are still below the bound. Other channels, even with a larger cross section, are well below the observed limits but will be tested during the HL-LHC runs.

f'(TeV)	$g_{Z'}$	σ_{tot}(fb)	$\sigma_{tt/bb}$(fb)	$\sigma_{\tau\tau/\mu\mu}$(fb)
5.0	0.28	11.21	4.20	0.70
6.0	0.23	7.79	2.92	0.49
7.0	0.20	5.72	2.15	0.36

Table 4.1: The cross sections for each decay channel based on $M_{Z'} = 1.4$ TeV with different choice of f'.

We only show the flavor conserving final states so far, but the Z' boson can also have flavor violating decays. However, their cross sections are already constrained by the absence of FCNCs. In the quark sector, the mixings are strongly constrained and thus the branching ratios for these decays are suppressed. However, in the lepton sector, a larger mixing is allowed and the search for flavor violating decays like $Z' \to \mu\tau$ might be viable.

Although other channels are unlikely to be the discovery channel, once the Z' boson is discovered, the next thing to do will be to look for the same resonance in other channels. Through the searches, we can decide the partial widths and figure out the couplings of the Z' boson to other fields. The structure of couplings can help us distinguish between different Z' models. For example, the Z' boson in our model couples universally to all the third generation SM fermions in the flavor basis. Even considering the transformation to the mass basis, it still has a unique partial width ratio

$$\Gamma_{tt} : \Gamma_{bb} : \Gamma_{\ell\ell} : \Gamma_{\nu\nu} \sim 3 : 3 : 1 : 1, \tag{4.5.10}$$

where $\Gamma_{\ell\ell}$ is the sum of all the charged lepton partial widths. The measurement will allow us to probe the nature of the Z' boson and the underlying $U(1)'$ symmetry.

4.6 Discussions

In this study, we are interested in the value of f', which is related to the breaking scale f, and the bound on $M_{Z'}$, which is important for the collider searches. In the last section, we found that a certain straight line (such as the blue line) in Fig. 4.1 corresponding to a predicted cross section $\sigma_{\mu\mu}(f'_0)$, which is given by

$$\text{Line: } \epsilon_{\mu\mu} = \frac{f'}{f'_0} \implies \sigma_{\mu\mu}(f'_0) = \sigma_{bb}\left(\frac{M_{Z'}}{4 \times f'_0}\right)^2, \tag{4.6.1}$$

where f'_0 represents the slope of the line, e.g. for the blue line in Fig. 4.1, $f'_0 = 7.7$ TeV. Using this relation, we can calculate the cross section $\sigma_{\mu\mu}$ for each point in the parameter space in Fig. 4.1 with a certain value of $M_{Z'}$. It allows us to combine "the constraints in the parameter space in f' v.s. $\epsilon_{\mu\mu}$ plot" (as shown in Fig. 4.1) with "the direct $\mu\mu$ channel search results from the ATLAS [76]" into "the viable parameter space in f' v.s. $M_{Z'}$ plot" as shown in Fig. 4.3.

The blue region is excluded by the $B_s - \bar{B}_s$ meson mixing, which gives the lower bound $M_{Z'} \gtrsim 1.2$ TeV. The bright blue line corresponds to the same parameter space as in Fig. 4.1 with $M_{Z'} \sim 1.2$ TeV. The yellow region, also excluded by the $B_s - \bar{B}_s$ meson mixing, sets the maximum value for f' as shown in Eq. (4.4.6), which can also be found directly in Fig. 4.1. Once the stronger constraint from $B_s - \bar{B}_s$ meson mixing is placed, the yellow line will move downward and the blue line will move rightward. The red region, which is excluded by $\tau \to 3\mu$, restricts the parameter space from below. It places the lower bound on f', which will be pushed upward if the constraint becomes stronger. We can also see the data fluctuations in dimuon search become the fluctuations on the red curve. The strength of the coupling $g_{Z'}$ with three different values is also labeled as the black straight line in the plot.

There are two regions worth noticed in the plot: (1) The region with the light Z' that corresponds to a small $g_{Z'}$ but a large f' region, i.e. $(g_{Z'}, f') \sim (0.2, 7 \text{ TeV})$. (2) For a natural CHM without a large fine-tuning, a smaller f (and thus $f' = 4f$) is preferred,

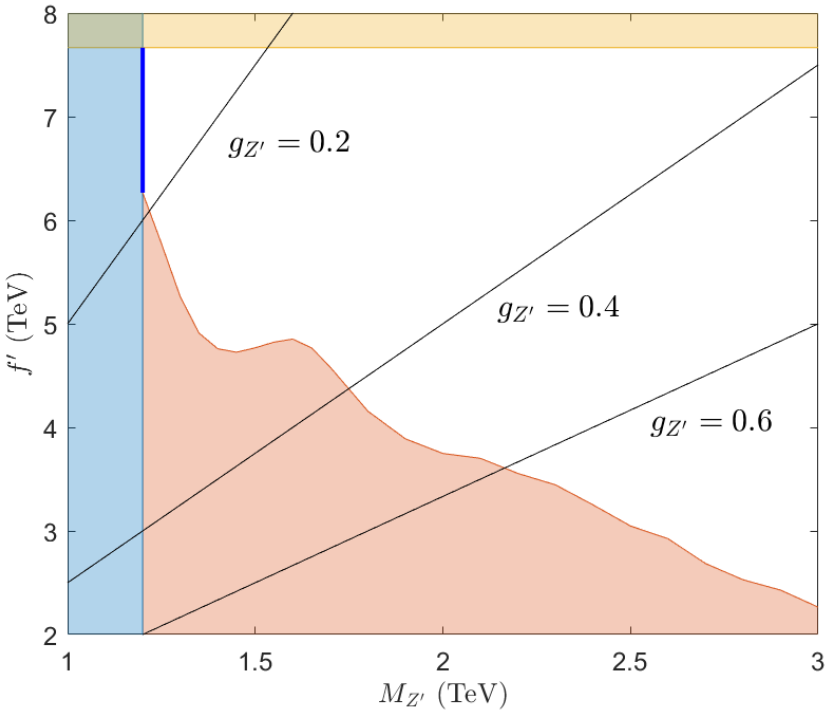

Fig. 4.3: Constraints on f' v.s. $M_{Z'}$ plot for $M_{Z'}$ below 3 TeV. The white region is currently allowed, where $\epsilon_{\mu\mu}$ and ϵ_{sb} are chosen to satisfy (4.4.2) from the requirement of the B anomalies. The shaded regions are excluded by the corresponding constraints from Fig. 4.1 combining with the direct searches, where we use the ATLAS 139 fb^{-1} dimuon searches. The three straight lines represent different values of $g_{Z'}$.

which corresponds to a larger $g_{Z'}$ region, such as $(g_{Z'}, f') \sim (0.5, 4 \text{ TeV})$ with a heavier Z'. Both regions are around the boundary. The direct searches will extend both blue and red exclusion regions rightward, so both points we mentioned will be probed soon. The lower bound on $M_{Z'}$ will be pushed to 2 TeV and most of the interesting parameter space will be explored during the HL-LHC era [77, 78].

4.7 Conclusions

In this paper, we presented a new Z' solution to the B anomalies, whose scale is related to the symmetry breaking scale of the underlying strong dynamics. We found that the anomaly-free $U(1)'$ symmetry can arise from $SM_3 - HF$, the difference between the third generation SM fermion number and the hyperfermion number. This type of $U(1)'$ is naturally broken at the TeV scale in many fundamental composite Higgs models, which

allow us to connect it with the hierarchy problem. We constructed a concrete model based on $SU(4)/Sp(4)$ minimal FCHM. The relation $f' = 2\,|Q_{HC}|f = 4f$ connects the flavor anomalies scale f' with the symmetry breaking scale f in the FCHM.

The potential for the Z' boson to explain the B anomalies is discussed in detail. Other flavor physics measurements, like neutral meson mixings and lepton flavor violation decays, put constraints on the allowed parameter space as shown in Fig. 4.1. The direct searches also give the bound on the mass of Z' as $M_{Z'} \gtrsim 1.2$ TeV. The combined constraints on the scale f' v.s. mass $M_{Z'}$ are shown in Fig. 4.3, which gives a clear picture about how the parameter space will be probed in the future. Some attractive regions are still viable and will be tested during the HL-LHC era.

Acknowledgements

I thank Hsin-Chia Cheng for many useful discussions. I am also grateful to Ben Allanach and Wolfgang Altmannshofer for reading the previous version and giving many helpful suggestions. This work is supported by the Department of Energy Grant number DE-SC-0009999.

References

[1] **CMS** Collaboration, S. Chatrchyan *et al.*, "Observation of a new boson at a mass of 125 GeV with the CMS experiment at the LHC," *Phys. Lett.* **B716** (2012) 30–61, [arXiv:1207.7235].

[2] **ATLAS** Collaboration, G. Aad *et al.*, "Observation of a new particle in the search for the Standard Model Higgs boson with the ATLAS detector at the LHC," *Phys. Lett.* **B716** (2012) 1–29, [arXiv:1207.7214].

[3] D. B. Kaplan and H. Georgi, "SU(2) x U(1) Breaking by Vacuum Misalignment," *Phys. Lett.* **136B** (1984) 183–186.

[4] D. B. Kaplan, H. Georgi, and S. Dimopoulos, "Composite Higgs Scalars," *Phys. Lett.* **136B** (1984) 187–190.

[5] J. Barnard, T. Gherghetta, and T. S. Ray, "UV descriptions of composite Higgs models without elementary scalars," *JHEP* **02** (2014) 002, [arXiv:1311.6562].

[6] G. Ferretti and D. Karateev, "Fermionic UV completions of Composite Higgs models," *JHEP* **03** (2014) 077, [arXiv:1312.5330].

[7] G. Cacciapaglia and F. Sannino, "Fundamental Composite (Goldstone) Higgs Dynamics," *JHEP* **04** (2014) 111, [arXiv:1402.0233].

[8] G. Cacciapaglia, C. Pica, and F. Sannino, "Fundamental Composite Dynamics: A Review," *Phys. Rept.* **877** (2020) 1–70, [arXiv:2002.04914].

[9] E. Katz, A. E. Nelson, and D. G. E. Walker, "The Intermediate Higgs," *JHEP* **08** (2005) 074, [hep-ph/0504252].

[10] B. Gripaios, A. Pomarol, F. Riva, and J. Serra, "Beyond the Minimal Composite Higgs Model," *JHEP* **04** (2009) 070, [arXiv:0902.1483].

[11] J. Galloway, J. A. Evans, M. A. Luty, and R. A. Tacchi, "Minimal Conformal Technicolor and Precision Electroweak Tests," *JHEP* **10** (2010) 086, [arXiv:1001.1361].

[12] **LHCb** Collaboration, R. Aaij *et al.*, "Measurement of Form-Factor-Independent Observables in the Decay $B^0 \to K^{*0}\mu^+\mu^-$," *Phys. Rev. Lett.* **111** (2013) 191801, [arXiv:1308.1707].

[13] **LHCb** Collaboration, R. Aaij *et al.*, "Test of lepton universality using $B^+ \to K^+\ell^+\ell^-$ decays," *Phys. Rev. Lett.* **113** (2014) 151601, [arXiv:1406.6482].

[14] **LHCb** Collaboration, R. Aaij *et al.*, "Angular analysis of the $B^0 \to K^{*0}\mu^+\mu^-$ decay using 3 fb^{-1} of integrated luminosity," *JHEP* **02** (2016) 104, [arXiv:1512.04442].

[15] **LHCb** Collaboration, R. Aaij *et al.*, "Test of lepton universality with $B^0 \to K^{*0}\ell^+\ell^-$ decays," *JHEP* **08** (2017) 055, [arXiv:1705.05802].

[16] **LHCb** Collaboration, R. Aaij *et al.*, "Search for lepton-universality violation in $B^+ \to K^+\ell^+\ell^-$ decays," *Phys. Rev. Lett.* **122** no. 19, (2019) 191801, [arXiv:1903.09252].

[17] **LHCb** Collaboration, R. Aaij *et al.*, "Measurement of CP-Averaged Observables in the $B^0 \to K^{*0}\mu^+\mu^-$ Decay," *Phys. Rev. Lett.* **125** no. 1, (2020) 011802, [arXiv:2003.04831].

[18] **LHCb** Collaboration, R. Aaij *et al.*, "Test of lepton universality in beauty-quark decays," (3, 2021) .

[19] W. Altmannshofer and P. Stangl, "New Physics in Rare B Decays after Moriond 2021," (3, 2021) .

[20] C. Cornella, D. A. Faroughy, J. Fuentes-Martín, G. Isidori, and M. Neubert, "Reading the footprints of the B-meson flavor anomalies," (3, 2021) .

[21] L.-S. Geng, B. Grinstein, S. Jäger, S.-Y. Li, J. Martin Camalich, and R.-X. Shi, "Implications of new evidence for lepton-universality violation in $b \to s\ell^+\ell^-$ decays," (3, 2021) .

[22] A. K. Alok, A. Dighe, S. Gangal, and D. Kumar, "Continuing search for new physics in $b \to s\mu\mu$ decays: two operators at a time," *JHEP* **06** (2019) 089, [arXiv:1903.09617].

[23] M. Algueró, B. Capdevila, S. Descotes-Genon, J. Matias, and M. Novoa-Brunet, "$\boldsymbol{b \to s\ell\ell}$ global fits after Moriond 2021 results," in *55th Rencontres de Moriond on QCD and High Energy Interactions*. 4, 2021. arXiv:2104.08921.

[24] A. Carvunis, F. Dettori, S. Gangal, D. Guadagnoli, and C. Normand, "On the effective lifetime of $B_s \to \mu\mu\gamma$," . (2, 2021) , [arXiv:2102.13390].

[25] W. Altmannshofer, S. Gori, M. Pospelov, and I. Yavin, "Quark flavor transitions in $L_\mu - L_\tau$ models," *Phys. Rev. D* **89** (2014) 095033, [arXiv:1403.1269].

[26] W. Altmannshofer and I. Yavin, "Predictions for lepton flavor universality violation in rare B decays in models with gauged $L_\mu - L_\tau$," *Phys. Rev. D* **92** no. 7, (2015) 075022, [arXiv:1508.07009].

[27] W. Altmannshofer, J. Davighi, and M. Nardecchia, "Gauging the accidental symmetries of the standard model, and implications for the flavor anomalies," *Phys. Rev. D* **101** no. 1, (2020) 015004, [arXiv:1909.02021].

[28] A. Crivellin, G. D'Ambrosio, and J. Heeck, "Explaining $h \to \mu^\pm\tau^\mp$, $B \to K^*\mu^+\mu^-$ and $B \to K\mu^+\mu^-/B \to Ke^+e^-$ in a two-Higgs-doublet model with gauged $L_\mu - L_\tau$," *Phys. Rev. Lett.* **114** (2015) 151801, [arXiv:1501.00993].

[29] A. Crivellin, J. Fuentes-Martin, A. Greljo, and G. Isidori, "Lepton Flavor Non-Universality in B decays from Dynamical Yukawas," *Phys. Lett. B* **766** (2017) 77–85, [arXiv:1611.02703].

[30] R. Alonso, P. Cox, C. Han, and T. T. Yanagida, "Anomaly-free local horizontal symmetry and anomaly-full rare B-decays," *Phys. Rev. D* **96** no. 7, (2017) 071701, [arXiv:1704.08158].

[31] R. Alonso, P. Cox, C. Han, and T. T. Yanagida, "Flavoured $B - L$ local symmetry and anomalous rare B decays," *Phys. Lett. B* **774** (2017) 643–648, [arXiv:1705.03858].

[32] C. Bonilla, T. Modak, R. Srivastava, and J. W. F. Valle, "$U(1)_{B_3-3L_\mu}$ gauge symmetry as a simple description of $b \to s$ anomalies," *Phys. Rev. D* **98** no. 9, (2018) 095002, [arXiv:1705.00915].

[33] B. C. Allanach, "$U(1)_{B_3-L_2}$ explanation of the neutral current $B-$anomalies," *Eur. Phys. J. C* **81** no. 1, (2021) 56, [arXiv:2009.02197]. [Erratum: Eur.Phys.J.C 81, 321 (2021)].

[34] B. C. Allanach and J. Davighi, "Third family hypercharge model for $R_{K^{(*)}}$ and aspects of the fermion mass problem," *JHEP* **12** (2018) 075, [arXiv:1809.01158].

[35] B. C. Allanach and J. Davighi, "Naturalising the third family hypercharge model for neutral current B-anomalies," *Eur. Phys. J. C* **79** no. 11, (2019) 908, [arXiv:1905.10327].

[36] R. Gauld, F. Goertz, and U. Haisch, "On minimal Z' explanations of the $B \to K^* \mu^+ \mu^-$ anomaly," *Phys. Rev. D* **89** (2014) 015005, [arXiv:1308.1959].

[37] A. J. Buras, F. De Fazio, and J. Girrbach, "331 models facing new $b \to s\mu^+\mu^-$ data," *JHEP* **02** (2014) 112, [arXiv:1311.6729].

[38] A. J. Buras and J. Girrbach, "Left-handed Z' and Z FCNC quark couplings facing new $b \to s\mu^+\mu^-$ data," *JHEP* **12** (2013) 009, [arXiv:1309.2466].

[39] D. Aristizabal Sierra, F. Staub, and A. Vicente, "Shedding light on the $b \to s$ anomalies with a dark sector," *Phys. Rev. D* **92** no. 1, (2015) 015001, [arXiv:1503.06077].

[40] A. Celis, J. Fuentes-Martin, M. Jung, and H. Serodio, "Family nonuniversal Z' models with protected flavor-changing interactions," *Phys. Rev. D* **92** no. 1, (2015) 015007, [arXiv:1505.03079].

[41] A. Falkowski, M. Nardecchia, and R. Ziegler, "Lepton Flavor Non-Universality in B-meson Decays from a U(2) Flavor Model," *JHEP* **11** (2015) 173, [arXiv:1509.01249].

[42] C.-W. Chiang, X.-G. He, and G. Valencia, "Z' model for $b \to s\ell\bar{\ell}$ flavor anomalies," *Phys. Rev. D* **93** no. 7, (2016) 074003, [arXiv:1601.07328].

[43] S. M. Boucenna, A. Celis, J. Fuentes-Martin, A. Vicente, and J. Virto, "Non-abelian gauge extensions for B-decay anomalies," *Phys. Lett. B* **760** (2016) 214–219, [arXiv:1604.03088].

[44] S. M. Boucenna, A. Celis, J. Fuentes-Martin, A. Vicente, and J. Virto, "Phenomenology of an $SU(2) \times SU(2) \times U(1)$ model with lepton-flavour non-universality," *JHEP* **12** (2016) 059, [arXiv:1608.01349].

[45] D. Bhatia, S. Chakraborty, and A. Dighe, "Neutrino mixing and R_K anomaly in $U(1)_X$ models: a bottom-up approach," *JHEP* **03** (2017) 117, [arXiv:1701.05825].

[46] P. Ko, Y. Omura, Y. Shigekami, and C. Yu, "LHCb anomaly and B physics in flavored Z' models with flavored Higgs doublets," *Phys. Rev. D* **95** no. 11, (2017) 115040, [arXiv:1702.08666].

[47] Y. Tang and Y.-L. Wu, "Flavor non-universal gauge interactions and anomalies in B-meson decays," *Chin. Phys. C* **42** no. 3, (2018) 033104, [arXiv:1705.05643]. [Erratum: Chin.Phys.C 44, 069101 (2020)].

[48] K. Fuyuto, H.-L. Li, and J.-H. Yu, "Implications of hidden gauged $U(1)$ model for B anomalies," *Phys. Rev. D* **97** no. 11, (2018) 115003, [arXiv:1712.06736].

[49] L. Bian, H. M. Lee, and C. B. Park, "B-meson anomalies and Higgs physics in flavored $U(1)'$ model," *Eur. Phys. J. C* **78** no. 4, (2018) 306, [arXiv:1711.08930].

[50] S. F. King, "$R_{K^{(*)}}$ and the origin of Yukawa couplings," *JHEP* **09** (2018) 069, [arXiv:1806.06780].

[51] G. H. Duan, X. Fan, M. Frank, C. Han, and J. M. Yang, "A minimal $U(1)'$ extension of MSSM in light of the B decay anomaly," *Phys. Lett. B* **789** (2019) 54–58, [arXiv:1808.04116].

[52] L. Calibbi, A. Crivellin, F. Kirk, C. A. Manzari, and L. Vernazza, "Z' models with less-minimal flavour violation," *Phys. Rev. D* **101** no. 9, (2020) 095003, [arXiv:1910.00014].

[53] B. Gripaios, M. Nardecchia, and S. A. Renner, "Composite leptoquarks and anomalies in B-meson decays," *JHEP* **05** (2015) 006, [arXiv:1412.1791].

[54] R. Barbieri, C. W. Murphy, and F. Senia, "B-decay Anomalies in a Composite Leptoquark Model," *Eur. Phys. J. C* **77** no. 1, (2017) 8, [arXiv:1611.04930].

[55] D. Marzocca, "Addressing the B-physics anomalies in a fundamental Composite Higgs Model," *JHEP* **07** (2018) 121, [arXiv:1803.10972].

[56] J. Fuentes-Martín and P. Stangl, "Third-family quark-lepton unification with a fundamental composite Higgs," *Phys. Lett. B* **811** (2020) 135953, [arXiv:2004.11376].

[57] C. Niehoff, P. Stangl, and D. M. Straub, "Violation of lepton flavour universality in composite Higgs models," *Phys. Lett. B* **747** (2015) 182–186, [arXiv:1503.03865].

[58] C. Niehoff, P. Stangl, and D. M. Straub, "Direct and indirect signals of natural composite Higgs models," *JHEP* **01** (2016) 119, [arXiv:1508.00569].

[59] A. Carmona and F. Goertz, "Lepton Flavor and Nonuniversality from Minimal Composite Higgs Setups," *Phys. Rev. Lett.* **116** no. 25, (2016) 251801, [arXiv:1510.07658].

[60] A. Carmona and F. Goertz, "Recent B physics anomalies: a first hint for compositeness?," *Eur. Phys. J. C* **78** no. 11, (2018) 979, [arXiv:1712.02536].

[61] R. Barbieri and A. Tesi, "B-decay anomalies in Pati-Salam SU(4)," *Eur. Phys. J. C* **78** no. 3, (2018) 193, [arXiv:1712.06844].

[62] F. Sannino, P. Stangl, D. M. Straub, and A. E. Thomsen, "Flavor Physics and Flavor Anomalies in Minimal Fundamental Partial Compositeness," *Phys. Rev. D* **97** no. 11, (2018) 115046, [arXiv:1712.07646].

[63] M. Chala and M. Spannowsky, "Behavior of composite resonances breaking lepton flavor universality," *Phys. Rev. D* **98** no. 3, (2018) 035010, [arXiv:1803.02364].

[64] V. Sanz and J. Setford, "Composite Higgs Models after Run 2," *Adv. High Energy Phys.* **2018** (2018) 7168480, [arXiv:1703.10190].

[65] **ATLAS** Collaboration, G. Aad *et al.*, "Combined measurements of Higgs boson production and decay using up to 80 fb^{-1} of proton-proton collision data at $\sqrt{s} =$ 13 TeV collected with the ATLAS experiment," *Phys. Rev. D* **101** no. 1, (2020) 012002, [arXiv:1909.02845].

[66] **HFLAV** Collaboration, Y. Amhis *et al.*, "Averages of b-hadron, c-hadron, and τ-lepton properties as of summer 2016," *Eur. Phys. J. C* **77** no. 12, (2017) 895, [arXiv:1612.07233].

[67] D. King, A. Lenz, and T. Rauh, "B$_s$ mixing observables and —V$_{td}$/V$_{ts}$— from sum rules," *JHEP* **05** (2019) 034, [arXiv:1904.00940].

[68] K. Hayasaka *et al.*, "Search for Lepton Flavor Violating Tau Decays into Three Leptons with 719 Million Produced Tau+Tau- Pairs," *Phys. Lett. B* **687** (2010) 139–143, [arXiv:1001.3221].

[69] W. Altmannshofer, S. Gori, M. Pospelov, and I. Yavin, "Neutrino Trident Production: A Powerful Probe of New Physics with Neutrino Beams," *Phys. Rev. Lett.* **113** (2014) 091801, [arXiv:1406.2332].

[70] **CCFR** Collaboration, S. R. Mishra *et al.*, "Neutrino tridents and W Z interference," *Phys. Rev. Lett.* **66** (1991) 3117–3120.

[71] M. Pospelov, "Secluded U(1) below the weak scale," *Phys. Rev. D* **80** (2009) 095002, [arXiv:0811.1030].

[72] **Muon g-2** Collaboration, B. Abi *et al.*, "Measurement of the Positive Muon Anomalous Magnetic Moment to 0.46 ppm," *Phys. Rev. Lett.* **126** no. 14, (2021) 141801, [arXiv:2104.03281].

[73] B. C. Allanach, J. M. Butterworth, and T. Corbett, "Collider constraints on Z' models for neutral current B-anomalies," *JHEP* **08** (2019) 106, [arXiv:1904.10954].

[74] A. D. Martin, W. J. Stirling, R. S. Thorne, and G. Watt, "Parton distributions for the LHC," *Eur. Phys. J. C* **63** (2009) 189–285, [arXiv:0901.0002].

[75] J. Alwall, R. Frederix, S. Frixione, V. Hirschi, F. Maltoni, O. Mattelaer, H. S. Shao, T. Stelzer, P. Torrielli, and M. Zaro, "The automated computation of tree-level and next-to-leading order differential cross sections, and their matching to parton shower simulations," *JHEP* **07** (2014) 079, [arXiv:1405.0301].

[76] **ATLAS** Collaboration, G. Aad *et al.*, "Search for high-mass dilepton resonances using 139 fb^{-1} of pp collision data collected at $\sqrt{s}$ =13 TeV with the ATLAS detector," *Phys. Lett. B* **796** (2019) 68–87, [arXiv:1903.06248].

[77] **ATLAS Collaboration** Collaboration, "Prospects for searches for heavy Z' and W' bosons in fermionic final states with the ATLAS experiment at the HL-LHC," tech. rep., CERN, Geneva, Dec, 2018.

[78] X. Cid Vidal *et al.*, "Report from Working Group 3: Beyond the Standard Model physics at the HL-LHC and HE-LHC," *CERN Yellow Rep. Monogr.* **7** (2019) 585–865, [arXiv:1812.07831].

Chapter 5

Conclusions

In this dissertation, we introduce three composite Higgs models aiming at solving different problems motivated by both theoretical considerations and experimental results. They are all based on larger cosets that allow additional symmetries and mechanisms beyond the minimal setup.

In *A More Natural Composite Higgs Model*, we show how an enlarged symmetry can help reduce the quadratic term and enhance the quartic term in the Higgs potential, which can minimalize the required fine-tuning. In *Composite Flavon-Higgs Models*, a flavor symmetry is included in the enlarged symmetry of CHMs, which can lead to the Froggatt-Nielsen mechanism and generate the mass hierarchy between the top and bottom quarks. In *A Flavorful Composite Higgs Model*, we find that a TeV-scale Z' boson can naturally arise in a fundamental composite Higgs model and provides a possible explanation to the neutral current B anomalies.

These models point out the richness of composite Higgs models with enlarged cosets. Moreover, they all introduce new physics at the TeV-scale phenomenology, which will be tested through direct and indirect searches in the LHC and other experiments. Especially, the B anomalies will be checked in the next few years by LHCb and Belle II experiments. If confirmed, that will be a revolution in the field of particle physics since the discovery of the Higgs boson. If the solution shows up at the TeV scale, it might unveil the deep connection between Higgs physics and flavor physics.